Deciphering the generation of bone marrow resident memory CD4 T cells in the spleen

D i s s e r t a t i o n

zur Erlangung des akademischen Grades

doctor rerum naturalium (Dr. rer. nat.)

im Fach Biologie

eingereicht an der

Lebenswissenschaftlichen Fakultät der Humboldt-Universität zu Berlin

von
Dipl.-Ing. Jana Sarkander

Präsidentin der Humboldt-Universität zu Berlin

Prof. Dr.-Ing. Dr. Sabine Kunst

Dekan der Lebenswissenschaftlichen Fakultät

Prof. Dr. Bernhard Grimm

Gutachter:
1. Prof. Dr. Andreas Radbruch
2. Prof. Dr. Andreas Thiel
3. Prof. Arturo Zychlinsky

Tag der mündlichen Prüfung: 12. August 2019

Abstract

Long-lived memory CD4 T lymphocytes play a crucial role in the generation, maintenance and reactivation of other memory lymphocytes. During an immune reaction, some antigen-experienced CD4 T cells relocate from secondary lymphoid organs (SLOs) to the bone marrow (BM) and reside and rest there as professional memory CD4 T cells. Despite the importance of CD49b and CD69 expression for the establishment and retention of BM memory CD4 T cells, it remains elusive how the precursors of BM memory CD4 T cells are generated in SLOs. This doctoral thesis aims at the phenotypical identification and functional characterization of splenic antigen-specific memory CD4 T cell precursors that ultimately populate the memory pool in the BM. By means of adaptive transfer of TCR-transgenic CD4 T cells and immunization with cognate peptide, the first part of this thesis identifies splenic CD49b$^+$T-bet$^+$/CXCR3$^+$ activated CD4 T cells as the precursors of BM memory CD4 T cells. Following their identification, the second part of the thesis deals with the characteristics of BM memory CD4 T cell precursors generated during priming and activation and describes that precursors of BM memory CD4 T cells are generated following enhanced cell proliferation and prolonged cognate interactions with dendritic cells (DCs) during the late activation phase of a primary immune response. Treatment with a cytostatic drug or blockage of CD28/B7 costimulatory pathway in the late activation phase in turn abrogates the generation of precursors of BM memory CD4 T cells. Moreover, fluorescent-dye labeling experiments demonstrate that the more CD49b$^+$CXCR3$^+$ activated CD4 T cells divide, the more they lose the expression of CCR7, a chemokine receptor crucial for the persistence in the T cell zone of SLOs, and gain the expression of IL-2Rβ, a cytokine receptor crucial for long-term survival. Since B cells have previously been described to modulate the formation of memory CD4 T cells in the spleen, the third part of this thesis investigates the role of B cells for the establishment of resting CD4 T cell memory in the BM by using B cell-depleted or B cell-deficient mice in combination with adoptive transfer of CD4 T cells. B cells negatively impact the accumulation of memory CD4 T cell precursors in the BM during the early phase of an immune response but do not affect the cell division of activated CD4 T cells in the spleen during the activation phase, raising further questions on the regulatory role of B cells for the generation of memory CD4 T cells in the BM. In sum, the results obtained in this thesis provide new insight into the generation of BM memory CD4 T cells that may help for the therapeutic

strengthening of immune memory in the context of vaccination or its abolishment within the scope of autoimmune diseases.

Zusammenfassung

Langlebige Gedächtnis-CD4 T Lymphozyten spielen eine entscheidende Rolle für die Bildung, Erhaltung und Reaktivierung anderer Gedächtnislymphozyten. Im Verlauf einer Immunreaktion wandern einige antigenerfahrene CD4 T Zellen aus den sekundär lymphoiden Organen (SLO) ins Knochenmark (KM), wo sie als professionelle Gedächtnis- CD4 T Zellen ruhen und überdauern. Trotz der Bedeutung der Expression von CD49b und CD69 für die Etablierung und Retention von KM-Gedächtnis-CD4 T Zellen, bleibt es weitghehend unverstanden wie deren Vorläuferzellen in SLO gebildet werden. Ziel dieser Dissertation ist die phänotypische Identifizierung und funktionelle Charakterisierung der Gedächtnis CD4 T Vorläuferzellen in der Milz, da diese Zellen letztendlich den Gedächtnispool im KM besiedeln. Mit Hilfe von adaptivem Transfer T-Zellrezeptor-transgener CD4 T Zellen und Peptidimmunisierung identifiziert der erste Teil dieser Arbeit CD49b$^+$T-bet$^+$/CXCR3$^+$ aktivierte CD4 T Zellen der Milz als Vorläuferzellen von KM-Gedächtnis-CD4 T Zellen. Im Anschluss beschäftigt sich der zweite Teil der Arbeit mit den Eigenschaften der Gedächtnis-CD4 T Vorläuferzellen während der Priming- und Aktivierungsphase. Es wird gezeigt, dass die Vorläuferzellen nach einer verstärkten Zellproliferation und längerer kognitiver Interaktion mit dendritischen Zellen während der späten Aktivierungsphase der primären Immunantwort gebildet werden. Die Behandlung mit einem Zytostatikum oder die Blockade des kostimulatorischen CD28/B7-Signalweges in der späten Aktivierungsphase verhindert wiederum die Generierung der Gedächtnisvorläuferzellen. Darüber hinaus wird gezeigt, dass mit zunehmender Anzahl an Zellteilungen die aktivierte CD49b$^+$CXCR3$^+$ CD4 T Zellen durchlaufen, sich die Expression des Chemokinrezeptors CCR7, der für den Zellverbleib in der T-Zellzone in SLO entscheidend ist, verringert. Im Gegenzug nimmt die Expression des Zytokinrezeptors IL-2Rβ, der für das langfristige Zellüberleben entscheidend ist, zu. Da zuvor beschrieben wurde, dass B Zellen die Bildung von Gedächtnis CD4 T Zellen in der Milz modulieren, untersucht der dritte Teil der Arbeit die Rolle von B Zellen während der Etablierung des CD4 T Zellgedächtnisses im KM unter Verwendung von B Zell-depletierten oder B Zell-defizienten Mäusen. Die Ergebnisse deuten darauf hin, dass B Zellen die Anreicherung von Gedächtnis CD4 T Vorläuferzellen im KM während der frühen Phase einer Immunantwort beeinträchtigen, jedoch die Proliferation aktivierter CD4 T Zellen nicht durch B Zellen beeinflusst wird. Die Ergebnisse dieser Arbeit liefern neue Einblicke in die Generierung von Gedächtnis-CD4 T Zellen des KM,

die für neue Ansätze zur therapeutischen Stärkung des Immungedächtnisses im Rahmen von Impfungen oder Zelldepletion bei Autoimmunerkrankungen beitragen können.

Table of Contents

Abbreviations

Ag	antigen
AICD	activation induced cell death
APC	antigen presenting cell
Bcl-6	B cell lymphoma- 6
BM	bone marrow
BSA	bovine serum albumin
BrdU	bromodeoxyuridine
CCR7	C-C chemokine receptor type 7
CFSE	carboxyfluorescein diacetate succinimidyl ester
CTL	cytotoxic T cell
CTLA-4	cytotoxic T-lymphocyte-associated protein 4
CXCR3	CXC chemokine receptor 3
CXCR5	CXC chemokine receptor 5
CyP	cyclophosphamide
DC	dendritic cell
DMEM	Dulbecco’s modified Eagle Medium
DMSO	dimethyl sulfoxide
DNA	desoxyribonucleic acid
DN	double negative
dsDNA	double stranded DNA
EDTA	ethylenediaminetetraacetic acid
Fab-fragment	variable region of an antibody
Fc-fragment	constant region of an antibody
FCS	fetal calf serum
FoxP3	forkhead box P3
GMFI	geometrical mean fluorescent intensity
GC	germinal center
FITC	fluorescein-5-isothiocyanat
HCl	hydrogen chloride

g	gravitational acceleration 9,81 m/s^2
i.p.	intraperitoneally
i.v.	intraveneously
ICOS	inducible T-cell costimulator
Ig	immunoglobulin
IHC	immunohistochemistry
IL	interleukin
IFN-γ	interferon-γ
IRF-4	interferon regulatory factor 4
kbp	kilo base pair
kDa	kilo Dalton
$KHCO_3$	potassium bicarbonate
Klf-2	Krüppel-like factor 2
LCMV	lymphocytic choriomeningitis virus
LN	lymph node
LP	lamina propria
LPS	lipopolysaccharide
mAb	monoclonal antibody
MACS	magnetically activated cell sorting
MP	memory phenotype
MFI	mean fluorescent intensity
$MgCl_2$	magnesium chloride
MHC	major histocompatibility complex class
mM	milli molar
Na_2CO_3	sodium carbonate
Na_2HPO_4	disodium phosphate
NaCl	sodium chloride
NaH_2PO_4	monosodium phosphate
$NaHCO_3$	sodium hydrogen carbonate
NH_4Cl	ammonium chloride
ON	over night
OVA	ovalbumin

PAMPs	pathogen-associated molecular patterns
PALS	periarteriolar lymphoid sheath
PBS	phosphate buffered saline
PC	plasma cell
PFA	para-formaldehyde
pH	pondus Hydrogenium
PI	propidium iodide
PP	Peyer's pathches
polyAb	polyclonal antibody
PRR	pattern recognition receptor
p.I.	post immunization/injection
PD-1	programmed cell death- receptor 1
RBC	red blood cell
RPMI	Rosewell Park Memorial Institute medium
RT	room temperature
SCID	severe combined immuno deficiency
SLO	secondary lymphoid organ
S1P1	sphingosine-1 phosphate receptor 1
Tg	transgene
TGF-β	tumor growth factor- β
T-bet	T-box expressed in T cells
TCA	trichloroacetic acid
TCR	T cell receptor
T_H	T helper cell
Tfh	T follicular helper cell
T_{EM}	effector memory T cell
T_{CM}	central memory T cell
T_{RM}	tissue resident memory T cell
Treg	regulatory T cell
TLR	Toll-like receptor
VCAM-1	vascular cell adhesion molecule 1
WT	wild type

1 Introduction

1.1 The adaptive immune system and the biology of CD4 T cells

The immune system is composed of the innate and the adaptive immune system which represent the two key defense strategies of vertebrates against all kinds of potentially harmful and infectious agents. The innate immune system is the major system found in plants, fungi, insects and primitive multicellular organisms and has evolved far earlier during evolution than the adaptive immune system. However, it is unable to form immunological memory and thus cannot provide long-lasting immunity. While the cells of the innate system recognize pathogens by conserved patterns and quickly respond in a non-specific and generic way, the adaptive immune system is characterized by an acquired response composed of a fast and highly specific cellular response via T cells and a strong and directed humoral response via B cells in terms of antibodies. Immune cells are able to distinguish between foreign substances that invaded the organism and self-molecules that are components of the own organism. Under some pathological conditions, however, the immune response may be directed to non-infectious agents or self-molecules leading to allergy or autoimmune diseases.

1.1.1 Antigen recognition

In order to effectively combat the wide range of pathogens an organism is frequently exposed to, the immune cells of the innate and adaptive immune system developed mechanisms to recognize antigens from viruses, bacteria or other disease-causing agents and organisms. An antigen is generally defined as a molecule or part of a molecule which is recognized by special pattern recognition receptors (PRR) and is able to induce an immune response (1). The surface of any pathogen contains special pathogen-associated molecular patterns (PAMP) which are recognized by PRRs e.g. toll-like receptors (TLR) (2). Antigens are typically peptides or proteins, lipids or polysaccharides.

B cells and their secreted antibodies recognize intact antigens, while T cells recognize degraded peptide fragments of antigens that have previously been engulfed, processed and ultimately presented by antigen presenting cells (APC) via the major histocompatibility complex (MHC) (3, 4).

The major APC for naïve T cells are dendritic cells (DC). However, also macrophages and B cells belong to the group of APC. DCs display the link between innate and adaptive immunity. They are distributed throughout the body in order to screen their environment for pathogens and ultimately present processed antigen to T cells in secondary lymphoid organs (SLO) (5). The type of antigen defines whether it will be presented via a MHC class I or MHC class II molecule. MHC class I molecules present peptides deriving from new proteins synthesized and degraded in the cytoplasm such as parts of viral proteins. MHC class II molecules present peptides deriving from protein degraded inside of endocytic vesicles (6, 7). The MHC I molecule is expressed on all nucleated cells, which excludes red blood cells (RBC). It is recognized by cytotoxic CD8 T cells, which induce apoptosis of the infected cell or tumor cell upon engagement of the T cell receptor (TCR) and the MHC I (8). The MHC II complex is only expressed on professional APCs that comprise DCs, macrophages and B cells, and is recognized by CD4 T cells, that are defined as helper T (Th) cells because of their ability to modulate activation and differentiation of other cells through the production of specific cytokines (9, 10). However, only DCs are able to prime naïve T cells and thus induce a primary immune response (11). DCs are derived from hematopoietic progenitor cells in the bone marrow (BM). They migrate as immature DCs through the blood into tissues where they constantly sample the environment for pathogens. Immature DCs are equipped with a highly active endocytic machinery and low T cell actiation potential (11). Upon encounter with a pathogen, PRRs expressed on the surface of the DC engage with microbial factors such as PAMP leading to DC activation and hence maturation that results in the migration from the site of antigen encounter into the T cell areas of SLOs in a CCR7 dependent manner. Furthermore, MHC molecules are upregulated as well as co-stimulatory molecules (11, 12). T cells localized in the T cell areas of SLOs recognize the MHC-antigen complex through the antigen-specific TCR. The majority of mature T cells express a TCR composed of the two glycoprotein chains α and β which are associated with the glycoprotein CD3 and the co-receptors CD4 or CD8. Both CD4 T cells and CD8 T cells, display diverse roles and can be further subdivided into specialized subsets according to their function, production of cytokines and localization.

1.1.2 CD4 T cell activation

The initial interaction between the T cell and the DC defines the following T cell response; while the specificity of the response is controlled by the TCR and the antigen-peptide presented via MHC molecules on the DC (Signal 1, Figure 1.1), the magnitude and type of response is dependent on costimulatory molecules and cytokines ex-

pressed by the antigen-presenting DC (13). Upon receipt of co-stimulatory signals (Signal 2a, Figure 1.1) via the CD28 or CD40L receptor through CD80/CD86 (B7) or CD40 molecules, respectively, strong responses of naïve T cells are induced which are important to mediate cell survival and expansion (14, 15). Other co-stimulatory receptors are CTLA-4 or PD-1 (Signal 2b, Figure 1.1). After activation of T cells, the expression of CTLA-4 is induced and competing with CD28 for co-stimulatory signals via CD80/CD86. CTLA-4 induces a negative regulation of T cell activation which in turn reduces the sensitivity for further stimulation (16, 17). Likewise, an engagement of PD-1 receptor expressed on activated T cells and PD-1L expressed on DCs inhibits the immune response through induction of interleukin (IL)-10 secretion by the APC (18). Notably, PD-1 expression in combination with the chemokine receptor molecule CXCR5 marks T follicular helper (Tfh) cells that will be introduced in section 1.1.3.

The third signal is promoted by cytokines and directs the differentiation of T cells into different effector subsets (Signal 3, Figure 1.1).

Upon completed T cell activation, the cell allows itself to proliferate through induction of autocrine IL-2 secretion. In turn, the expression and engagement of all three subunits of the IL-2 receptor (αβγ) activates the T cell's proliferation pathway. Each of the three subunits exhibits a different affinity for IL-2: The low affinity monomeric IL-2Rα (CD25) may bind IL-2 but is incapable of transducing a signal, the intermediate affinity dimeric IL-2Rβγ is capable of signal transduction, whereas the high affinity trimeric IL-2Rαβγ has the highest affinity for IL-2 and is responsible for the majority of physiologically relevant IL-2 signaling.

The clonal proliferation serves two major purposes: On the one hand, cells need to expand in order to differentiate into effector cells and express suitable chemokine receptors that enable the migration to the site of infection. On the other hand, clonal proliferation provides a greater number of cells that help both B cells and CD8 T cells. In particular, CD4 T cells are essential for B cell germinal centre formation, class switching and affinity maturation and a lack of CD4 T cells impairs the generation of high-affinity memory B cells and plasma cells (19-22). Not less importantly, CD4 T cells responding to antigens associated with those driving the CD8 T cells are required when inflammatory signals upon immunization or infection are low. In this context, CD4 T cells most likely function by directly providing IL-2 or by properly activating the DCs that are presenting antigen to the CD8 T cells (23, 24). In addition, CD4 T cells are essential for the maintenance and expansion of memory CD8 T cells during secondary immune responses (25-28).

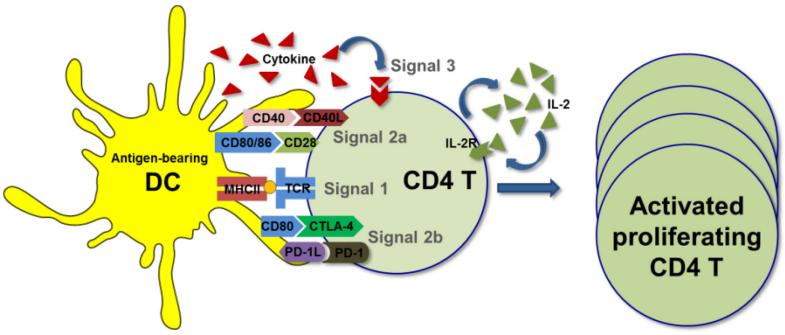

Figure 1.1: Priming of naïve CD4 T cells by DCs and formation of an immunological synapse. The scheme depicts the three signals between a DC and a CD4 T cell leading to T cell activation and subsequent proliferation induced by autocrine IL-2 signaling. Signal 1 comprises binding between the peptide-MHCII complex with the TCR, as shown in the center of the DC-T cell interaction. In the upper part, positive co-stimulatory interactions are shown (Signal 2a), specifically CD80/CD28 and CD40/CD40L, while in the lower part of the DC-T cell interaction, negative co-stimulatory interactions are shown (Signal 2b). Here, PD-L1/PD-1 and CD80/CTLA-4. The integration within the T cell of these two types of interactions will determine the activation state of the T cell. On the upper part of the scheme, cytokine priming (Signal 3),here through IL-12, is indicated. Depending on the combination of cytokines delivered by DC and T cells during their interaction, different types of immune responses result.

1.1.3 Diversity of CD4 effector T cell responses

Activated CD4 T cells can differentiate and be commonly subdivided into five subsets that are characterized by a variety of distinct functions and characteristics: Th1, Th2, Th17, regulatory T cells (Tregs) and T follicular helper cells (Tfh).

Th1 cells are the main effector cells against intracellular pathogens such as bacteria and viruses. They are generated under the direction of IL-12 secreted by the priming DC and the transcription factor T-bet (T-box expressed in T cells, *Tbx21*). T-bet is exclusively found in the lymphoid system and considered the master regulator of Th1 differentiation (29). Naïve T cells do not express T-bet, but once the TCR is stimulated, IFN-γ- STAT1 and IL-12R- STAT4 signaling pathways induce its expression (29-31). Mice lacking expression of T-bet show a severe deficiency in IFN-γ expression in CD4 T cells as well as in antigen-specific CD8 T cells and DCs (32-35). Th1 cells further activate and increase the phagocytic activity of macrophages through IFN-γ signaling (36) and increase the proliferation of cytotoxic T cells (CTLs) (37). Th1 cells are marked by the chemokine receptor CXCR3 that is expressed on effector and memory Th1 cells and is transactivated and regulated by T-bet (29). Furthermore, CXCR3 is important for the migration of antigen-specific CD4T cells out of the T cell zone into the interfollicular site of T cell and DC interactions (38) and for directing activated T cells to inflammatory sites in the periphery (39).

Conversely to Th1 cells, IL-4 and the transcription factor GATA-3 promote a differentiation towards the Th2 lineage that mediates protection against nematodes and contribute to allergic responses through production of the effector cytokines IL-4, IL-5 and IL-13 (34, 40). Furthermore, IL-10 production by Th2 cells efficiently suppresses IL-2

and IFNγ production in T cells and IL-12 production by APCs and thus effectively inhibits a type I response (Th1 response) (41).

IL-17 is the eponym of pro-inflammatory Th17 cells which play an important role in the maintenance of mucosal barrier function by mediating protection against extracellular bacteria and fungi (42). In addition, Th17 cells have been shown to direct the pathogenesis of autoimmune and inflammatory disorders (43, 44). In the presence of IL-6, IL-1β, IL-23, IL-21 and TGF-β, activated CD4 T cells express the retinoic orphan receptor (ROR)γt and differentiate into Th17 cells (45-48).

The counter-part to pro-inflammatory T helper subsets are Treg cells which express the forkhead-winged helix transcription factor Foxp3 and are crucial for tolerance to self-antigens, preventing autoimmune disorders and suppressing pro-inflammatory effector T cells (49-51). Depending on the context of their generation, natural regulatory T cells (nTreg), adaptive (aTreg) or inducible Treg (iTreg) are distinguished.

While the above mentioned effector Th subsets are able to perform their effector function outside of the lymphoid organ, Tfh cells display the major subset providing B cell help for high-affinity antibody responses in germinal centers of lymphoid organs and for memory B cell differentiation (52-54). Tfh cells are associated with constitutive expression of the B cell follicle homing receptor CXCR5, PD-1, inducible T-cell costimulator (ICOS), the transcription factor Bcl-6 and secretion of IL-21 (55-57).

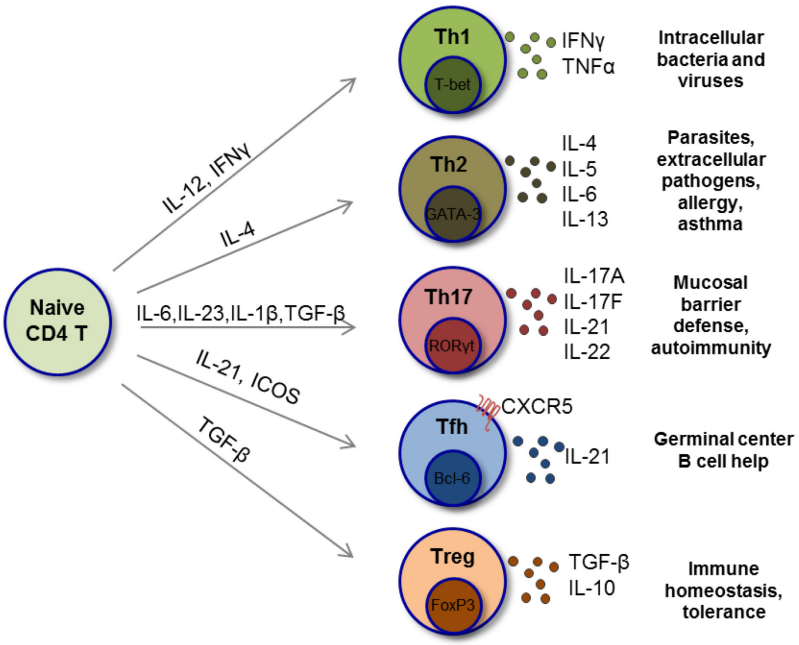

Figure 1.2: Signals in CD4 T cell differentiationpathways, indicating transcription factors and inducing factors such as cytokines or co-stimulatory factors. Adopted from (52).

1.2 Immunological memory

1.2.1 General introduction to immunological memory

In 1796, Edward Jenner observed that milkmaids were protected against smallpox due to their exposure to the pus in the blisters from cowpox. He could not foresee back then, that his discovery would lead to the first global immunization program that ultimately led to the eradication of this severe human infectious disease (58). As the vaccination era moved forward, Louis Pasteur, Robert Koch and Paul Ehrlich contributed greatly by developing inactivated and attenuated agents from highly virulent pathogens that induced immunity (59, 60). Still today, vaccination is considered the most successful medical treatment available. We know now that the most important biological consequence of the adaptive immune system is the formation of protective immunological memory upon infection or vaccination which enables the immune system to respond more rapidly and effectively to a pathogen that has been encountered previously (60). On the contrary, in the context of autoantigens, allergens or persistent pathogens immunological memory greatly contributes to chronic inflammatory disorders and immunopathology (61).

Immunological memory generated after infection or vaccination ultimately leads to a dual inhibitory mechanism to fight off re-encountered pathogens. On the one hand, long-lived plasma cells that develop from B cells continuously provide circulating high-affinity antibodies (humoral immunity). On the other hand, cellular immunity is maintained by persisting T cells that escape from default contraction after the clearance of the pathogen and are able to induce rapid recall responses more efficiently than their naïve counterparts (60) (Figure 1.3). Long-lived plasma cells are established in the bone marrow (BM) where they continuously secrete large amounts of antibodies but rest in terms of proliferation and differentiation in specialized survival niches consisting of CXCL12-secreting stromal cells and APRIL-providing eosinophils (62-69). Interestingly, a substantial population of memory CD8 T cells also resides in the BM in stromal niches providing IL-15 and IL-7 as survival factors and it has been demonstrated that these cells rest in terms of proliferation (70-74).

Historically, the utmost developments in research on immunological memory have occurred in the fields of memory B and CD8 T cells due to the limited range of effector phenotypes, inherent phenotypic conformity between primary and secondary effector cells and the relatively restricted immunological field of activity of these cells (75, 76). Whereas antibody-secreting plasma cells mostly target extracellular pathogens, cyto-

toxic CD8 T cells are particularly specialized in killing the body's own cells infected with pathogens. In contrast, CD4 T cell memory has been more difficult to study owed to multiple distinct CD4 T cell effector lineages and functions, less proliferative capacity and limited evidence for memory cells and secondary effector responses (76, 77). A recent tactic to shed more light on CD4 T cell memory involves compartmentalized approaches by restraining studies to comparable or overlapping phenotypes (76, 78). However, the better studied CD8 T cell memory largely provides the outline for studies on CD4 T cell memory.

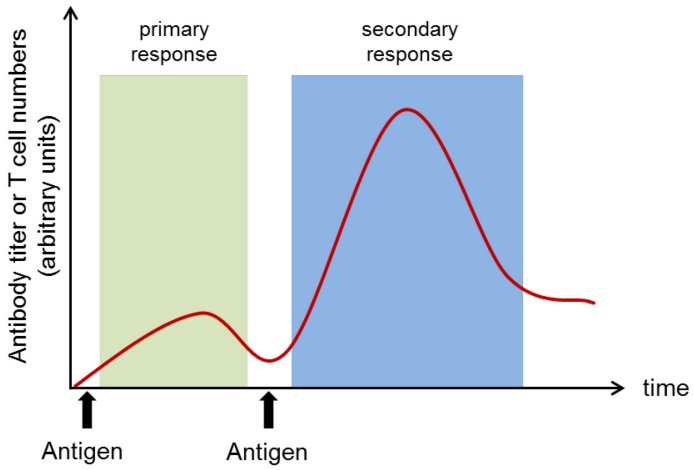

Figure 1.3: One of the key features of the adaptive immune response is the formation of immune memory. Upon infection or vaccination, B and T cells get activated, differentiate and expand upon first encounter with the antigen. During the contraction phase of the primary immune response the majority of effector cells undergo apoptosis, while a small proportion of clones will differentiate into memory cells and survive in specialezed compartments and niches of the body. Memory cells remain in the body for years (or even a lifetime). Upon second encounter with the antigen, the memory cells react faster, more efficient and vigorously than during the primary immune response.

1.2.2 Subsets and compartmentalization of memory CD4 T cells

After the clearance of the pathogen the majority of activated CD4 T cells undergo apoptosis, leaving behind a minor population that is broadly heterogeneous and conventionally divided into distinct subsets based on their expression of surface molecules, which ultimately define their localization in the body as well as their cytokine susceptibility and cytokine secretion potential. Memory CD4 T cells are maintained in the absence of antigen by survival signals and homeostatic proliferation (79-82).

Historically, memory CD4 T cells have been divided into central memory CD4 T cells (T_{CM}) and effector memory CD4 T cells (T_{EM}) based on the ability or inability to provide immediate effector function and the distinct expression of homing receptors that enables cells to re-enter SLO or migrate to non-lymphoid tissues (83). T_{CM} are defined by their expression of the chemokine receptor CCR7 and the L-selectin adhesion molecule (CD62L), both of which are also expressed on naïve T cells and required for cell

extravasation through high endothelial venules (HEV) and migration to periarteriolar sheaths (PALS, also named T cell zone) of SLOs (84, 85). Genetic CCR7 deficiency leads to an expanded accumulation of T cells in the blood, the red pulp of the spleen and the BM whereas LN and splenic PALS are devoid of naïve T cells (85). Just like naïve CD4 T cells, T_{CM} cells re-circulate between SLOs, lymph and blood. In comparison to their naïve counterparts however, T_{CM} are more sensitive to antigenic stimulation and provide more efficient help to B cells due to high CD40L expression.

T_{EM} are predominantly found in peripheral tissues allowing them to provide immediate protection upon re-infection. Notably, T_{EM} cells do not express CCR7 and CD62L and display a diverse set of chemokine receptors and adhesion molecules that enables their homing to inflamed tissues (83, 86). In addition, T_{EM} rapidly secrete effector cytokines upon re-stimulation when compared to T_{CM}. It has further been suggested that T_{CM} can replenish the T_{EM} population whereas the type and site of infection (systemic or local) define the relative role of either subset during secondary responses (87).

The classical paradigm of memory CD4 T cell division into T_{CM} and T_{EM} has recently been challenged by emerging evidence of CD4 T cell memory in epithelial barrier tissues such as the gut, skin, respiratory- and reproductive tract (88). These cells have been entitled tissue resident memory T cells (T_{RM}) and are constitutively poised to rapidly respond to local pathogen re-encounter. Whereas T_{EM} are able to recirculate between certain non-lymphoid tissues, lymph and blood, T_{RM} exclusively persist within one compartment without recirculating (89). T_{RM} cells are characterized by high expression of CD69 and reduced expression of CD62L and the transcription factors Klf2 and Eomes. T_{RM} cells localized to epithelial layers of intestine and skin additionally express $\alpha_E\beta_7$ (CD103) that is induced upon exposure to local TGFβ (90).

In addition to T_{CM}, T_{EM} and T_{RM}, the existence of memory Tfh cells has recently also been postulated and characterized by their ability to rapidly provide help to memory B cells in SLOs (78, 91-95).

The BM has been well-known to host long-lived plasma cells and memory CD8 T cells. Recent evidence demonstrated that in mice, a substantial proportion of activated CD4 T cells characterized as $CD44^{hi}CD62L^{lo}CCR7^{-}$ cells preferentially migrate into the BM during primary immune responses (96). In the BM, memory CD4 T cells reside and rest in specialized survival niches composed of IL-7 secreting VCAM-1^{+} Collagen-XI^{+} stromal cells (96-101). During the memory phase of an immune response against LCMV-peptide GP_{61-80}, about 90% of previously adoptively transferred antigen-specific CD4 T cells re-locate to the BM (96). BM memory CD4 T cells highly express Ly-6C, CD69

and Integrin α2 (CD49b), the latter enabling activated cells the homing to their niche in the BM (96-99).

Murine BM memory CD4 T cells are characterized by a Th1 phenotype (96). Interestingly, the repertoire of human BM memory CD4 T cells is considerably enriched for systemic pathogens such as cytomegalovirus (pp65), tetanus toxoid, measles, mumps and rubella when compared to memory T cells of peripheral blood (102, 103). Another study further reported that in rats, IL-5 secreting CD4 T cells migrate from airway to the BM after antigen inhalation (104).

BM memory CD4 T cells induce a more rapid and efficient secondary response than their splenic counterpart in terms of cytokine production and upregulation of co-stimulatory molecules This suggests that BM memory CD4 T cells rapidly migrate into SLOs upon re-exposure to antigen to provide B cell help and promote a high-affinity antibody response (96).

1.3 Generation of memory CD4 T cells

While the vast majority of activated CD4 T cells undergo apoptosis after clearance of the pathogen, a small proportion survives the contraction phase and differentiates into long-lived memory cells. However, it still remains enigmatic which cells within the pool of antigen-specific activated CD4 T cells possess the potential to differentiate into different types of memory CD4 T cells and which are the cellular and molecular cues leading to memory formation. The classical paradigm that offers the basis for the study of memory CD4 T cell generation provides the T cell response. Early investigations particularly focused on the Th1 and Th2 paradigm to understand memory formation. Further research in the field identified the multiple effector lineages with different migration and cytokine patterns that bedeviled a simplified model to explain CD4 T cell memory formation. To date, no unifying model exists, that takes the diverse complexity of memory CD4 T cell generation into account (105). However, the different models discussed in the field have generally in common that effector CD4 T cells that overcome the contraction phase require a shift from a phenotypically and functionally active to an inactive but functionally alert state (76).

1.3.1 Factors governing memory CD4 T cell generation

1.3.1.1 Frequency of antigen-specific naïve CD4 T cells

The frequency of antigen-specific naïve CD4 T cells directly affects the primary immune response and hence the quantities of cells that ultimately populate the memory pool (106). Even though endogenous naïve CD4 T cell numbers differ according to their pathogen-specificity, studies using T cell libraries found approximately 100 antigen-specific naïve CD4 T cells per mouse spleen (107, 108). However, these naïve cells differ greatly in their “fitness” and not all naïve antigen specific CD4 T cells are later represented in the memory pool indicating that diversity in TCR signaling and antigen load play a decisive role for memory formation (109). In addition, an increasing frequency in antigen-specific naïve CD4 T cells has been shown to foster interclonal competition for TCR-p:MHCII signaling which in turn may lead to skewing of primary and secondary CD4 T cell responses (76, 110).

1.3.1.2 Quality and duration of TCR-p:MHCII interaction

The availability and amount of antigen presented to the TCR via p:MHCII molecule on DCs, the TCR affinity for the antigen and the duration of the cognate interaction determine the quality of TCR signaling (76, 111, 112). Numerous naïve clones with unique

TCRs are engaged upon antigen challenge. The TCR signal strength threshold required for memory formation had generally been assumed to be intermediate to robust, whereas too strong signaling merely led to terminal differentiated effector cells prone to death (113). In line with this hypothesis, some studies suggested that only high functional avidity clones are able to transit from effector to memory stage (114-116). By contrast, in the context of infection or lymphopenia, memory cells even developed from very low affinity clones indicating that functional binding avidity of the TCR is not exclusively responsible for positive memory selection (117-121). Increasingly convincing evidence suggests that complete CD4 T cell priming, maximal proliferation and subsequent memory formation depend on prolonged and sustained TCR-p:MHCII signaling and that an optimal cognate interaction even ensues over several days (122). In line with these findings, in particular TCR clones that displayed a slow dissociation rate between the TCR and p:MHCII on DCs have been shown to preferentially populate the memory pool supporting the importance of sustained cognate TCR-p:MHCII interactions for memory formation (123).

1.3.1.3 Co-stimulation and IL-2 signaling milieu

Complete CD4 T cell priming requires co-stimulatory signals and a suitable cytokine environment in addition to adequate TCR signaling. Whereas newly expressed CD40L by CD4 T cells is critical for priming and clonal expansion of activated CD4 T cells (15), pre-formed CD40L has been shown to be internalized and stored in memory CD4 T cells enabling them to rapidly mount a secondary response upon antigen re-challenge (124). In addition, CD80/86 expression on antigen-loaded DCs lowers the threshold sensitivity to TCR- p:MHCII signaling by binding to CD28 expressed on the activated CD4 T cells, thus fostering maximal clonal expansion and in turn memory formation (125). Furthermore, the lower activation threshold induced by CD28 prompts transcription of IL-2 and apoptotic inhibitors such as Bcl-XL which in turn leads to enhanced proliferation and survival (126).

IL-2 primarily functions as T cell growth factor. Through induction of cell cycle entry and reinforcement of TCR signals, IL-2 influences the CD4 T cell lineage outcome and mediates survival signals during default contraction (76). In addition, IL-2 is expressed in high quantities in Th1 favouring conditions upon activation and IL-2 signaling during priming is critical for CD4 and CD8 T cell memory formation (23, 127-130). Furthermore, late IL-2 signaling has been described to mediate survival through downregulation of apoptotic pathways in effector T cells and by inducing IL-7 receptor expression (127, 130). In contrast, IL-2 signaling during priming of CD8 T cells may also lead to terminal differentiation and hence activation-induced cell death (AICD) (131). Notably,

opposing signals from the Bcl-6 transcription factor and the IL-2R have been demonstrated to generate Th1 central and effector memory cells, respectively (93). However, even though Tfh-like cells may populate the central memory pool (78, 93), the Th1 effector pool also gives rise to memory cells, indicating that the cells are not terminally differentiated (78, 132). Furthermore, *in vitro* addition of IL-2 and TGF-β was shown to rescue activated effector CD4 T cells from programmed apoptosis (133) and late cognate TCR-p:MHCII interactions induced autocrine IL-2 signaling which mediated the effector to memory transition in an influenza infection model (127).

1.3.1.4 The role of B cells for memory CD4 T cell formation

B cells are potent APCs and nearly as effective as DCs in presenting antigen (134). However, DCs are exclusively capable of priming naïve CD4 T cells in the PALS of the spleen whereas B cells are essential for the generation of Tfh cells in germinal centers (52). Much effort has been made to investigate the role of B cells for the establishment of splenic CD4 T cell memory by studying the expansion and maintenance of antigen-specific CD4 T cells from B cell-depleted or -deficient mice (135-139). Interestingly, other evidence revealed that long-term T cell memory may be influenced through persisting immunogenic complexes composed of secreted antibody (Ab) bound to antigen on follicular dendritic cells (FDC) (140, 141), while an immune complex independent formation and preservation of CD4 T cell memory by B cells has been postulated as well (139). During a model of acute LCMV infection, B cell deficiency doubled the rate of Th1 cell contraction which in turn led to a drastic reduction of memory CD4 T cells despite an initially normal expansion phase and antigen-independent B cell signaling (139). Another study showed that B cell depleted mice were able to generate primary virus-specific Th1 cells, whereas T-bet$^+$ memory precursors were reduced which eventually caused a decrease in memory cell numbers (136). Similar findings indicating that B cells are important for splenic memory CD4 T cell formation were reported, even though the exact underlying mechanism remains elusive (137, 138).

1.3.2 Hypothetical models of memory CD4 T cell generation

1.3.2.1 Linear differentiation model

The rather simplified linear differentiation model states that naïve CD4 T cells get activated upon antigen encounter which leads to proliferation and differentiation into effector cells of which some survive a default contraction phase and become long-lived memory cells (Figure 1.4 A). At the same time, this concept suggests that the generated memory cells retain their primary effector phenotype upon antigen re-encounter,

which has been convincingly demonstrated in experiments using IFN-γ reporter mice (132) or in Th1 and Th2 adoptive transfer experiments (142).

1.3.2.2 The decreasing potential/progressive differentiation model

The decreasing potential/progressive differentiation model uses the linear differentiation model as a basic outline but includes the strength and duration of TCR signaling and takes the role of co-stimulatory signals upon primary activation into account (76, 105). The model suggests that effector T cell functions gradually diminish as a consequence of persisting antigenic stimulation. Thus, the ability of the effector cell pool to provide for the memory pool is progressively restricted in proportion to increasing signaling (76). Studies focussing on this model particularly suggest that only cells of intermediate differentiation status are capable of receiving and responding to memory survival signals whereas terminally differentiated effector cells are inevitably committed to apoptosis (116). Furthermore, the model suggests that the existence of T_{CM} and T_{EM} cells may be a consequence of this progressive differentiation model (143). Others have suggested that the duration of antigen-exposure determines the differentiation state of memory precursors. While short antigen exposure preferentially led to $CD62L^{hi}$ T_{CM} cells, a prolonged antigen exposure favourably yielded $CD62L^{lo}$ T_{EM} cells (144).

1.3.2.3 Divergent differentiation/disparate fate model

The divergent differentiation/ disparate fate model suggests that the two daughter cells of a naïve CD4 T cell possess heterogeneous capacities to become either an effector or a memory cell, a decision that could be passive or educational. The model proposes that an activated CD4 T cells disproportionately distributes factors between the two daughter cells that are either decisive for survival and differentiation into a memory cell or equip the cell with an increased effector function and hence terminal differentiation (76, 105). Notably however, this model neglects an involvement of duration of antigen exposure for memory formation. Studies analyzing asymmetric cell division with regards to effector and memory formation provide convincing evidence on how multiple phenotypes arise from a single antigen-specific activated CD4 T cell (145-147). Further evidence on the directive role of asymmetric cell division for divergent differentiation was provided by Choi et al., who demonstrated that multiple repetitions of this event during the expansion phase are decisive for the simultaneous formation of $Bcl\text{-}6^{+}$ Tfh and $Blimp\text{-}1^{+}$ Th1 effector lineages (148). This further suggests that asymmetric cell division may be an adequate model to explain the generation of some types of memory cells (76, 78). However; further research on the effect of asymmetric cell division of CD4 T cells for the formation of memory CD4 T cells is necessary.

1.3.2.4 B cell-influenced/ Sustained TCR-p:MHCII interaction model

The B cell-influenced /sustained cognate TCR-p:MHCII interaction model combines two different aspects that have been reported to affect memory CD4 T cell formation and are described in section 1.3.1.2 and 1.3.1.4.

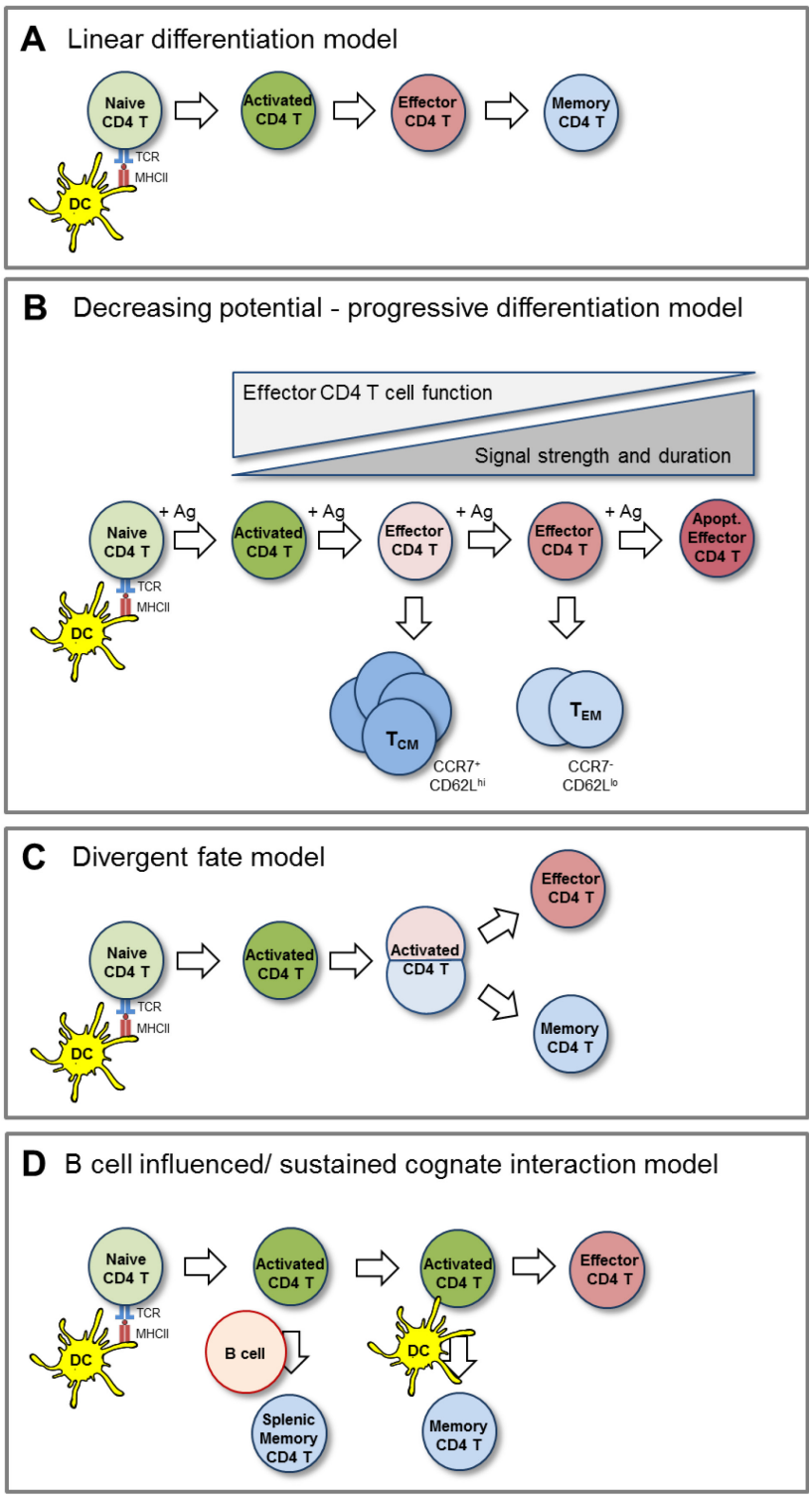

Figure 1.4: Hypothetical models of memory CD4 T cell generation. **A:** Linear differentiation model. **B:** Decreasing potential/ progressive differentiation model. **C:** Divergent fate model. **D:** B cell influenced /sustained TCR:pMHCII interaction model

1.4 BM memory CD4 T cell- specific markers

1.4.1 Ly-6C

Ly-6C is a member of the Ly-6 superfamily of GPI-anchored cell surface glycoproteins and is expressed by plasma cells, subsets of myeloid cells and subsets of T cells in mice, but not in humans. Although its function and regulation is still poorly defined, Ly-6C acts as a co-stimulatory molecule for T cells (149). Moreover, Ly-6C has been proposed as a marker of memory CD8 T cells (150) and has been shown to support homing of CD8 T_{CM} cells into lymph nodes, but also to mark $CD44^{hi}$ CD8 T in the BM of Balb/c mice (151). Importantly, Ly-6C particularly discriminates resting BM memory CD4 T cells from other memory phenotype $CD44^{hi}CD62L^{lo}$ CD4 T cells of unknown etiology, antigen-specificity and function as 80 % of all Ly-$6C^{hi}$ $CD44^{hi}CD62L^{lo}$ CD4 T were found to be resident in the BM (96). In the BM, all $CD44^{hi}CD62L^{lo}$ CD4 T cells express Ly-6C, even though about 40 % of cells express Ly-6C highly and 60 % at an intermediate level. Upon antigen re-challenge, Ly-$6C^{hi}$ memory CD4 T cells of the BM rapidly secrete cytokines and CD40L and thus efficiently provide help to B cells for affinity maturation (96). In the spleen of unchallenged WT mice, merely 5 % of memory phenotype $CD44^{hi}CD62L^{lo}$ CD4 T cells were found to express Ly-6C (96). However, recent evidence by Marshall et al. also suggested that a differential expression of Ly-6C and T-bet distinguishes splenic effector and memory Th1 cells in an LCMV infection model and particularly splenic Ly-$6C^{lo}$T-bet^{int} CD4 T cells displayed greater longevity and populated the splenic memory pool (152).

1.4.2 CD69

Until recently, the type II C-lectin receptor CD69 has mostly been regarded as an activation marker, since T cells express CD69 rapidly upon stimulation of the TCR (153, 154). However, emerging evidence has been published in the last years implying a prominent role for CD69 as a retention molecule for both, CD8 and CD4 T_{RM} cells (88) and a major population of BM resident memory CD8 T cells highly expresses CD69 (73). In line with the role of CD69 as a retention molecule for TRM cells, the formation of resting BM memory CD4 T cells has been shown to be impaired for antigen-specific CD4 T cells lacking CD69 expression and in turn leading to a defective secondary response (97, 99). Notably, it is well established that lymphocytes upregulate expression of sphingosine 1-phosphate receptor-1 (S1P1) to sense S1P gradients in lymph, blood and tissues, thereby governing egress from lymphoid tissues (155). The transcription

factor Krüppel-like factor 2 (Klf2) drives the expression of S1P1 (156) and retention and establishment of CD8 T_{RM} in different tissues has been observed upon downregulation of Klf2 and S1P1 (157). Importantly, CD69 can physically interact with S1P1 after exposure to IFNα/β leading to S1P1 internalization and degradation and consequently blocked S1P-mediated lymphocyte egress from lymphoid structures (158-160). Accordingly, inhibition or deficiency in CD69 may be expected to increase lymphocyte egress from SLOs into the periphery, but increased cell numbers in peripheral blood were not observed in adoptively transferred antigen-specific $CD69^{-/-}$ CD4 T cells at various time points after immunization (97) leaving room for further investigations on the role of CD69 for memory CD4 T cell establishment in the BM.

1.4.3 CD49b

CD4 and CD8 T cells express CD49b after antigenic stimulation, which entitles CD49b to be called a T cell activation marker (161). In addition, CD49b has been described as a general marker of memory CD4 T cells, as about 50 % of CD4 T cells harboring the memory pool maintained long-term CD49b expression (162). CD49b is also named integrin-α2 and forms the very-late activation antigen (VLA-2) in conjunction with CD29 (also named integrin-β1). CD49b is involved in cell adhesion owed to its function as collagen receptor (98, 163) and VLA-2 selectively binds collagen I, II and XI (164, 165). CD49b expression is greatly enriched in memory phenotype $CD44^{hi}$ and antigen-specific memory CD4 T cells of the BM and blocking CD49b by injection of non-depleting CD49b antibodies or genetic deletion of CD49b in CD4 T cells impairs the accumulation of antigen-experienced CD4 T cells in the BM (96, 98). CD49b controls the establishment of BM CD4 T cell memory by modulating the trans-migration of activated CD4 T cells into the BM via sinusoids and subsequent interaction with collagen-expressing stromal cells (98), indicating that activated $CD49b^{+}$ CD4 T cells possess BM tropism and that CD49b is required for the migration to their survival niche. Moreover, CD49b expression on memory CD4 T cells identifies cells with an increased ability to produce IL-2 and TNF-α upon *in vitro* stimulation (162). Interestingly, also β_1-integrin (CD29), the β-subunit of VLA-2, is critical for the retention of antigen-specific CD4 T cells in the BM (166).

1.5 Thesis objectives

Memory CD4 T cells of the BM are generated from antigen-experienced CD4 T cells in SLOs during the primary immune response during which they have been empowered to overcoming the contraction phase and survive in the absence of antigen in stromal niches that provide survival signals (96, 103). Some activated CD4 T cells migrate into the BM in CD69- and CD49b- dependent manners and BM memory CD4 T cells highly express Ly-6C. However, it remains elusive how BM memory CD4 T cells are generated during a primary immune response in SLOs, how the splenic precursors may be identified within the pool of activated CD4 T cells and which are the cellular and molecular cues leading to their generation and instructing them to migrate towards the BM.

The first part of this thesis aims at identifying the phenotype of splenic precursors of BM memory CD4 T cells within the pool of polyfunctional memory phenotype (MP) CD4 T cells and antigen-specific TCR transgenic CD4 T cells. Since the expression of CD49b, CD69 and Ly-6C has been previously described to mark or modulate the generation of BM memory CD4 T cells, these molecules set the ground for the identification of splenic precursors of BM memory CD4 T cells. In long-lasting immune reactions provoked by virus or persisting antigen/adjuvant combinations such as aluminum hydroxide or Freund's adjuvant, memory phenotype $CD44^{hi}CD62L^{lo}$ CD4 T cells also persist in the SLOs for extended time periods (167, 168). Cognate peptide immunizations in combination with LPS or Monophosphoryl lipid A as adjuvant however, induce a directed, but time limited and not persisting immune reaction leading to a vast reduction of activated CD4 T cells in SLOs within one week after transfer and immunization (96, 169). Thus, to track the generation of precursors of BM memory CD4 T cells in the spleen, adoptive TCR-transgenic CD4 T cell transfer and cognate peptide plus LPS immunizations were applied. Following the identification of precursors of BM memory CD4 T cells within the pool of splenic activated CD4 T cells, the second part of the thesis aims at elucidating the characteristics and requirements of their generation during priming and activation with a particular focus on their proliferative capacities in combination with cellular localization during the activation process. Since B cells have been previously described to modulate splenic memory CD4 T cell formation, the third part of this thesis aims at investigating whether B cells are also involved in the establishment of resting CD4 T cell memory in the BM. By using B cell-depleted or B cell-deficient mice in combination with an adoptive CD4 T cell transfer and immunization model, the role of B cells for the accumulation of antigen-specific precursors of BM memory CD4 T cells is examined.

2 Materials and Methods

2.1 Materials

2.1.1 Chemicals and reagents

Chemical or reagent	Providing company
Anti-mouse CD3 T-cell Activation Plate (pre-coated)	BD BioCoat, USA
Azide	Life Technologies, USA
Anti-Biotin MicroBeads	Miltenyi Biotec, Germany
Anti-FITC MicroBeads	Miltenyi Biotec, Germany
Anti-Thy1.2 MicroBeads	Miltenyi Biotec, Germany
Streptavidin MicroBeads	Miltenyi Biotec, Germany
Anti-CD4 MicroBeads (clone L3T4) for naive CD4 T cell sorting for *in vitro* culture	Miltenyi Biotec, Germany
Anti-CD4-Fab antibody (clone YTS19.1) for naïve CD4 T cell sorting	DRFZ, Germany
Anti-CD4- FITC antibody (clone GK1.5) for B cell sorting	DRFZ, Germany
Anti-CD8a- FITC antibody (clone 53-6.7) for B cell sorting	DRFZ, Germany
Anti-Mac-1 FITC antibody (clone M1/70.15.11) for B cell sorting	DRFZ, Germany
Anti-B220-Biotin (clone RA3.6B2) for activated CD4 T cell sorting	DRFZ, Germany
Anti-CD8a-Biotin (clone 53-6.72) for activated CD4 T cell sorting	DRFZ, Germany
Anti-MHCII-Biotin (clone M5/114) for activated CD4 T cell sorting	DRFZ, Germany
Anti-IgD (clone 11.26c) for B cell depletion	DRFZ, Germany
Isotype control (clone 1d10) for B cell depletion	DRFZ, Germany
Mouse anti-rat IgG antibody (clone MAR18.5) for B cell depletion	DRFZ, Germany
Bovine Serum Albumin (BSA)	Pan Biotech, Germany
Bromodeoxyuridine (BrdU)	Sigma-Aldrich, Germany
β-Mercaptoethanol	Sigma-Aldrich, Germany
Carboxyfluorescein succinimidyl ester (CFSE)	BioLegend, USA
Cyclophosphamide	Sigma-Aldrich, Germany

InVivoMAb recombinant CTLA-4-Ig	Hölzel Biotech, Germany
DMSO	Sigma-Aldrich, Germany
DNAse	Sigma-Aldrich, Germany
EDTA	Roth, Germany
Fetal Calf Serum (FCS)	Sigma-Aldrich, Germany
Fluorescent Mounting medium	DAKO Cytomation, Denmark
Formaldehyde 37 %	Merck, Germany
n-Hexan	Sigma-Aldrich, Germany
IgG from human serum	Sigma-Aldrich, Germany
Imject® Alum	Thermo Scientific, USA
LCMV-peptide gp61-80	Genecust, Luxembourg
Lipopolysaccharide (O111:B4 ; LPS)	Sigma-Aldrich, Germany
Na_2HPO_4	Riedel-de-Haen, Germany
NaCl	Roth, Germany
NaH_2PO_4	Sigma-Aldrich, Germany
NH_4Cl	Sigma-Aldrich, Germany
Endograde Ovalbumin (OVA)	Hyglos GmbH, Germany
Para-formaldeyde 4%	Roth, Germany
Penecilline- Streptomycine	Life Technologies, USA
Propidium iodide	Merck, Germany
RPMI 1640 + GlutaMAX™-I	Life Technologies, USA
Sucrose	Roth, Germany
Trypan-blue	Sigma-Aldrich, Germany
Türk's solution	Merck, Germany

Table 1: Chemicals and reagents

2.1.2 Buffers, media, solutions and kits

Buffer/ media/solution	**Recipe/ providing company**
PBS buffer (pH 7.2- 7.4)	2.7 mM KCl, 1.5 mM KH_2PO_4, 137 mM NaCl, 8.1 mM Na_2HPO_4
PBS/ BSA buffer	5 g/L BSA in PBS
PBS/BSA/EDTA buffer	2 mM EDTA in PBS/BSA buffer
PBS/BSA/Azide (FACS buffer)	PBS/0.1 % BSA, 0.01 % Sodium azide
RBC lysis buffer (pH 7.2)	155 mM NH_4Cl, 10 mM $KHCO_3$, 0.1 mM EDTA, 1000 ml H_2O dest.
RPMI medium	Rosewell Park Memorial Institute medium 1640 + Gluta-Max™-I (2mM L-Glutamine), 10 % FCS, 1 % Pen/Strep, 1 % β-Mercaptoethanol
IHC Staining buffer	PBS, 5 % FCS

30 % Sucrose	PBS, 30 % sucrose, 0.01 % Azide
Cell fixation buffer	PBS, 2 % Formaldehyde
IHC fixation buffer	PBS, 4 % Para-formaldehyde
SCEM embedding media for frozen samples	SECTION-LAB Co, Japan
Perm/Wash Buffer for intracellular cytokine staining	10x Perm/Wash buffer (BD Biosciences) diluted to 1x Perm/Wash buffer wqith H_2O dest.
FoxP3 staining buffer kit for intranuclear T-bet or Ki-67 staining	eBioscience, Life Technologies, USA
Mouse naïve CD4 T cell isolation kit (MOJO kit)	BioLegend, USA
MOJO buffer	PBS, 0.5 % BSA, 2mM EDTA
BrdU staining buffer kit	BioLegend, USA
Trypan Blue solution	0.4 % Stock (Sigma-Aldrich) 1:4 diluted in PBS
Türks solution	1:20 dilution for blood leukocyte count

Table 2: Buffers, media, solutions and kits

2.1.3 Laboratory equipment

Equipment	Providing company
AkkuBlock	Labnet International Inc., USA
BD FACS Aria	Beckton Dickinson, USA
BD Canto II	Beckton Dickinson, USA
BD LSRII	Beckton Dickinson, USA
BD Fortessa	Beckton Dickinson, USA
Fridge 4°C, - 20°C	Liebherr, Germany
Freezer -80°C	Thermo Fisher Scientific Inc., USA
Heraeus Fresco 21	Thermo Fisher Scientific Inc., USA
Heraeus Fresco 17	Thermo Fisher Scientific Inc., USA
Incubator HeraCell 2401, 37°C, %% CO_2	Thermo Fisher Scientific Inc., USA
Inverted light microscope Hund	Helmut-Hund GmbH, Germany
Labofuge 400R	Thermo Fisher Scientific Inc., USA
Laminar flow workbench HeraSafe KS	Thermo Fisher Scientific Inc., USA
LS magnetic cell separation column	Miltenyi Biotec, Germany
LSM 710 confocal microscope	Carl Zeiss MicroImaging, Germany
MOJO magnet	BioLegend, USA
Microm HM560 Cryostar	Thermo Fisher Scientific Inc., USA
Multifuge X3R	Thermo Fisher Scientific Inc., USA
Nanodrop 2000	Thermo Fisher Scientific Inc., USA
QuadroMACS magnet	Miltenyi Biotec, Germany

Vortex Mixer	Neolab, Germany
Waterbath	Memmert, Germany

Table 3: Laboratory equipment

2.1.4 Software

Software	Providing company
Adobe© InDesign©	Adobe Systems, Ireland
FlowJo V10	FlowJo, LLC (since 2017 BD Biosciences), USA
Diva Sofware	BD Biosciences, USA
Mendeley Reference Management	Mendeley Ltd, USA
GraphPadPrism 8.0.2	GraphPad Software Inc., USA
Image Lab	Bio-Rad Laboratories GmbH, Germany
MACSQuantify	Miltenyi Biotec, Germany
Microsoft Office	Microsoft Inc., USA
Zen 2012	Carl Zeiss MicroImaging, Germany

Table 4: Software

2.1.5 Antibodies used for flow cytometry and IHC

Antibody	Clone	Providing company
Arm. Hamster IgG	HTK888	BioLegend
B220	RA3.6B2/ REA755	BioLegend, Miltenyi Biotec
Bcl-6	K112-91	BD Biosciences
BrdU	BU20A	BioLegend
CD11b (Mac-1)	M1/70.15.11	DRFZ
CD11c	N418	DRFZ, BioLegend
CD122 (IL-2Rb)	TM-b1	Miltenyi Biotec
CD19	1D3	DRFZ
CD197 (CCR7)	4B12	BioLegend
CD127	A7R 34	BioLegend
CD25	3C7	DRFZ
CD279 (PD-1)	29F.1A12	BioLegend
CD3	145-2C11	BioLegend
CD4	GK1.5	DRFZ
CD4	RM4-5	BioLegend
CD4	YTS19.1	DRFZ
CD4	RM4-5	BioLegend

CD44	IM7	BioLegend
CD45	30-F11	BioLegend
CD49b	HMa2	BioLegend
CD62L	MEL-14	BioLegend
CD69	H1.2F3	eBiosciences, DRFZ
CD8a	53-6.7	BioLegend
CD8	RA3.6B2	DRFZ
CD90.1 (Thy1.1)	HIS51	BioLegend
CD90.1 (Thy1.1)	Ox-7	DRFZ
CD90.2 (Thy1.2)	20-H12	BioLegend
CXCR3	REA724	Miltenyi Biotec
CXCR3	CXCR3-173	Miltenyi Biotec
CXCR5 (CD185)	SPRCL5	BioLegend
CXCR5 (CD185)	L138D7	BioLegend
DO11.10 (OVA-TCR)	KJ1.26	BioLegend, DRFZ
Donkey anti-Rabbit IgG	Polyclonal 40-46	BioLegend
IL-2	JES6-5H4	Miltenyi Biotec
Ki-67	RTK2758	Miltenyi Biotec
Ly-6C	HK1.4	BioLegend
MHCII (I-A/I-E)	M5/114.15.2	BioLegend
Mouse IgG1, κ	MOPC-21	BioLegend
Mouse IgG2a, κ	G155-178, MOPC-173	BioLegend, DRFZ
NK1.1	PK136	Miltenyi Biotec
NKp46	29A1.4	BioLegend, DRFZ
Rat IgG1, κ	RTK2071	BioLegend
Rat IgG2b, κ	RTK4530	BioLegend
Rat IgG2a,κ	RTK2758	BioLegend
RBC	Ter119	DRFZ
Streptavidin	-	BioLegend
T-bet	4B10	BioLegend
TCRVa2	B20.1	BioLegend
TCRVb2	B20.6	BioLegend

Table 5: Antibodies used for flow cytometry and IHC

2.2 Methods

2.2.1 Mice

All mice were housed under specific pathogen-free conditions and used at 6-16 weeks of age. All mouse experiments were performed in accordance with the German Law for Animal Protection and with permission from the local veterinary offices, and in compliance with the guidelines of the Institutional Animal Care and Use Committee. Mice strains are listed in table 6.

Mouse strain	Function	Origin
C57BL/6	WT recipient	Charles River, Germany
Balb/c	WT recipient	Charles River, Germany
T-bet$^{-/-}$	Ubiquitously lacking T-bet expression	(29), In-house bred (DRFZ)
DO11.10	OVA-TCR Tg, express TCR specific for Ovalbumin	(170), In-house bred (DRFZ)
DO11.10x T-bet$^{-/-}$	OVA-specific CD4 T cells lack expression of T-bet	In-house bred (DRFZ)
SMARTAx PL	LCMV-TCR Tg (SMARTA), express TCR specific for lymphocytic choriomeningitis virus (LCMV)-epitope gp61-80, crossed to PL (Thy1.1^{+}) mice	(171) In-house bred (DRFZ)
SMARTAx T-bet ZsGreen	LCMV-TCR Tg (SMARTA) crossed to T-bet ZsGreen reporter mice	T-betZsGreen: (172), In-house bred (DRFZ)
Rag-1$^{-/-}$	Deficiency in the V(D)J recombination activation gene Rag-1 leads to lack of mature B and T cells	(173), In-house bred (DRFZ)
SCID	Spontaneous Prkdc scid mutation leads to deficiency of functional B and T cells	Charles River, Germany

Table 6: Mouse strains and their origin

For immunizations, mice were injected intraperitoneally (i.p.) with antigen plus adjuvant in PBS in a total volume of 200 µl. Antigens and adjuvants are listed in table 7.

Molecule	Antigen or Adjuvant	Origin
LCMV-peptide gp-61-80	antigen	Genecust, Luxemburg
Endograde Ovalbumin (OVA)	antigen	Hyglos GmbH, Germany
Lipopolysaccharide (O111:B4 ; LPS)	adjuvant	Sigma-Aldrich, Germany
Imject® Alum	adjuvant	Thermo Scientific, USA

Table 7: Antigens and adjuvants used for immunizations

2.2.2 Naïve CD4 T cell sorting

For positive sorting of splenic antigen-specific CD4 T cells in figures 3.1.5- 6 and 3.1.8-9, the Fab fragments of anti-CD4 antibody and Streptavidin MicroBeads (Miltenyi Biotec) were used. Briefly, splenocytes were treated with 1 ml RBC lysis buffer for 1.5 min, washed, centrifuged and the pellet resuspended in 3 ml PBS/BSA/Azide (FACS buffer) containing anti-CD4-Fab-Biotin antibody (dilution 1:100, clone YTS19.1, DRFZ) and incubated for 20 min on ice. After washing with 7 ml of FACS buffer, cells were centrifuged at 300 x g for 5 min at 4°C and the supernatant discarded. The pellet was resuspended in 900 µl FACS buffer and 100 µl of streptavidin MicroBeads (MACS Miltenyi Biotec) added and the suspension incubated for 15 min at 4°C. Cells were washed with 9 ml of FACS buffer, centrifuged and the pellet resuspended in 1 ml FACS buffer. For MACS positive sorting of anti-CD4 labeled cells, a LS column (Miltenyi Biotec) was equilibrated with 3 ml FACS buffer and the cell suspension loaded onto the column. After washing 3 times with 3 ml of FACS buffer, the negative fraction was discarded (unlabeled cell fraction) and the column removed from the magnet. 5 ml of FACS buffer were applied to the column and cells flushed out (positive magnetically labeled CD4 T cell fraction). Cells were centrifuged and re-suspended in ice-cold PBS and the cell number adjusted to 0.5- 1x10^6 cells in 200 µl PBS and cells transferred intravenously (i.v.).

For figures 3.1.10-12, 3.2.1- 7 and 3.3.1-3, naïve antigen-specific CD4 T cells were negatively sorted with the Mojo cell sorting kit (BioLegend) according to the manufacturer's protocol. Briefly, a single cell suspension of splenocytes (no RBC lysis) was incubated with a biotinylated antibody mix for 15 min on ice in the dark. Without washing, Streptavidin coupled magnetic nanobeads were added and the suspension incubated for 15 min on ice in the dark. Then, MOJO buffer (PBS, 0.5 % BSA, 2mM EDTA)

was added to dilute the suspension and the polystyrene tube put into the MOJO magnet (BioLegend). All magnetically labeled cells, but not naïve CD4 T cells, were attached to the tube wall due to the magnetic force. After 5 min, naïve CD4 T cells were transferred to a new tube, centrifuged and re-suspended in PBS. The cell number was enumerated by trypan blue exclusion and the cell number adjusted to approximately 0.5- 1x10^6 cells in 200 µl PBS. For purity check of SMARTA Thy1.1$^+$ CD4 T cells, a small amount of cells was stained with anti-Thy1.1 (clone Ox-7, DRFZ), anti-CD4 (clone GK1.5, DRFZ), anti-TCRvα2 (clone B20.1, BioLegend) and anti-CD44 (clone IM7, BioLegend) and the purity evaluated by flow cytometry. For purity check of DO11.10 CD4 T cells, a small amount of cells was stained with anti-DO11.10 (clone KJ1.26, DRFZ) and anti-CD4 (clone GK1.5, DRFZ) and the purity evaluated by flow cytometry.

2.2.3 Splenic B cell sorting

For negative sorting of splenic B cells, splenocytes were stained with FITC-conjugated anti-Mac1 (clone M1/70.15.11, DRFZ), anti-CD4 (clone GK1.5, DRFZ) and anti-CD8a (clone 53-6.7, DRFZ) antibodies for 20 min on ice (after RBC lysis) followed by anti-FITC and anti-Thy1.2 MicroBeads (Miltenyi Biotec) incubation. The stained samples were then sorted by a magnetic cell separation system (MACS, Miltenyi Biotec). Cells were centrifuged and re-suspended in ice cold PBS and the cell number adjusted to 10^7 cells in 200 µl PBS and transferred intravenously.

2.2.4 CFSE labeling of naïve CD4 T cells

Carboxyfluorescein succinimidyl ester (CFSE) is a dye that can be used to monitor lymphocyte proliferation, both *in vitro* and *in vivo*, due to the progressive halving of CFSE fluorescence within daughter cells upon each cell division. Approximately 7-8 cell divisions can be identified before the CFSE fluorescence is too low to be distinguished above the autofluorescence background. CFSE is able to passively diffuse into cells, where its acetate groups are cleaved by intracellular esterases, and the molecules converted to fluorescent esters. It is retained within the cell and covalently couples to intracellular molecules via its succinimidyl group. Due to this covalent coupling reaction, fluorescent CFSE can be retained within the cell for a long period and is not transferred to adjacent cells (174). For the analysis of the proliferative capacity, naïve LCMV-specific (SMARTA) CD4 T cells were sorted as described above and labeled with CFSE according to the manufacturer's protocol (BioLegend) shortly before adop-

tive transfer and immunization. Briefly, sorted naïve CD4 T cells were re-suspended in 5 µM CFSE working solution and incubated for 20 min at 37°C in the dark. Next, the staining was quenched by adding 5 times the original staining volume of RPMI cell culture medium (Gibco, Life Technologies) containing 10% FCS. The cells were centrifuged and the pellet re-suspended in pre-warmed cell culture medium and incubated for 10 min at 37°C. Next, cells were centrifuged and taken up in ice-cold PBS, the cell number adjusted to 0.5 – 1x10^6 cells in 200 µl PBS and cells transferred intravenously.

2.2.5 Cell isolation from spleen, bone marrow and blood

Mice were sacrificed by cervical dislocation. Approximately 300-500 µl peripheral blood (PB) was taken up in PBS/BSA/EDTA and spleens and femurs in FACS buffer. 5 ml RBC lysis buffer were added to PB and incubated at RT for 5 min followed by washing step in FACS buffer, centrifugation at 300 x g for 5 min and pellet-resuspension in appropriate amounts of FACS buffer. Spleens were meshed and filtered through a 100 µm filter. Bones were cut at the ends and flushed using a syringe with a 22G needle and cells filtered through a 100 µm filter. Cell suspensions were centrifuged at 300 x g for 5 minutes at 4°C, the pellets re-suspended in 1 ml red blood cell (RBC) lysis buffer and incubated for 1.5 min. Next, RBC lysed samples were washed with up to 10 ml FACS buffer, centrifuged and the pellets re-suspended in 1 ml FACS buffer for further procedures.

2.2.6 Surface, intracellular and intranuclear staining for flow cytometry

Cell staining and flow cytometric acquisition and analyses were conducted according to the guidelines for the use of flow cytometry and cell sorting in immunological studies (175). For cell surface staining, 0.5- 1x 10^7 cells were stained for 20 min on ice with monoclonal antibodies in titrated dilutions. To exclude dead cells during flow cytometric acquisition, cells were stained with 1 µg/ml propidium iodide (PI, Sigma) shortly before measurement.

Intranuclear staining of T-bet, Bcl-6 or Ki-67 was performed using the one-step protocol of the Foxp3/transcription factor staining buffer kit (eBioscience) according to the manufacturer's guidelines. Briefly, after surface antigen staining, cells were washed in FACS buffer, centrifuged at 300 x g and the pellet dissociated by pulsed-vortexing. Next, 500 µl of FoxP3 Fix/perm working solution were added and the cells incubated at RT for 30-60 min in the dark. Without washing, 1 ml of permeabilization buffer was

added, the cells centrifuged at RT and the pellet resuspended in 100 µl of permeabilization buffer including the recommended amount of fluorochrome-conjugated antibody against T-bet (clone 4B10, BioLegend), Bcl-6 (clone K112-91, BD Biosciences) or Ki-67 (clone REA183, Miltenyi Biotec). The cells were incubated at RT in the dark for 30 min and afterwards washed twice in permeabilization buffer. For flow cytometric analyses, cells were re-suspended in an appropriate amount of FACS buffer without PI.

For intracytosolic staining of IL-2, 0.5- 1x 10^7 cells were stained for surface antigens and subsequently fixed in 1 ml 2 % formaldehyde in the dark at RT for 15 min. Without washing, 10 µl of 10 % BSA was added and the tube rotated gently. After washing and centrifugation, cells were permeabilzed by washing twice in 1x BD Perm/Wash buffer (BD Biosciences) and subsequently incubated in 1x BD Perm/Wash buffer for 15 min at RT in the dark. After centrifugation, cells were stained for intracellular IL-2 in 50 µl 1x BD Perm/Wash buffer containing anti-IL-2 antibody (clone JES6-5H4, Miltenyi Biotec) for 30 min at 4°C in the dark. Next, cells were washed twice in 1x BD Perm/Wash buffer and resuspended in FACS buffer without PI for flow cytometric analysis.

After washing and centrifugation, stained cells were acquired on a BD Fortessa, BD LSRII or BD Canto (BD Biosciences). Flow cytometric data was analyzed with FlowJo v10 software (FlowJo, LLC /BD Biosciences).

2.2.7 Cell counting

The viability of cells from spleen or BM was assessed by trypan blue exclusion. A Neubauer-counting chamber was used for manual cell counting. The cells were diluted in 0.1% trypan blue solution and 10 µl of the cell suspension used for counting. The chamber contains 4 big squares, which contain 16 smaller squares. Four big squares were counted for each sample. The average cell count of four squares were multiplied by a given dilution factor times the Neubauer-chamber factor 10^4, which gave the concentration of cells per 1 ml. A light microscope was used for counting. A single femur was estimated to harbor 6.3% of total BM, therefore the conversion factor 16 was used to enumerate total cell numbers in the BM of an individual mouse (176).

PB leukocytes were counted in a defined volume of blood by using Türk's solution and total blood volume was calculated from body weight, assuming that mice contain 72 ml blood per kg body weight. The frequencies of CD4 T cells were then determined by flow cytometry, and their absolute numbers per mouse were calculated with respect to the total blood volume of that mouse.

2.2.8 BrdU treatment and staining

Mice were injected i.p. with 1 mg/ml Bromodeoxyuridine (BrdU) in PBS on indicated days. For detection of $BrdU^+$ cells, splenocytes were first stained for cell surface markers as described above and subsequently stained for BrdU according to the manufacturer's protocol (BioLegend). Briefly, cells were re-suspended by pulse-vortexing once and 1 ml freshly prepared 1x BrdU staining buffer working solution added, mixed gently and incubated at RT for 30 min in the dark. Next, cells were washed twice in FACS buffer and centrifuged at 300 x g at RT for 5 min. Next, 100 µl of DNase I working solution (0.3 mg/ml) was added and cells incubated for 1 hour at 37°C in the dark. Afterwards, cells were washed twice in FACS buffer and the pellet re-suspended in FACS buffer containing fluorochrome conjugated anti-BrdU antibody (clone BU20A, BioLegend) and incubated for 30 min at RT in the dark. After washing twice, cells were re-suspended in FACS buffer and measured by flow cytometry.

2.2.9 Cyclophosphamide treatment

For proliferation blocking experiments cyclophosphamide (50 mg/kg, Sigma-Aldrich) in PBS was administered i.v. at indicated time points. PBS was injected into the control group.

2.2.10 CTLA-4 Ig treatment

Mice were treated with 200 µg CTLA-4 Ig (InVivoMab, BioXcell) or 200 µg IgG from human serum (Sigma-Aldrich) i.p. at indicated time points.

2.2.11 Antibody-mediated B cell depletion

B cells were depleted by antibody-mediated antigen-receptor cross-linking as previously described (177). Briefly, mice were injected i.p. with either 200 µg of anti-IgD (clone 11.26c, DRFZ) or isotype control (clone 1d10, DRFZ) followed by i.p. injection of 200 µg of mouse anti-rat IgG antibody (clone MAR18.5, DRFZ). The efficiency of B cell depletion was examined by flow cytometry using an anti-B220 antibody (clone REA755, Miltenyi Biotec) on the day of analysis. Two days after induction of B cell depletion, naive CD4 T cells were transferred i.v.

2.2.12 Naïve CD4 T cell sorting for *in vitro* activation

A single cell suspension of splenocytes from a WT Balb/c or T-bet$^{-/-}$ mouse was prepared and RBCs lysed as described above. After washing and centrifugation at 300 xg for 5 min at 4°C, cells were filtered through a 100 µm mesh and re-suspended in 900 µl FACS buffer plus 100 µl anti-CD4 MicroBeads (clone L3T4, Miltenyi Biotec) and incubated for 15 min at 4°C in the dark. Next, cells were washed in 9 ml FACS buffer, centrifuged and re-suspended in 1 ml FACS buffer prior to magnetic cell separation by means of the MACS system (Miltenyi Biotec). Briefly, a LS column was equilibrated with 3 ml FACS buffer, the cell suspension added and the column washed 3 times with 3 ml of FACS buffer. The negative fraction of unlabeled cells (flow-through) was discarded, the tube below the column changed and the column released from the magnet. 5 ml of FACS buffer were added to the column and flushed. The positive fraction containing CD4 T cells was centrifuged and the pellet re-suspended in 1 ml FACS buffer. Subsequently, cells were stained for 20 min on ice for surface antigens using antibodies against CD62L (clone MEL-14, DRFZ), CD4 (clone GK1.5, DRFZ), CD90.2 (clone HO13, DRFZ), CD25 (clone 3C7, BioLegend) and CD44 (clone IM7, BioLegend). After a washing step, cells were re-suspended in FACS buffer (containing 1 µg/ml PI) and naïve CD4 T cells sorted at a BD Aria cell sorter (BD Biosciences). Naïve CD4 T cells were gated as CD4^{+}CD90.2^{+}CD62L^{+} PI^{-}CD25^{-}CD44^{low} cells. 3 x 10^{5} naive WT or T-bet$^{-/-}$ CD4 T cells were plated on an pre-coated anti-mouse CD3 T-cell activation plate (96 well plate, BD BioCoat, BD Biosciences) in 100 µl of RPMI cell culture medium (Gibco, Life Technologies) containing 10 % FCS and incubated for 24 or 48 hours at 37°C. After 24 or 48 hours, cells were harvested from the plate, washed in FACS buffer and stained for surface antigens using antibodies against CD49b (clone HMa2, BioLegend), CD69 (clone H1.2F3, BioLegend), CD25 (clone 3C7, BioLegend), CD62L (clone MEL-14, DRFZ) and CD44 (clone IM7, BioLegend) and cells acquired at a BD Fortessa flow cytometer.

2.2.13 Sorting and transfer of activated Ag-specific CD4 T cells

Activated OVA-TCR specific (DO11.10) CD4 T cells, DO11.10 x T-bet$^{-/-}$ CD4 T cells or LCMV-specific CD4 T cells were negatively sorted on day 6 after immunization from spleens of transferred WT Balb/c (transferred with DO11.10 CD4 T cells) or WT C57BL/6 mice (transferred with LCMV-specific CD4 T cells) in order to re-transfer them into SCID or Rag-1 mice, respectively. After RBC lysis, splenocytes were incubated with biotinylated antibodies against B220 (clone RA3.6B2, DRFZ), MHCII (clone M5/114, DRFZ) and CD8 (clone 53-6.72, DRFZ) for 20 min on ice in the dark. After

washing off excess antibodies with FACS buffer and centrifugation, cells were resuspended in appropriate amount of FACS buffer containing anti-Biotin-MACS beads and incubated for 15 min at 4°C in the dark according to the manufacturer's protocol (1:10 dilution, Miltenyi Biotec). Next, cells were washed with 9 ml of FACS buffer, centrifuged and the pellet re-suspended in 1 ml FACS buffer. For MACS negative sorting of antigen-specific CD4 T cells, a LS column (Miltenyi Biotec) was equilibrated with 3 ml FACS buffer and the cell suspension loaded onto the column. After washing 3 times with 3 ml of FACS buffer, the negative fraction was collected (containing unlabeled CD4 T cells). The column contained $B220^{+}MHCII^{+}CD8^{+}$ labeled cells and was discarded. After centrifugation, the cells were re-suspended in PBS and the cell number adjusted to 10^{7} cells in 200 µl and transferred i.v. into SCID or $Rag1^{-/-}$ mice. After two hours, spleen, BM and PB were analyzed for the accumulation of antigen-specific CD4 T cells by flow cytometry.

2.2.14 Transcriptome Analysis/ Microarray

Data on *Tbx21* (T-bet) mRNA levels in $CD44^{hi}CD62L^{lo}$ CD4 T cells of spleen and BM (Figure 3.1.2 A) was generated from microarray data previously published (96). Briefly, whole splenocytes and BM cells were harvested from WT C57BL/6 mice, RBC lysed, surface antigens stained and $CD4^{+}B220^{-}CD44^{hi}CD62L^{lo}$ cells sorted by flow cytometric cell sorting. Total RNA from sorted cells was prepared with QIAGEN RNeasy Mini kit and DNA microarray analysis of gene expression was performed (Affymetrix). The data represents three individual gene arrays for each of the BM and spleen cells (n=3). *p<0.05 Bonferroni corrected Student's t test.

2.2.15 Immunohistochemistry and confocal microscopy

For immunofluorescence staining, samples were fixed in 4% paraformaldehyde overnight and equilibrated in 30% sucrose in PBS. Samples were frozen and cryosectioned using Kawamoto's film method (178). In order to stain surface markers, six micrometer sections were rehydrated in PBS twice for 2 min. After a blocking step in 5% FCS/PBS for 30 min at RT, sections were stained with antibodies in 5% FCS/PBS for 2 hours at RT. Next, sections were washed twice in PBS for 5 min and if necessary a secondary antibody applied. Monoclonal antibodies against Thy1.1 (clone HIS51, BioLegend), B220 (clone RA3-6B2, BioLegend), CD4 (clone RM4-5, BioLegend) or CD11c (clone N418, BioLegend) were used for staining. After another washing step in PBS, sections where washed in tap water for 1 min in order to eliminate the salt. Sections were then

mounted with 10 µl fluorescent mounting medium (DAKO) and stored in the dark at 4°C until microscopy. All confocal microscopy was carried out using a Zeiss LSM710 with a 20 × /0.8 numerical aperture objective lens. Image acquisition was performed using Zen 2010 Version 6.0 and images were analyzed by Zen 2012 Light Edition software (Carl Zeiss MicroImaging).

2.2.16 Statistical analyses

Graphs were plotted and statistical analyses carried out with Graph Pad Prism 8.0.2. Data are presented as mean ± SEM unless otherwise indicated. Statistical tests applied are indicated in the figure caption. Testing of statistically significant differences between groups was conducted after normality testing (Gaussian distribution). If normality testing was positive, the unpaired two-tailed Student's *t* test with Welch's correction was applied for comparison of two groups. If samples were not subject to Gaussian distribution, the non-parametric unpaired Mann-Whitney U test was applied for comparison of two groups.

If more than two groups (or subsets) were compared, statistical significance between groups/subsets was determined by Kruskal-Wallis test with Dunn‘s multiple comparison test (after negative normality testing) or one-way ANOVA with Dunnett‘s multiple comparison test (positive normality testing). In figure 3.1.2 A, statistical significant difference between spleen and BM cells was determined by Bonferroni corrected unpaired Student's *t* test.

P values as a measure of statistical significance between groups are indicated as *$p<0.05$, ** $p< 0.01$, ***$p< 0.001$, ****$p < 0.0001$ or *ns* when differences between groups were not significant.

3 Results

3.1 Identification of splenic precursors of BM memory CD4 T cells

While the vast majority of activated CD4 T cells undergo apoptosis after clearance of the pathogen, it is still poorly understood which subpopulations within the pool of antigen-specific activated CD4 T cells possess the potential to differentiate into memory precursor cells and ultimately populate the memory CD4 T cell pool. It was previously shown that in mice, some antigen-specific memory CD4 T cells reside in the BM (96). The first part of this thesis deals with the identification of precursors of BM memory CD4 T cells in the spleen.

3.1.1 Many CD49b$^+$CD69$^+$ memory phenotype CD4 T cells express Ly-6C in the BM

Memory CD4 T cells of the BM highly express the surface molecule Ly-6C (96). Furthermore, the establishment of antigen-specific CD4 T cell memory in the BM was described to occur in CD69- and CD49b- dependent manners (97-99). In order to investigate whether splenic precursors of BM memory CD4 T cells can be identified and discriminated on the basis of the expression of CD49b, CD69 and Ly-6C, the endogenous polyfunctional memory phenotype (MP) compartment of CD4 T cells in spleen and BM of WT C57BL/6 mice was examined by flow cytometry. MP CD4 T cells can be identified as CD4$^+$B220$^-$CD44^{hi}CD62L^{lo} cells. Interestingly, about 8 % of cells within the pool of MP CD4 T cells co-express CD49b and CD69 in the spleen and about 20 % in the BM (Figure 3.1.1). Even though it is reported that only few splenic activated CD4 T cells express Ly-6C (96), CD49b$^+$CD69$^+$ splenic MP CD4 T cells were found to harbour the major population of 10.05 % (±1.18 SEM) Ly-6C$^+$ cells in comparison to 4.47 % (±0.87 SEM) CD49b$^+$- single-positive, 1.61 % (±0.42 SEM) CD69$^+$- single positive cells or 1.9 % (±0.47 SEM) CD49b$^-$CD69$^-$ (DN) cells (Figure 3.1.1, spleen). In the BM, 33.08 % (±2.65 SEM) of CD49b$^+$CD69$^+$ cells include Ly-6C$^+$ cells while the other populations only include minor frequencies of Ly-6C$^+$ cells (CD49b$^+$: 5.97 % (±1.34 SEM), CD69$^+$: 4.46 % (±1.15 SEM), DN (double negative): 2.41 % (±0.88 SEM), Figure 3.1.1, BM). This result confirms that more MP CD4 T cells of the BM express CD49b, CD69 and Ly-6C and that a small population expressing these markers can be found in the pool of splenic MP CD4 T cells.

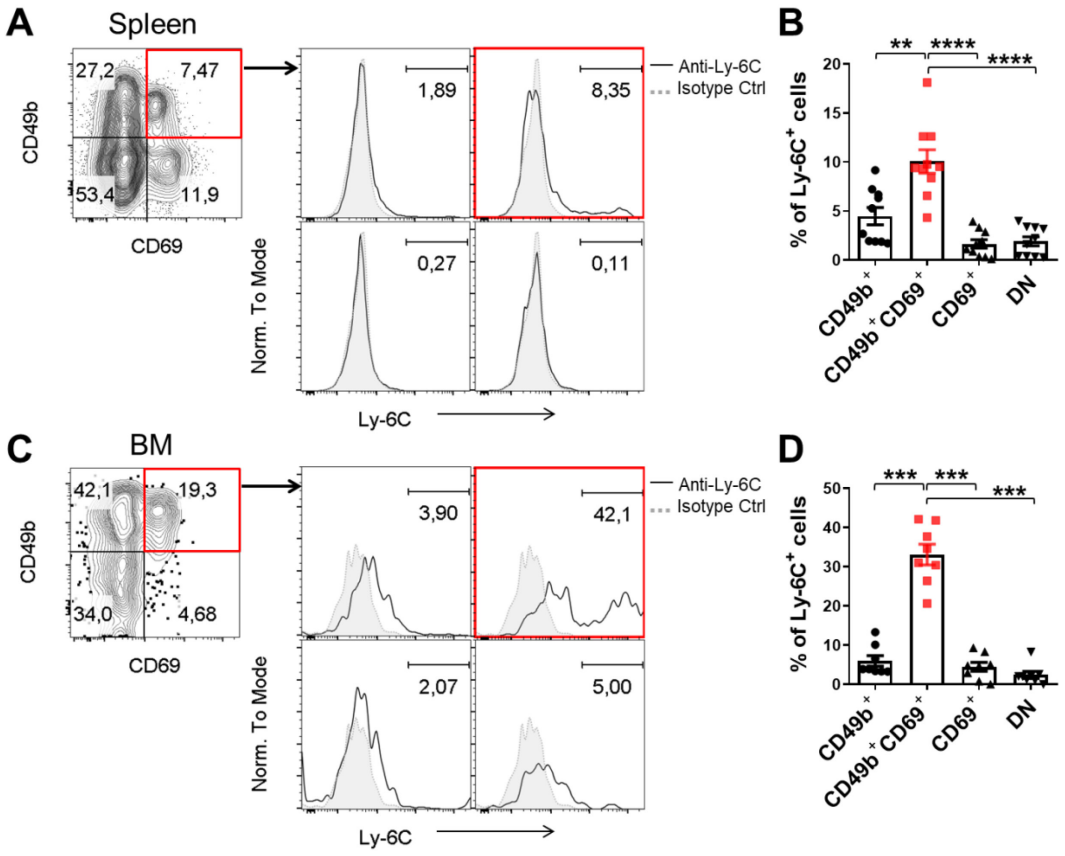

Figure 3.1.1: Memory phenotype CD44^{hi}CD62L^{lo} CD4 T cells of spleen and BM express CD49b, CD69 and Ly-6C and are enriched in the BM. Whole splenocytes and BM cells were harvested from WT C57BL/6 mice, RBC lysed, surface antigens stained, and cells analyzed by flow cytometry. Live CD4^{+}B220^{-} T cells were gated on CD44^{hi} and CD62L^{lo} cells and further examined for CD49b and CD69 expression (countour blot). The subsets of CD49b and CD69 expressing cells were then analyzed for expression of Ly-6C (histograms). The subset of CD49b^{+}CD69^{+} co-expressing cells is framed in red and the percentage indicated in each gate. **A:** Representative contour blot of splenic memory phenotype CD4^{+}CD44^{hi}CD62L^{lo} T cells regarding CD49b and CD69 expression and histograms indicating Ly-6C expression of subsets of CD49b and CD69 expressing cells. CD49b^{+}CD69^{+} cells are framed in red, the percentages indicated in each gate. **B:** Bar graph displays percentages of subsets of CD49b and/or CD69 expressing memory phenotype CD4^{+}CD44^{hi}CD62L^{lo} T cells in the spleen. Data represent pooled results from four independent experiments (total n=10). Data are presented as mean ± SEM. Statistical significance was (after normality testing) determined by unpaired two-tailed Student's t test with Welch's correction as $^{*}p < 0.05$, $^{**}p < 0.01$, $^{***}p < 0.001$, $^{****}p < 0.0001$. **C:** Representative contour blot of BM memory phenotype CD4^{+}CD44^{hi}CD62L^{lo} T cells regarding CD49b and CD69 expression and histograms indicating Ly-6C expression in subsets of CD49b and CD69 expressing cells. CD49b^{+}CD69^{+} cells are framed in red, the percentages indicated in each gate. **D:** Bar graph displays percentages of subsets of CD49b and/or CD69 expressing memory phenotype CD4^{+}CD44^{hi}CD62L^{lo} T cells in the BM. Data represent pooled results from three independent experiments, each experiment with either one, three or four mice (total n=8). Data are presented as mean ± SEM. Statistical significance was after negative normality testing determined by Mann-Whitney U test as $^{*}p < 0.05$, $^{**}p < 0.01$, $^{***}p < 0.001$.

3.1.2 CD49b^{+}CD69^{+} MP CD4 T cells differentially express T-bet

For a global assessment of the differences in gene expression between CD4^{+}CD44^{hi}CD62L^{lo} memory phenotype cells from the spleen and BM, a transcriptome comparison was carried out prior to this study (96). 1756 transcripts were differentially expressed, with 96 % of them being downregulated in BM MP CD4 T cells compared to splenic MP CD4 T cells, demonstrating that MP CD4 T cells of the BM are in a resting state. Interestingly, the transcript of *Tbx-21*, encoding the Th1 response driving major transcription factor T-bet, was significantly upregulated in MP CD4 T cells of the BM

compared to the splenic population (Figure 3.1.2, A). Accordingly, the expression of T-bet was determined in MP CD4 T cells in spleen and BM by flow cytometry (Figure 3.1.2, B). In both, spleen and BM CD49b^{+}CD69^{+} MP CD4 T cells were significantly enriched for T-bet^{+} cells compared to the other subsets. In the spleen, 40.81 % (±3.25 SEM) of CD49b^{+}CD69^{+} cells included T-bet^{+} cells whereas 23.08 % (±2.10 SEM) of CD49b^{+} -cells, 22.5 % (±1.83 SEM) of CD69^{+} -cells and only 15.07 % (±1.35 SEM) of CD49b^{-}CD69^{-} (DN - double negative) cells included T-bet^{+} cells (Figure 3.1.2, B and C). In the BM, 25.76 % (±4.22 SEM) of CD49b^{+}CD69^{+} cells included T-bet+ cells whereas 4.17 % (±1.24 SEM) of CD49b^{+} -cells, 9.6 % (±2.06 SEM) of CD69^{+} -cells and only 2.93 % (±0.47 SEM) of CD49b^{-}CD69^{-} (DN - double negative) cells included T-bet^{+} cells (Figure 3.1.2, D and E). This result suggests that expression of T-bet marks CD49b^{+}CD69^{+} BM memory CD4 T cells and their splenic precursors.

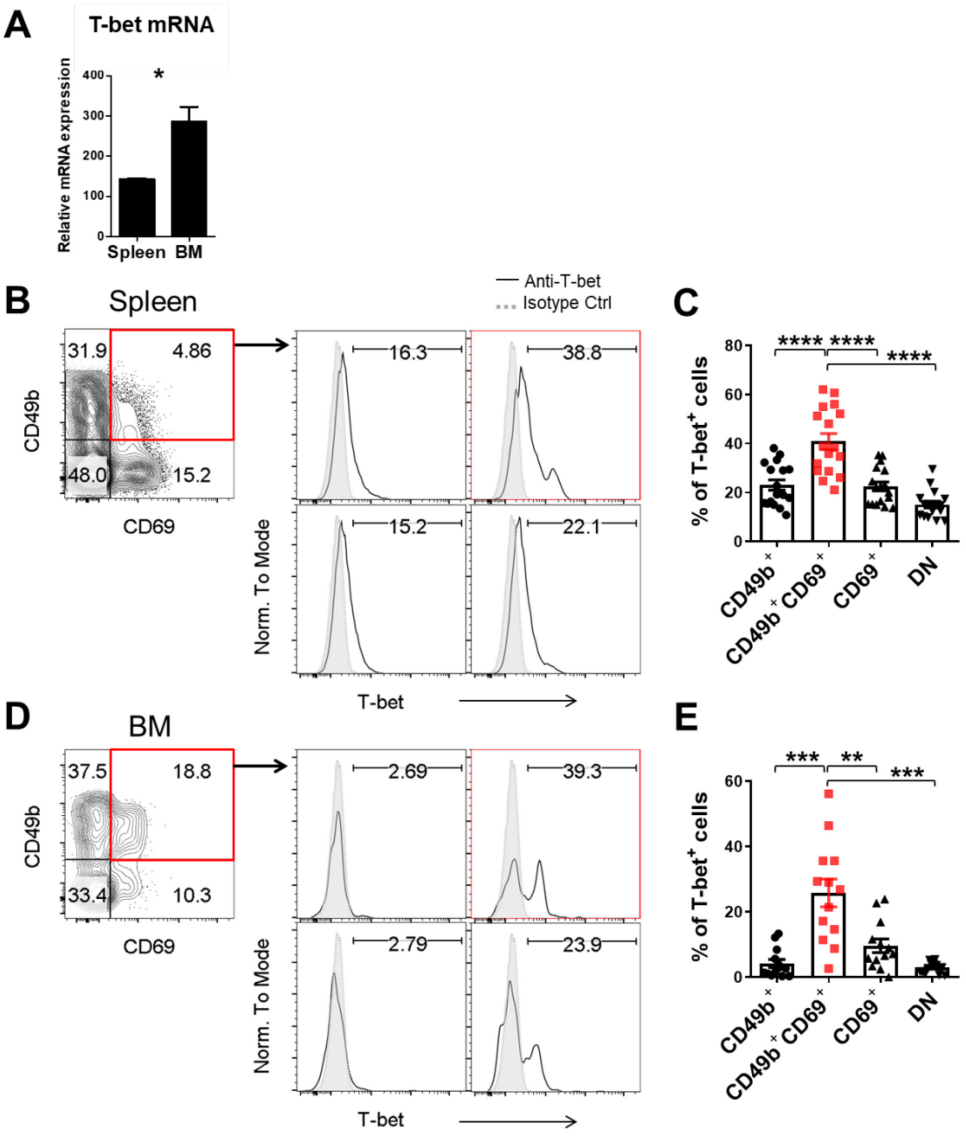

Figure 3.1.2: The transcription factor T-bet (*Tbx21*) is highly expressed in memory phenotype CD49b^{+}CD69^{+} CD4 T cells of spleen and BM. **A:** Expression of T-bet (*Tbx21*) mRNA in FACS-sorted CD4^{+}CD44^{hi}CD62L^{lo} T cells of spleen and BM. Whole splenocytes and BM cells were harvested from WT C57BL/6 mice, RBC lysed, surface antigens stained

and $CD4^+B220^-CD44^{hi}CD62L^{lo}$ cells sorted by flow cytometric cell sorting. Total RNA from sorted cells was prepared with QIAGEN RNeasy Mini kit and DNA microarray analysis of gene expression was performed (Affymetrix). The data represents three individual gene arrays for each of the BM and spleen cells (n=3). *p<0.05 Bonferroni corrected Student's t test. **B+D:** Splenic and BM $CD49b^+CD69^+$ memory phenotype CD4 T cells contain significantly higher percentages of T-bet$^+$ cells compared to other subsets. Representative contour blots of spleen (B) and BM (D) memory phenotype $CD4^+CD44^{hi}CD62L^{lo}$ T cells are displayed regarding the expression of CD49b and CD69. Histograms indicate T-bet expression in subsets of CD49b and CD69 expressing cells. Whole splenocytes (B) and BM cells (D) were harvested from WT C57BL/6 mice, RBC lysed, surface antigens stained, cells fixed and permeabilized with a transcription factor staining kit and stained for T-bet. Next, cells were analyzed by flow cytometry. $CD4^+B220^-$ T cells were gated on $CD44^{hi}$ and $CD62L^{lo}$ cells and further examined for CD49b and CD69 expression (contour blot). The subsets of CD49b and CD69 expressing cells were then analyzed for expression of T-bet (histograms). The subset of $CD49b^+CD69^+$ cells is framed in red and the percentage of T-bet$^+$ cells indicated in each gate. **C:** Bar graph displays percentages of T-bet$^+$ cells in subsets of CD49b and/or CD69 expressing memory phenotype $CD4^+CD44^{hi}CD62L^{lo}$ T cells in the spleen. Data represent pooled results from five independent experiments, each experiment with 3-4 mice (total n=17). Data are presented as mean ± SEM. Statistical significance was (after normality testing) determined by unpaired two-tailed Student's t test with Welch's correction as $^{****}p < 0.0001$. **E:** Bar graph displays percentages of T-bet$^+$ cells in subsets of CD49b and/or CD69 expressing memory phenotype $CD4^+CD44^{hi}CD62L^{lo}$ T cells in the BM. Data represent pooled results from four independent experiments, each experiment with 3-4 mice (total n=13). Data are presented as mean ± SEM. Statistical significance was (after normality testing) determined by unpaired two-tailed Student's t test with Welch's correction as $^{**}p < 0.01$, $^{***}p < 0.001$.

3.1.3 T-bet deficiency impairs the appearance of $CD49b^+CD69^+$ MP CD4 T cells in spleen and BM

Since T-bet was found to be differentially expressed in $CD49b^+CD69^+$ MP CD4 T cells of spleen and BM, the expression of CD49b and CD69 on MP CD4 T cells was analyzed in mice lacking T-bet expression (T-bet$^{-/-}$). Whereas splenic WT MP CD4 T cells included a reasonable population of 7.2 % (± 0.55 SEM) $CD49b^+CD69^+$ MP CD4 T cells, a significant reduction of this population was observed in T-bet$^{-/-}$ mice (4.3 % ±0,23 SEM) (Figure 3.1.3 A and B). In the BM, $CD49b^+CD69^+$ MP CD4 T cell percentages significantly decreased from 17.3 % ± (1.9 SEM) in WT mice to 2.8 % (± 0.79 SEM) in T-bet$^{-/-}$ mice. This effect was also observed in the total number of $CD49b^+CD69^+$ cells in the BM in the absence of T-bet (WT: $2.97x10^4$ ± $3.88x10^3$ SEM, T-bet$^{-/-}$: $6.41x10^3$ ± $1.6x10^3$ SEM) (Figure 3.1.3 A-C). In the spleen however, only the percentages of $CD49b^+CD69^+$ MP CD4 T cells were reduced, but cell numbers of splenic $CD49b^+CD69^+$ MP CD4 T cells were not affected (WT: $1.50x10^5$ ± $1.45x10^4$ SEM, T-bet$^{-/-}$: $1.58x10^5$ ± $1.39x10^4$) (Figure 3.1.3, A and C). This result does not surprise, as T-bet deficient mice knowingly suffer from splenomegaly and naturally include more lymphocytes of all subsets (179). Interestingly, also total numbers of CD4 T cells and $CD44^{hi}CD62L^{lo}$ MP CD4 T cells in the spleen were not affected by the absence of T-bet expression (Figure 3.1.3 D, Spleen). Furthermore, CD4 T cell numbers and MP CD4 T cells in the BM were not affected in T-bet$^{-/-}$ mice (Figure 3.1.3 D, BM). This result indicates that T-bet expression may not be required for the accumulation of antigen-experienced CD4 T cells in the BM.

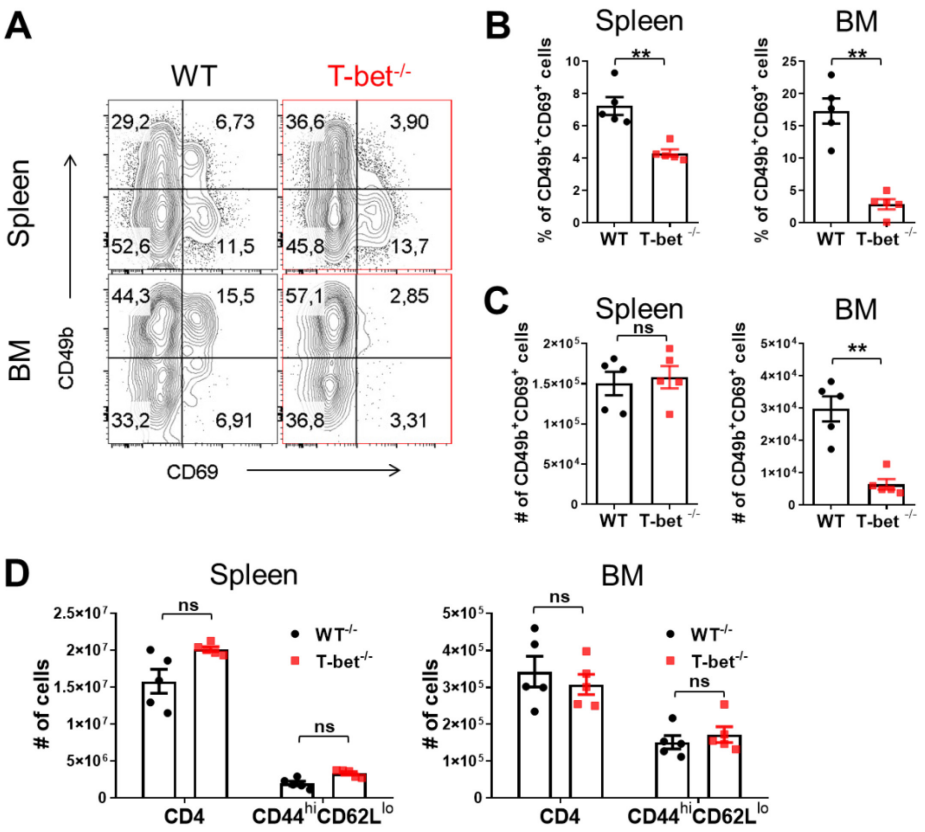

Figure 3.1.3: T-bet deficiency impairs the simultaneous expression of CD49b and CD69 in MP CD4 T cells in spleen and BM but does not affect the total numbers of MP CD4 T cells. Whole splenocytes and BM cells were harvested from WT Balb/c and T-bet$^{-/-}$ mice, RBC lysed, surface antigens stained and MP CD4^{+}CD44^{hi}CD62L^{lo} T cells analyzed for expression of CD49b and CD69 by flow cytometry and total cell numbers enumerated. **A:** Representative countour plots of spleen and BM are displayed. Percentages of CD49b^{+}CD69^{+} MP CD4 T cells are indicated within the respective gate. **B:** Percentages of CD49b^{+}CD69^{+} MP CD4 T cells compared between WT and T-bet$^{-/-}$ mice in spleen (left bar graph) and BM (right bar graph). **C:** Absolute cell numbers of CD49b^{+}CD69^{+} MP CD4 T cells compared between WT and T-bet$^{-/-}$ mice in spleen (left bar graph) and BM (right bar graph). **D:** Absolute cell numbers of CD4 T cells (spleen, WT:1,58x10^{7}± 1.6x10^{6} SEM, T-bet$^{-/-}$: 2.01x10^{7} ± 3.3x10^{6} SEM; BM: WT: 3.42x10^{5} ± 4.15x10^{4} SEM, T-bet$^{-/-}$: 3.07x10^{5} ± 2.75x10^{4} SEM) and CD44^{hi}CD62L^{lo} CD4 T cells (spleen, WT: 1.96x10^{6} ± 2.9x10^{5} SEM, T-bet$^{-/-}$: 3.33x10^{6} ± 2.23x10^{5} SEM; BM: WT: 1.50x10^{5} ± 1.8x10^{4} SEM, T-bet$^{-/-}$: 1.71x10^{5} ± 2.14x10^{4} SEM) of spleen (left bar graph) and BM (right bar graph) compared between WT Balb/c and T-bet$^{-/-}$ mice. Data represent pooled results from two independent experiments, each with 2-3 mice per group (total n=5 per group). Data are presented as mean ± SEM. *p < 0.05, **p < 0.01, ***p < 0.001, Statistical significance was determined by Mann-Whitney U test as ns=not significant.

3.1.4 T-bet deficiency impairs the expression of Ly-6C in CD49b^{+} MP CD4 T cells

Expression of T-bet has been described to be indispensable for expression of Ly-6C in Vα14i NKT cells (180). Since resting BM memory CD4 T cells highly express Ly-6C, expression levels of Ly-6C in MP CD4 T cells of the spleen and BM were determined in T-bet deficient mice. T-bet deficiency was found to significantly abrogate Ly-6C expression in splenic MP CD4 T cells (WT: 1.56 % ± 0.16 SEM, T-bet$^{-/-}$: 0.52 % ± 0.18 SEM) and more drastically also in the BM (WT: 9.88 % ± 0.87 SEM, T-bet$^{-/-}$: 2.3 % ±0.84 SEM) (Figure 3.1.4 A and B). In order to dissect which cells within the pool of MP CD4 T cells displayed the defect in Ly-6C expression, subsets of CD49b and/or CD69 expressing cells were analyzed. In the spleen of WT mice 1.14 % (±0.10 SEM) co-

expressed CD49b and Ly-6C whereas this population was lacking in the spleen of T-bet-deficient mice (0.14 % ± 0.03 SEM). This effect was even more prominent in the BM, where 7.52 % (± 0.75 SEM) of MP CD4 T cells were found to be CD49b$^+$Ly-6C$^+$ whereas in the BM of T-bet$^{-/-}$ mice only 1.10 % (± 0.51 SEM) of MP CD4 T cells were found to be co-expressing CD49b and Ly-6C. In summary, pprimarily CD49b$^+$ expressing cells, including CD49b$^+$CD69$^+$ cells, lacked Ly-6C expression in the absence of T-bet (Figure 3.1.4 C and D).

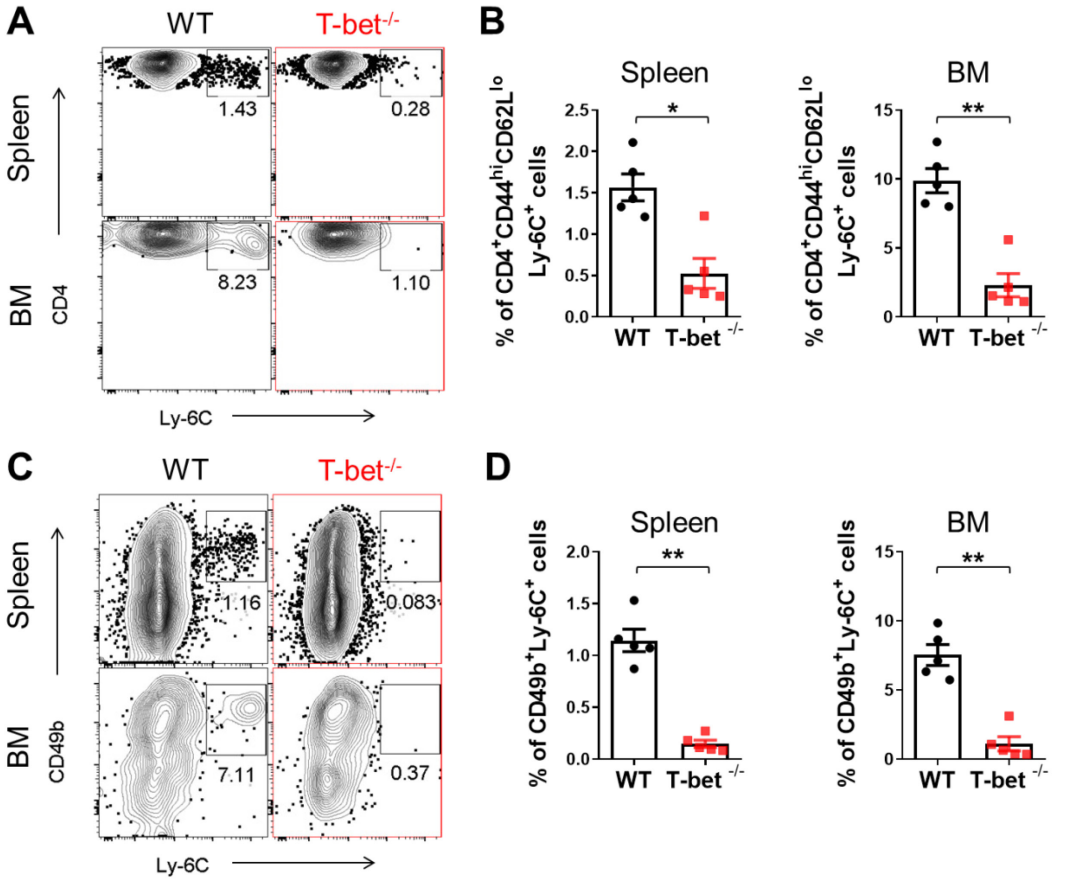

Figure 3.1.4: T-bet deficiency impairs the expression of Ly-6C within the CD49b$^+$ subset of MP CD4 T cells in spleen and BM. Whole splenocytes and BM cells were harvested from WT Balb/c and T-bet$^{-/-}$ mice, RBC lysed, surface antigens stained and MP CD4$^+$CD44^{hi}CD62L^{lo} T cells analyzed for expression of CD49b, CD69 and Ly-6C by flow cytometry. **A:** Representative contour blots display the percentage of Ly-6C$^+$ cells in MP CD4$^+$CD44^{hi}CD62L^{lo} T cells in spleen and BM of WT and T-bet$^{-/-}$ mice. The percentages of Ly-6C$^+$ cells are indicated in each gate. Displayed blots have been previously gated on live CD4$^+$B220$^-$CD44^{hi}CD62L^{lo} cells. **B:** Bar graphs display percentages of CD4$^+$B220$^-$CD44^{hi}CD62L^{lo}Ly-6C$^+$ cells in spleen (left bar graph) and BM (right bar graph) cells of WT and T-bet$^{-/-}$ mice. Data represent pooled results from two independent experiments, each experiment with two to three mice per group (total n=5 per group). Data are presented as mean ± SEM. Statistical significance was determined by Mann-Whitney U test as $^*p < 0.05$, $^{**}p < 0.01$. **C:** Representative contour blots display the percentage of CD49b$^+$Ly-6C$^+$ cells in MP CD4$^+$CD44^{hi}CD62L^{lo} T cells in spleen and BM of WT and T-bet$^{-/-}$ mice. The percentages of CD49b$^+$Ly-6C$^+$ cells are indicated in each gate. Displayed blots have been previously gated on live CD4$^+$B220$^-$CD44^{hi}CD62L^{lo} cells. **D:** Bar graphs display percentages of CD4$^+$B220$^-$CD44^{hi}CD62L^{lo} CD49b$^+$Ly-6C$^+$ cells in spleen (left bar graph) and BM (right bar graph) cells of WT and T-bet$^{-/-}$ mice. Data represent pooled results from two independent experiments, each experiment with two to three mice per group (total n=5 per group). Data are presented as mean ± SEM. Statistical significance between groups was determined by Mann-Whitney U test as $^*p < 0.05$ or $^{**}p < 0.01$.

3.1.5 Some antigen-specific CD49b$^+$ CD4 T cells highly co-express T-bet and Ly-6C

To examine how activated CD49b$^+$CD69$^+$ CD4 T cells are generated in the spleen during a directed primary immune response, an adoptive transfer model of antigen-specific CD4 T cells was utilized. Ovalbumin (OVA)-specific TCR (DO11.10)- Tg CD4 T cells were transferred into WT Balb/c host mice, immunized with OVA plus LPS and splenic activated OVA-specific CD4 T cells analyzed with regard to expression of CD49b, CD69, T-bet and Ly-6C at day 6 post immunization (p.I.) (Figure 3.1.5 A). Interestingly, a notable population of Ly-6C$^+$T-bet$^+$ cells was found to be harbored within the the CD49b$^+$-(6.2 % ± 0.92 SEM) and CD49b$^+$CD69$^+$- (4.5 % ± 0.65 SEM) subpopulations of OVA-TCR specific activated CD4 T cells whereas CD69$^+$ cells (1.74 % ± 0.34 SEM) and DN (double negtive) cells (DN: 1.22 % ± 0.12 SEM) contained only minor percentages. These results indicate that during a primary antigen-directed immune response against OVA, particularly CD49b$^+$ OVA-specific CD4 T cells (including CD49b$^+$CD69$^+$ cells) concomitantly express Ly-6C and T-bet, but not CD69$^+$ OVA-specific CD4 T cells. Furthermore, this result demonstrates that Ly-6C expression is also negligible in CD69$^+$ (single positive) antigen-specific CD4 T cells.

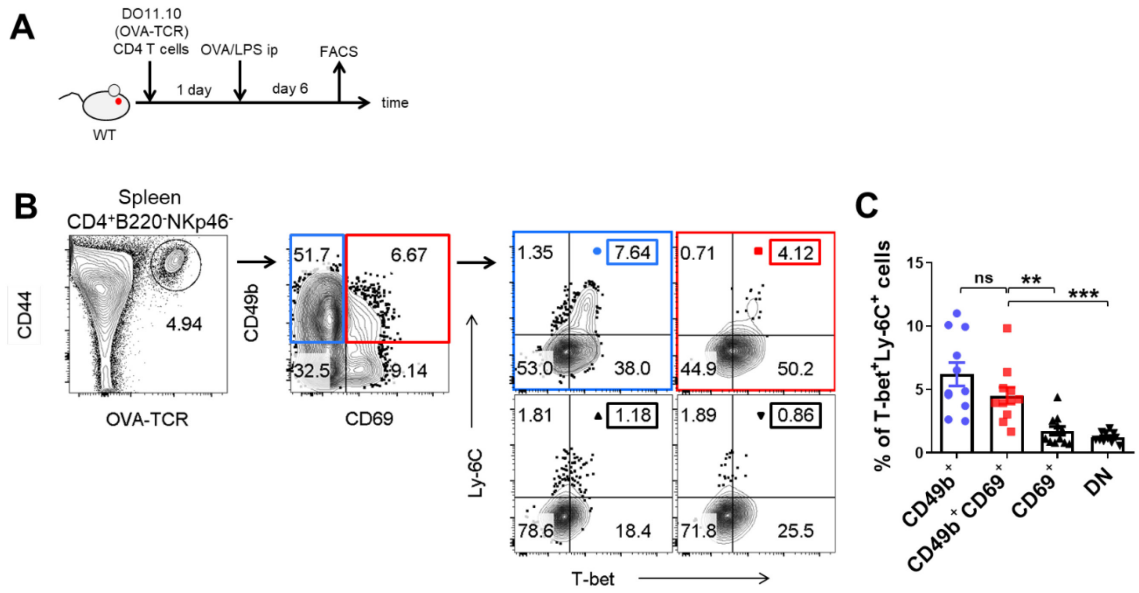

Figure 3.1.5: Some CD49b$^+$ and CD49b$^+$CD69$^+$ OVA-specific activated CD4 T cells co-express T-bet and Ly-6C on day 6 of the primary immune response. **A:** Experimental outline. WT Balb/c mice were transferred with naïve OVA-TCR specific (DO11.10) CD4 T cells, immunized with 100 µg OVA-peptide and 10 µg LPS and splenocytes were analyzed on day 6 after immunization by flow cytometry. **B:** Representative contour blots and gating strategy: Splenic CD4$^+$B220$^-$ NKp46$^-$ T cells were gated on OVA-TCR specific activated CD4 T cells (left blot) and subsequently analyzed for the expression of CD49b and CD69 (middle blot). Next, four subsets of CD49b and/or CD69 expressing cells were analyzed for the co-expression of T-bet and Ly-6C (right contour blots). CD49b$^+$ OVA-specific CD4 T cells are framed in blue, CD49b$^+$CD69$^+$ OVA-specific CD4 T cells are framed in red. **C:** Bar graph displays percentages of T-bet$^+$Ly-6C$^+$ cells in the four subsets of CD49b and/or CD69 expressing OVA-TCR specific CD4 T cells. Percentages are framed in **B**. Data represent pooled results from four independent experiments, each experiment with 2-3 mice (total n=11). Data are presented as mean ± SEM. Statistical significance was conducted after normality testing and determined by unpaired two-tailed Student's t test with Welch's correction as ns= not significant, $^{**}p < 0.01$ or $^{***}p < 0.001$.

3.1.6 T-bet deficiency impairs the expression of Ly-6C in antigen-specific CD49b$^+$ CD4 T cells

In order to examine the effect of T-bet deficiency in antigen- specific CD4 T cells on the expression of CD49b, CD69 and Ly-6C during a primary response against OVA, T-bet$^{-/-}$ OVA-specific CD4 T cells were transferred into WT Balb/c host mice, followed by immunization with OVA plus LPS. On day 6 after immunization, splenocytes were analyzed and enumerated for OVA-specific CD4 T cells by flow cytometry (Figure 3.1.6, A). The percentages of activated OVA-specific CD4 T cells were comparable on day 6 p.I. when mice were transferred with T-bet sufficient (WT) OVA-TCR CD4 T cells (5.47 % ± 0.22 SEM) and T-bet$^{-/-}$ OVA-TCR CD4 T cells (6.3 % ± 1.08 SEM) (Figure 3.1.6 C). Interestingly, also the percentages of CD49b$^+$CD69$^+$ activated OVA-TCR$^+$ CD4 T cells did not differ regardless of T-bet expression (WT: 6.07 % ± 0.61 SEM, T-bet$^{-/-}$: 8.27 % ± 1.27 SEM). This result indicates that T-bet does not regulate the concomitant expression of CD49b and CD69 in OVA-specific CD4 T cells during a primary immune response in the spleen (Figure 3.1.6 B-D). On the other hand, the frequency of Ly-6C$^+$ cells within OVA-specific CD4 T cells significantly dropped from 3.17 % (± 0.57 SEM) in T-bet sufficient OVA-TCR$^+$ CD4 T cells to 0.87 % (± 0.16 SEM) in OVA-TCR$^+$ CD4 T

cells lacking the expression of T-bet (Figure 3.1.6 E and F). Similar to CD49b$^+$ MP CD4 T cells, also CD49b$^+$ OVA-specific CD4 T cells (including CD49b$^+$CD69$^+$ cells) selectively lost expression of Ly-6C when OVA-TCR CD4 T cells lacked T-bet expression (WT: 2.42 % ± 0.45 SEM, T-bet$^{-/-}$: 0.40 % ± 0.04 SEM) (Figure 3.1.6 E and G).

Taken together, these results indicate that expression of T-bet is indispensable for Ly-6C expression in antigen-specific CD49b$^+$ CD4 T cells. However, the formation of activated CD49b$^+$CD69$^+$ CD4 T cells is not affected in the absence of T-bet.

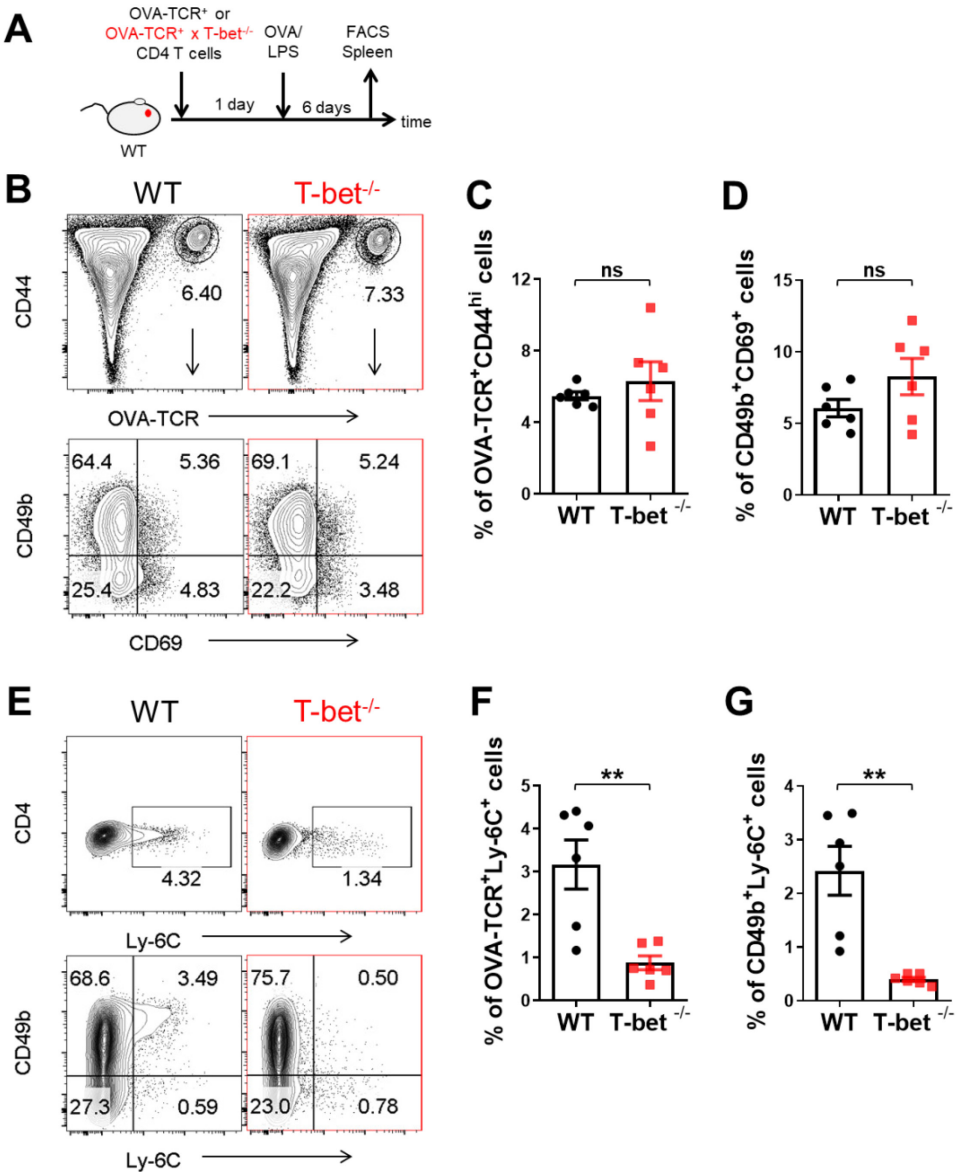

Figure 3.1.6: T-bet deficiency impairs the expression of Ly-6C in CD49b$^+$ OVA-TCR specific activated CD4 T cells. **A:** Experimental outline. Purified OVA-TCR$^+$ (DO11.10) Tbx21$^{+/+}$ or Tbx21$^{-/-}$ CD4 T cells were transferred into WT Balb/c mice followed by immunization with 100 µg OVA-peptide and 10 µg LPS. On day 6 after immunization, splenic OVA-TCR$^+$ CD4 T cells were analyzed by flow cytometry for the expression of CD49b, CD69 and Ly-6C after gating on CD4$^+$ B220$^-$ NKp46$^-$ CD44^{hi} OVA-TCR$^+$ cells.**B:** Loss of T-bet in OVA-TCR specific CD4 T cells does not impair the frequency of OVA-TCR$^+$CD44^{hi} CD4 T cells by day 6 after immunization nor the simultaneous expression of CD49b and CD69 in OVA-TCR$^+$CD44^{hi} cells. Representative contour blots: CD49b and CD69 expressing cells were previously gated on CD4$^+$ B220$^-$ NKp46$^-$ CD44^{hi} OVA-TCR$^+$ cells. **C:** Bar graph displays percentages of WT OVA-TCR$^+$CD44^{hi} cells and T-

bet$^{-/-}$OVA-TCR^{+}CD44^{hi} cells in the spleen on day 6 after immunization. **D:** Bar graph displays percentages of CD49b^{+}CD69^{+} cells in WT OVA-TCR^{+}CD44^{hi} cells and T-bet$^{-/-}$OVA-TCR^{+}CD44^{hi} cells in the spleen on day 6 after immunization. **B-D:** Data represent pooled results from two independent experiments, each experiment with three mice per group (total n=6 per group). Data are presented as mean ± SEM. Statistical significance between groups was determined by Mann-Whitney U test as ns= not significant. **E-G:** Loss of T-bet in OVA-TCR specific CD4 T cells leads to a loss of Ly-6C expression in CD49b^{+} cells. Representative contour blots: Ly-6C expressing cells were previously gated on CD4^{+} B220^{-} NKp46^{-} CD44^{hi}OVA-TCR^{+} cells and then displayed as CD4^{+} Ly-6C^{+} cells. Percentage of Ly-6C^{+} cells is indicated in the gate. **F:** Bar graph displays percentages of Ly-6C^{+} cells in WT OVA-TCR^{+}CD44^{hi} cells and T-bet$^{-/-}$OVA-TCR^{+}CD44^{hi} cells in the spleen on day 6 after immunization. **G:** Bar graph displays percentages of CD49b^{+}Ly-6C^{+} cells in WT OVA-TCR^{+}CD44^{hi} cells and T-bet$^{-/-}$OVA-TCR^{+}CD44^{hi} cells in the spleen on day 6 p.I. **E-G:** Data represent pooled results from two independent experiments, each experiment with three mice per group (total n=6 per group). Data are presented as mean ± SEM. Statistical significance between groups was determined by Mann-Whitney U test as $^{**}p < 0.01$.

3.1.7 T-bet deficiency does not impair the co-expression of CD49b and CD69 *in vitro*

In order to exclude bystander and compensatory effects in mice ubiquitously lacking T-bet expression, the effect of T-bet deficiency on synchronistic CD69 and CD49b expression was analyzed after *in vitro* activation of naïve CD4 T cells. To that end, splenic naïve CD4 T cells from WT or T-bet$^{-/-}$ mice were sorted and cultured under anti-CD3 stimulating conditions for 24 or 48 h and the expression of CD49b and CD69 examined by flow cytometry (Figure 3.1.7 A). After 24 hours, WT and T-bet$^{-/-}$ CD4 T cells predominantly expressed CD69 in equal proportions (WT: 87.56 % ± 5.37 SEM, T-bet$^{-/-}$: 93.52 % ± 1.88 SEM). Interestingly, CD49b expression could not be detected after 24 hours of anti-CD3 stimulation in both WT and T-bet$^{-/-}$ CD4 T cells. After 48 hours, nearly all CD4 T cells of both, WT and T-bet$^{-/-}$ mice, equally co-expressed CD49b and CD69 (WT: 95.41 % ±1.27 SEM, T-bet$^{-/-}$: 91.72 % ±1.37 SEM) (Figure 3.1.7 B and C). This result suggests that T-bet expression is dispensable for the co-expression of CD49b and CD69 after primary activation of CD4 T cells.

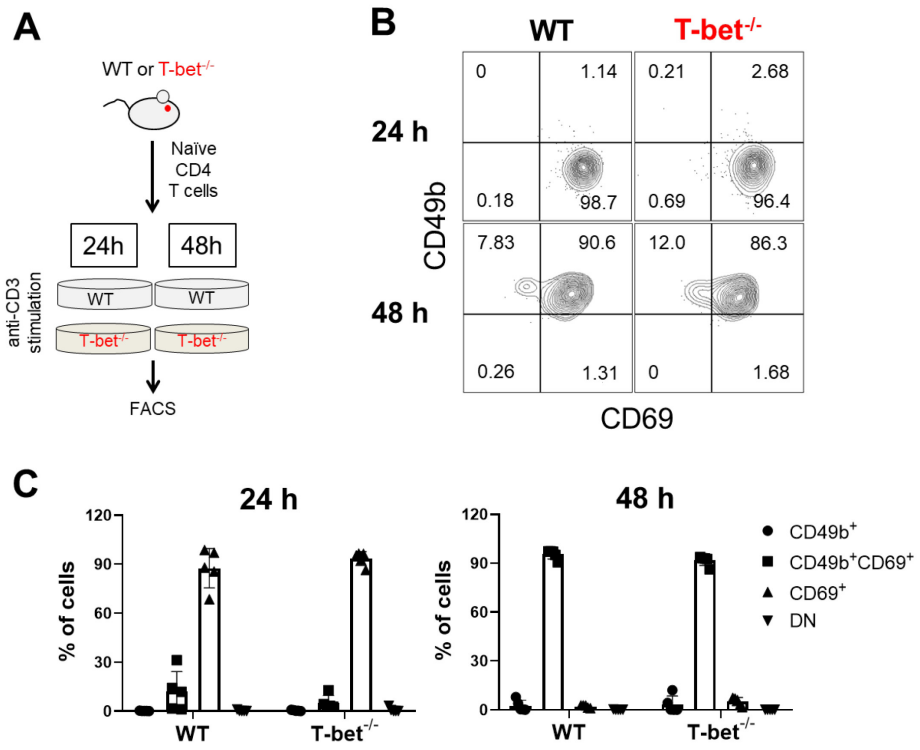

Figure 3.1.7: T-bet deficient activated CD4 T cells simultaneously express CD49b and CD69 upon CD3 stimulation *in vitro*. **A:** Experimental outline. Splenic WT or T-bet$^{-/-}$ naïve CD4 T cells were sorted by flow cytometric cell sorting (live CD4^{+}B220^{-}CD25^{-}CD44^{lo}CD62L^{hi}) and cultured under CD3 stimulating conditions for 24 or 48 hours. At 24 and 48 hours cells were harvested and CD49b and CD69 expression analyzed by flow cytometry. **B:** Representative contour blots displaying CD49b and CD69 expression of WT and T-bet$^{-/-}$ CD3 stimulated CD4 T cells at 24 and 48 hours. Numbers indicate percentages of positive cells in the respective gate. **C:** Bar graphs display percentages of CD49b^{+} cells, CD49b^{+}CD69^{+} cells, CD69^{+} cells and DN (double negative cells) at 24 and 48 hours after *in vitro* CD3 stimulation. Data represent pooled results from two independent experiments, each experiment with 2-3 mice per group (total n=5 per group). Data are presented as mean ± SEM

3.1.8 T-bet is not required for the accumulation of antigen-specific CD4 T cells in the BM

T-bet directly trans-activates a broad spectrum of chemokine receptors that are involved in lymphocyte migration and homing. To test if the migratory capacity of activated CD4 T cells to locate to the BM is impaired in the absence of T-bet, naïve T-bet$^{-/-}$ OVA-specific CD4 T cells were transferred into WT Balb/c host mice followed by immunization with OVA plus LPS (Figure 3.1.7 A). On day 6 after immunization, splenocytes of transferred and immunized WT Balb/c mice were harvested and B220^{+} cells, MHCII^{+} cells and CD8^{+} T cells excluded by magnetic activated cell sorting (MACS, Miltenyi Biotec). The resulting cell suspension (containing activated OVA-specific CD4 T cells) was transferred into Severe Combined Immuno Deficiency (SCID) mice and the spleen and BM were analyzed for accumulated OVA-TCR^{+} CD4 T cells 2 hours after transfer. SCID mice are unable to generate T or B cells, because V(D)J recombination does not occur due to a rare recessive mutation on chromosome 16 that determines the activity of an enzyme involved in DNA repair. Since SCID mice do not possess

lymphocytes, this model facilitates the detection of transferred lymphocytes that were generated in a different organism. Comparable percentages of OVA-specific CD4 T were detected independently of T-bet expression in the spleen (WT: 0.83 % ± 0.142 SEM, T-bet$^{-/-}$: 0.74 % ± 0.107 SEM) and BM (WT: 0.61 % ± 0.115 SEM, T-bet$^{-/-}$: 0.47 % ± 0.15 SEM) (Figure 3.1.8 B-E). This result suggests that T-bet expression, or the downstream targets of T-bet, is redundant for the migration of antigen-specific CD4 T cells towards the BM.

Finally, to examine the physiological impact of T-bet deficiency on the accumulation and maintenance of activated antigen-specific CD4 T cells in the BM during the primary phase of an immune response, purified naïve *Tbx21*$^{+/+}$ (WT) or *Tbx21*$^{-/-}$ (T-bet$^{-/-}$) Thy1.1^{+} LCMV–TCR (SMARTA) CD4 T cells were transferred into WT C57BL/6 mice followed by immunization with LCMV peptide $GP_{61–80}$ plus LPS. On day 6 after immunization, the Thy1.1^{+} CD4 T cells in spleen and BM were analyzed by flow cytometry (Figure 3.1.8 F). On day 6 after immunization, spleen and BM cells were analyzed for the frequencies of Thy1.1^{+}-specific CD4 T cells. A comparable expansion of LCMV-TCR specific Thy1.1^{+} CD4 T cells was observed independently of T-bet expression in the spleen (WT: 3.61 % ± 0.4 SEM, T-bet$^{-/-}$: 4.1 % ± 0.36 SEM) (Figure 3.1.8 I and J). Also in the BM, T-bet$^{-/-}$ LCMV-TCR specific Thy1.1^{+} CD4 T cells accumulated similarly to WT cells (WT: 1.89 % ± 0.34 SEM, T-bet$^{-/-}$: 1.66 % ± 0.28 SEM) (Figure 3.1.8 G and H). Thus, the capability of antigen-specific CD4 T cells to accumulate in the BM is not impaired in the absence of T-bet expression, which is in accordance with MP CD4 T cell accumulations in T-bet$^{-/-}$ mice (Figure 3.1.3 D).

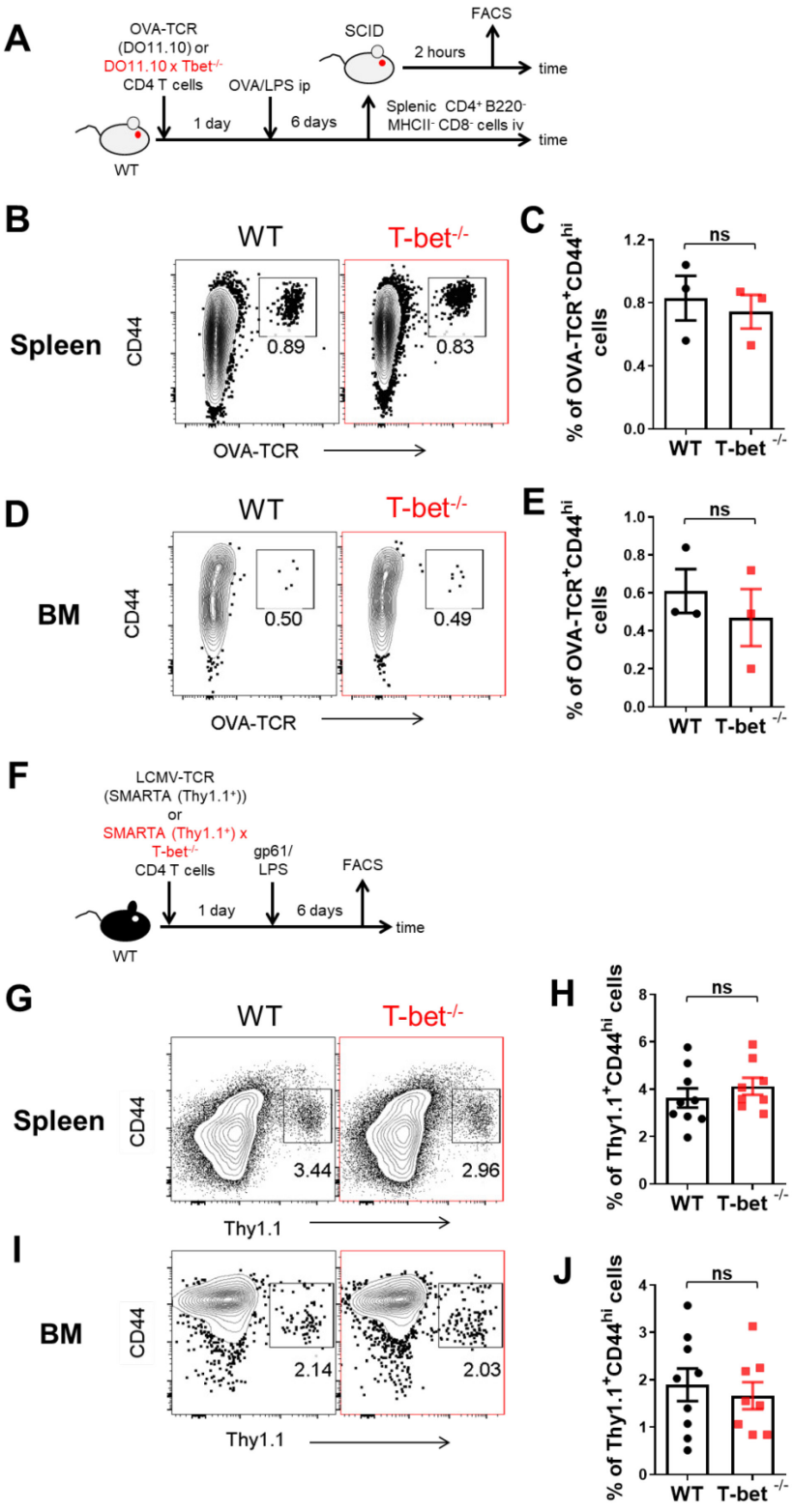

Figure 3.1.8: T-bet deficiency does not impair the migration of activated antigen-specific CD4 T cells into the BM. **A:** Experimental outline. Purified *Tbx21*$^{+/+}$ or *Tbx21*$^{-/-}$ OVA-TCR^{+} (DO11.10) CD4 T cells were transferred into WT Balb/c mice followed by immunization with 100 µg OVA-peptide plus 10 µg LPS. On day 6 after immunization, whole splenocytes were harvested, RBC lysed and B220^{+} cells, MHCII^{+} and CD8^{+} T cells excluded by magnetic activated cell sorted (MACS, Miltenyi Biotec). B220^{-} MHCII^{-}CD8^{-} cells were transferred intravenously into SCID mice and spleen and BM harvested and analyzed for OVA-TCR^{+} CD4 T cells by flow cytometry 2 hours after transfer. **B-D:** Representative contour blots with gates representing the frequency of CD44^{hi}OVA-TCR^{+}T-bet$^{+/+}$ or T-bet$^{-/-}$ cells in spleen (**B**) and BM (**D**). **C:** Bar graph displays percentages of WT OVA-TCR^{+}CD44^{hi} cells and T-bet$^{-/-}$OVA-TCR^{+}CD44^{hi} cells in the spleen of SCID mice 2 hours after transfer. Data represents results from one experiments with three mice per group. Data are presented as mean ± SEM. Statistical significance between groups was determined by Mann-Whitney U test as ns= not significant. **E:** Bar graph displays percentages of WT OVA-TCR^{+}CD44^{hi} cells and T-bet$^{-/-}$OVA-TCR^{+}CD44^{hi} cells in the

BM of SCID mice 2 hours after transfer. Data represents results from one experiments with three mice per group. Data are presented as mean ± SEM. Statistical significance between groups was determined by Mann-Whitney U test as ns= not significant. **F:** T-bet is not required for the accumulation of antigen-specific CD4 T cells in the BM. Experimental outline. Purified *Tbx21*$^{+/+}$ or *Tbx21*$^{-/-}$ Thy1.1$^+$ LCMV–TCR (SMARTA) CD4 T cells were transferred into WT C57BL/6 mice followed by immunization with 100 µg LCMV $GP_{61–80}$ plus 10 µg LPS. On day 6 after immunization, the Thy1.1$^+$ CD4 T cells in the spleen and BM were analyzed by flow cytometry. **G:** Representative contour blots show a Thy1.1$^+$ (LCMV-TCR$^+$) population in CD4$^+$CD44^{hi}B220$^-$NK1.1$^-$PI$^-$ cells in the spleen (**G**) and BM (**I**) on day 6 after immunization. **H** & **J:** Bar graph displays percentages of WT *Tbx21*$^{+/+}$ Thy1.1$^+$CD44^{hi} cells and *Tbx21*$^{-/-}$Thy1.1$^+$CD44^{hi} cells in the spleen (**H**) and BM (**J**) on day 6 p.I. Data represent pooled results from two independent experiments, each experiment with 4-5 mice per group (total n=9 for WT and n=8 for T-bet$^{-/-}$). Data are presented as mean ± SEM. Statistical significance between groups was determined by Mann-Whitney U test as ns= not significant.

3.1.9 CD49b$^+$T-bet$^+$ antigen-specific CD4 T cells are detected at highest percentage in the BM

Albeit the unknown role of T-bet for BM memory CD4 T cells, the transcription factor is physiologically not required for the accumulation of antigen-specific CD4 T cells in the BM. Nonetheless, T-bet may serve as a potential marker for identification of antigen-specific memory CD4 T cell precursors in the spleen. In order to test this, T-bet-ZsGreen BAC Tg mice that express ZsGreen fluorescent protein under the control of *Tbx21* regulatory elements (172) were crossed to lymphocytic choriomeningitis virus (LCMV)- TCR (SMARTA) Tg mice, that express a TCR specific for the LCMV- epitope gp61-80 and can be identified by the expression of the congenic marker Thy1.1. Purified Thy1.1$^+$ T-bet-(ZsGreen) reporter LCMV-specific CD4 T cells were transferred into WT C57BL/6 mice followed by immunization with LCMV peptide $GP_{61–80}$ plus LPS. On day 6 after immunization, spleen, blood, and BM were analyzed for the accumulation of Thy1.1$^+$ LCMV-TCR specific CD4 T cells by flow cytometry (Figure 3.1.9 A-C). Intriguingly, CD49b$^+$T-bet$^+$ LCMV-specific CD4 T cells were detected at the lowest percentage in the spleen 13.7 % ± 1.8 SEM), at the midst in the blood (34.1 % ± 3.6 SEM), and at the highest in the BM (59.9 % ± 3.1 SEM) (Figure 3.1.9 B-C). The increasing percentages towards the BM suggest that CD49b$^+$T-bet$^+$ LCMV- specific CD4 T cells selectively migrate from the spleen into the BM via blood. These results further indicate that CD49b$^+$T-bet$^+$ antigen-specific CD4 T cells define the potential precursors of BM memory CD4 T cells.

The precursors of long-lived plasma cells egress from splenic B cell follicles towards the BM in a CXCR4-CXCL12-dependent manner via splenic red pulp and blood (181, 182). To examine the localization of T-bet$^+$ antigen-specific CD4 T cells in the spleen, a histological analysis was performed on above analyzed mice and the localization of T-bet$^+$ and T-bet$^-$ Thy1.1$^+$LCMV-TCR specific CD4 T cells was assessed by confocal microscopy (Figure 3.1.9 D). On day 6 after immunization, most T-bet (ZsGreen)$^-$ Thy1.1$^+$LCMV-TCR specific CD4 T cells remained in the white pulp, including B cell follicles and PALS. However, the majority of T-bet (ZsGreen)$^+$ Thy1.1$^+$LCMV-specific CD4 T cells localized in the red pulp, suggesting that T-bet (ZsGreen)$^+$ precursors of

BM memory CD4 T cells preferentially localize in splenic red pulp and migrate via blood towards the BM in a similar fashion as the precursors of long-lived plasma cells (183, 184).

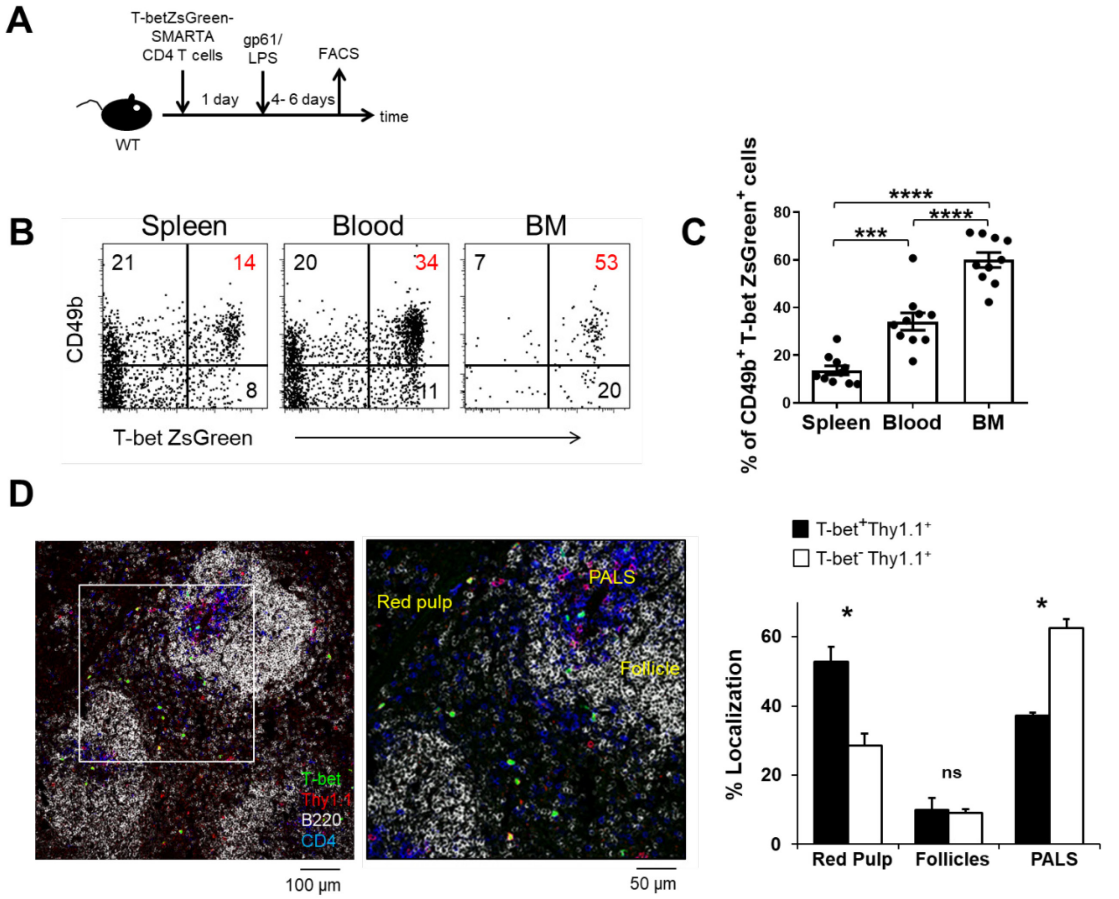

Figure 3.1.9: CD49b$^+$T-bet$^+$ antigen-specific CD4 T cells are detected at the highest percentage in the BM. **A:** Experimental outline. Purified Thy1.1$^+$ T-bet-ZsGreen reporter LCMV–TCR CD4 T cells were transferred into WT C57BL/6 mice followed by immunization with 100 µg LCMV-gp-61 and 10 µg LPS. On day 6 p.I. CD4$^+$Thy1.1$^+$B220$^-$NK1.1$^-$PI$^-$ cells in the spleen, blood, and BM were analyzed by flow cytometry for the expression of CD49b and T-bet-ZsGreen. **B:** Gating blots display CD49b and T-bet-ZsGreen expressing cells in a Thy1.1$^+$ population in CD4$^+$CD44^{hi}B220$^-$NK1.1$^-$PI$^-$ cells in the spleen, blood and BM. Percentages of CD49b$^+$T-bet-ZsGreen$^+$ cells are indicated in red. **C:** Bar graph displays percentages of CD49b$^+$T-bet-ZsGreen$^+$ cells in the spleen, blood and BM. Data represent pooled results from three independent experiments, each experiment with 3-4 mice (total n=10). Data are presented as mean ± SEM. Statistical significance between spleen, blood and BM was determined by unpaired Student's t test with Welch's correction as ****$p < 0.0001$ and ***$p < 0.001$. **D:** T-bet-expressing antigen-specific CD4 T cells preferentially egress from white pulp into red pulp. Localization of T-bet$^+$ (ZsGreen$^+$) Thy1.1$^+$ CD4 T cells in a spleen section. Frozen sections were prepared from the spleen of host mouse in Panel **B** was stained with anti-Thy1.1 (red), anti-B220 (gray), and anti-CD4 (blue) antibodies. Bar chart represents the localization of T-bet$^+$Thy1.1$^+$ and T-bet$^-$Thy1.1$^+$ cells in each area of the spleen. n=100-200 (from 3 mice). Data represent the mean ± SD. *$p < 0.05$. Student's t test.

3.1.10 Splenic CD49b$^+$CXCR3$^+$ antigen-specific CD4 T cells migrate into and remain in the BM

T-bet directly trans-activates the chemokine receptor CXCR3 (29, 185) and CXCR3 expression by T cells in lymph nodes has been assigned a potential role for the induction of CD8 and CD4 T cell memory (186-188).

In order to test whether CXCR3 is expressed in T-bet$^+$CD49b$^+$ BM memory CD4 T cell precursors, purified Thy1.1$^+$T-bet-ZsGreen reporter LCMV-TCR-specific CD4 T cells were transferred into WT C57BL/6 mice followed by immunization with LCMV peptide $GP_{61–80}$ plus LPS. On day 6 after immunization, splenic CD49b$^+$T-bet$^+$ (ZsGreen$^+$) Thy1.1$^+$ CD4 T cells were analyzed for the expression of CXCR3 by flow cytometry (Figure 3.1.10 A and B). While CD49b$^+$-single positive cells and CD49b$^-$T-bet (ZsGr)$^-$ (DN) cells only expressed low levels of CXCR3 (11.54 % ± 1.6 SEM and 7.9 % ± 0.9 SEM, respectively), 70.32 % (± 6.7 SEM) of CD49b$^+$T-betZsGr$^+$ cells highly expressed CXCR3. As anticipated, 44.2 % (± 4.6 SEM) of T-bet-ZsGr$^+$ -single positive cells also expressed CXCR3 (Figure 3.1.10 A and B).

To further analyze if CXCR3 is expressed in conjunction with CD49b on antigen-specific memory precursor and early memory CD4 T cells of the spleen and BM, purified Thy1.1$^+$ LCMV-TCR-specific CD4 T cells were transferred into WT C57BL/6 mice followed by immunization with LCMV peptide $GP_{61–80}$ plus LPS. On day 6 and 21 after immunization, spleen and BM cells were analyzed by flow cytometry (Figure 3.1.10 C). On day 6 after immunization, 13.76 % (± 1.66 SEM) of splenic Thy1.1$^+$ cells included CD49b$^+$CXCR3$^+$ cells, while this percentage slightly increased to 17.6 % (± 5.7 SEM) on day 21 after immunization (Figure 3.1.10 C). However, total splenic Thy1.1$^+$ cell numbers decreased significantly over time since the during the contraction phase most activated antigen-specific CD4 T cells undergo apoptosis. Already by day 6 after immunization, 68.2 % (± 7.5 SEM) of Thy1.1$^+$ cells were found to be CD49b$^+$CXCR3$^+$ cells in the BM. This population of BM Thy1.1$^+$ cells remained stable up to day 21 after immunization (70.6 % ± 7.5 SEM).

These results indicate that splenic activated antigen-specific CD49b$^+$CXCR3$^+$ CD4 T cells possess a BM tropism and that CXCR3 may be used as superior marker to T-bet for the identification of splenic precursors of BM memory CD4 T cells.

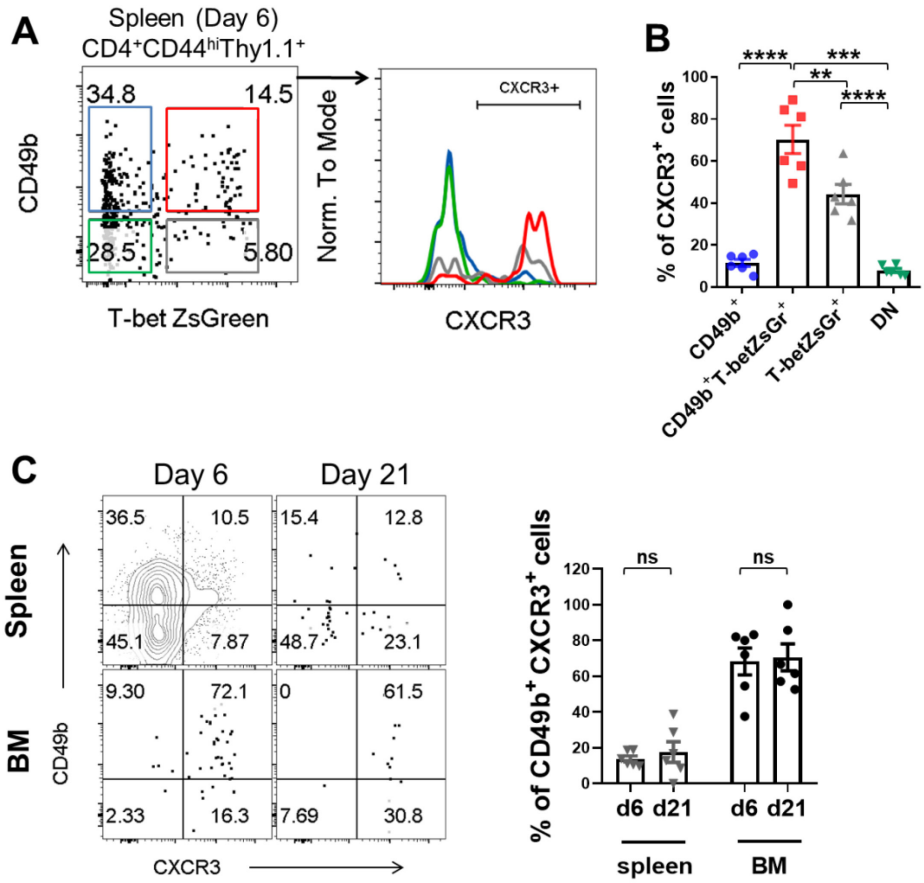

Figure 3.1.10: CD49b$^+$T-bet$^+$ antigen-specific CD4 T cells highly express CXCR3 and accumulate in the BM. **A:** Purified Thy1.1$^+$ T-bet-ZsGreen reporter LCMV–TCR CD4 T cells were transferred into C57BL/6 mice followed by immunization with 100 µg LCMV-gp-61 and 10 µg LPS. On day 6 p.l., the CD49b$^+$T-bet$^+$ (ZsGreen$^+$) population in CD4$^+$Thy1.1$^+$B220$^-$NK1.1$^-$PI$^-$ cells in the spleen was analyzed for the expression of CXCR3 by flow cytometry. Gating blot displays CD49b and T-betZsGreen expressing cells in a Thy1.1$^+$ population in CD4$^+$CD44^{hi}B220$^-$NK1.1$^-$PI$^-$ cells in the spleen on day 6 p.l. and further gating these populations (blue: CD49b$^+$, red: CD49b$^+$ T-bet ZsGreen$^+$, grey: T-bet ZsGreen$^+$, green: double negative (DN)) for their expression of CXCR3 (histogram). **B:** Bar graph displays percentages of CXCR3$^+$ cells in splenic subsets of CD49b and T-bet-ZsGreen expressing cells in CD4$^+$CD44^{hi}Thy1.1$^+$ cells. Data represent pooled results from two independent experiments with 3 mice per experiment (total n=6). Data are presented as mean ± SEM. Statistical significance between subsets was determined by one-way ANOVA with Tukey's multiple comparison test as ****$p < 0.0001$ and ***$p < 0.001$. **C:** Purified Thy1.1$^+$ LCMV–TCR CD4 T cells were transferred into C57BL/6 mice followed by immunization with 100 µg LCMV-gp-61 and 10 µg LPS. On days 6 and 21 p.l. the Thy1.1$^+$ cell population within CD4$^+$CD44^{hi}B220$^-$NK1.1$^-$PI$^-$ cells in spleen and BM was analyzed for the expression of CD49b and CXCR3 by flow cytometry (gating blots). Bar graph displays percentages of CD49b$^+$CXCR3$^+$ cells in splenic CD4$^+$CD44^{hi}Thy1.1$^+$ cells on day 6 and 21 p.l. in spleen and BM. Data represent pooled results from two independent experiments with 3 mice per experiment (total n=6). Data are presented as mean ± SEM. Statistical significance between groups was determined by Mann-Whitney U test as ns= not significant.

3.1.11 CD69 marks BM-resident memory CD4 T cells, but not their splenic precursors

In order to get insight into the heterogeneity of activated antigen-specific CD4 T cells with respect to CD49b and CD69 expression, T follicular helper cells were analysed after transfer of OVA-specific CD4 T cells into WT Balb/c host mice followed by immunization with OVA precipitated in the adjuvant aluminum hydroxide (Alum) which facilitates the induction of Tfh cells. On day 8 after immunization, OVA-specific Tfh cells were analyzed according to expression of CXCR5, PD-1 and Bcl-6 in relation to CD49b and CD69 expression indicating that the Tfh cell population does not include precursors of BM memory CD4 T cells since CD49b expression is crucial for the formation of BM CD4 T cell memory (Supplementary figure 1) (96, 98, 172).

In order to further investigate on the role of CD69 for the generation of BM memory CD4 T cells in relation to CD49b and T-bet/CXCR3 co-expression, BM MP CD4 T cells of WT Balb/c mice were analyzed (Figure 3.1.11 A and B). MP CD4 T cells of the BM comprised all four subpopulations of CD49b- and/or CXCR3- expressing cells although $CD49b^+CXCR3^+$ cells displayed the most frequent population. Interestingly, 54.7 % (± 2.8 SEM) of $CD49b^+CXCR3^+$ MP CD4 T cells included $CD69^+$ cells in the BM, of compared to 16.62 % (± 2.13 SEM) of $CD49b^+$ (single-positive) cells, 24.18 % (± 0.9 SEM) of $CXCR3^+$ (single-positive) and 23.5 % (± 2.3 SEM) of DN (double negative) cells (Figure 3.1.11 A and B).

Next, in order to assess the expression of CD69 in splenic antigen-specific $CD49b^+CXCR3^+$ memory precursor CD4 T cells, naïve OVA-specific CD4 T cells were transferred into WT Balb/c mice followed by immunization with OVA-peptide and LPS. On day 6 after immunization, the splenic $CD49b^+CXCR3^+$ population in $CD4^+OVA\text{-}TCR^+$ cells was analyzed by flow cytometry (Figure 3.1.11 C). Furthermore, the frequencies of $CD69^+$ cells in subpopulations of CD49b - and/or CXCR3 - expressing cells did not differ significantly from one another. However, $CXCR3^+$ (single positive) cells but not $CD49b^+CXCR3^+$ cells contained most $CD69^+$ cells with a frequency of 27.47 % (± 1.6 SEM) compared to the other sub-populations ($CD49b^+$: 15.07 % ± 0.45 SEM, $CD49b^+CXCR3^+$: 17.3 % ± 1.9 SEM, DN: 17.7 % ± 0.5 SEM).

In the memory phase (day 37 p.I.), only 2.1 % (± 0.15 SEM) of OVA-TCR- specific CD4 T cells in the spleen were co-expressing CD49b and CD69, whereas the BM contained 43.2 % (± 4.0 SEM) of $CD49b^+CD69^+$ cells within the pool of OVA-TCR-specific CD4 T cells by day 37 (Figure 3.1.11 F and G) indicating that CD69 is indeed a marker for BM memory CD4 T cells. While the spleen still hosted a minor population of 6.8 % (± 0.6

SEM) of CD49b$^+$CXCR3$^+$ cells by day 37 p.I., 63.6 % (± 6.8 SEM) of OVA-TCR-specific CD4 T cells in the BM were CD49b$^+$CXCR3$^+$ cells (Figure 3.1.11 F and H).

In sum this data indicates that CD69 may be seen as an activation marker, but not a memory precursor marker for splenic CD4 T cells. During the memory phase, CD49b, CD69 and CXCR3 are suitable markers to identify BM memory CD4 T cells.

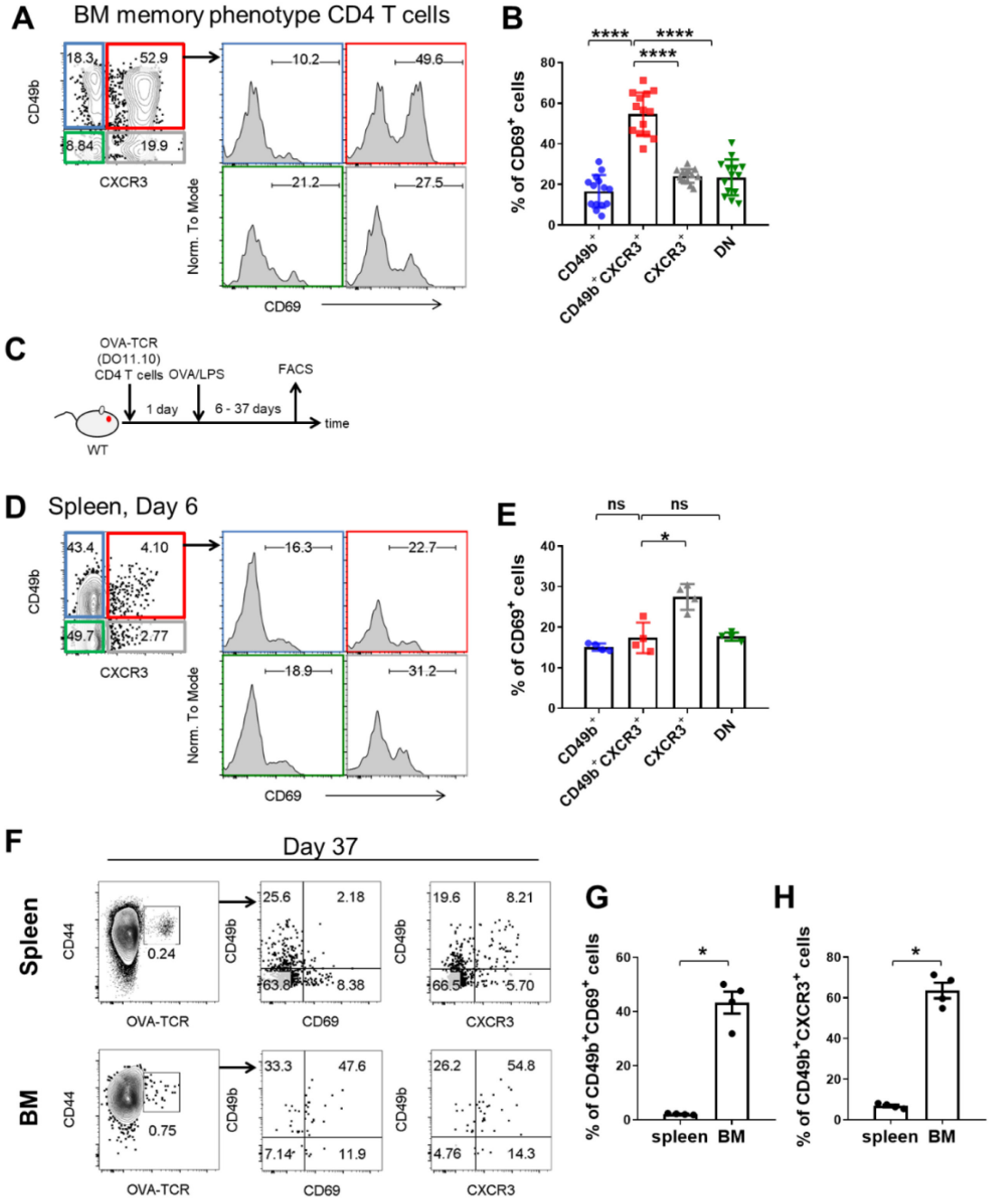

Figure 3.1.11: CD69 expression marks BM memory CD4 T cells but not their splenic precursors. **A:** Gating blot displays CD49b and CXCR3 expressing cells in memory phenotype CD4$^+$CD44^{hi}B220$^-$NK1.1$^-$PI$^-$ cells in the BM and further gating these populations (blue: CD49b$^+$, red: CD49b$^+$CXCR3$^+$, grey: CXCR3$^+$, green: double negative (DN)) displays their expression of CD69 (histograms). The percentage of CD69$^+$ cells in the respective subsets is indicated in the histogram. **B:** Bar graph displays percentages of CD69$^+$ cells in BM subsets of CD49b and CXCR3 expressing cells in memory phenotype CD4 T cells. Data represent pooled results from four experiments with 3-4 mice per experiment (total n=14). Data are presented as mean ± SEM. Statistical significance between subsets was determined by one-way ANOVA with Dunnett's multiple comparison test as ****$p < 0.0001$. **C:** Experimental outline. Purified OVA-TCR$^+$

(DO11.10) CD4 T cells were transferred into WT Balb/c mice followed by immunization with 100 µg OVA-peptide and 10 µg LPS. On day 6 or 37 p.I. OVA-TCR$^+$ CD4 T cells of spleen (d6, d37) or BM (d37) were analyzed by flow cytometry for the expression of CD49b, CXCR3 and CD69. **D:** Gating blot displays CD49b and CXCR3 expressing cells in OVA-TCR$^+$CD4$^+$CD44^{hi}B220$^-$NK1.1$^-$PI$^-$ T cells of the spleen on day 6 p.I. Further gating these populations (blue: CD49b$^+$, red: CD49b$^+$CXCR3$^+$, grey: CXCR3$^+$, green: double negative (DN)) displays their expression of CD69 (histograms). The percentage of CD69$^+$ cells in the respective subsets is indicated in the histogram. **E:** Bar graph displays percentages of CD69$^+$ cells in splenic subsets of CD49b and CXCR3 expressing cells in OVA-TCR$^+$CD4$^+$CD44^{hi}B220$^-$NK1.1$^-$PI$^-$ T cells on day 6 p.I. Data represent results from one experiment with n= 4. Data are presented as mean ± SEM. Statistical significance between subsets was determined by Kruskal-Wallis test with Dunn's multiple comparison as *$p < 0.05$ or ns= not significant. **F:** Gating blot displays OVA-TCR$^+$CD44^{hi} cells in spleen (upper blot) and BM (lower blot) on day 37 p.I. Further gating of OVA-TCR$^+$CD44^{hi} cells reveals expression pattern of CD49b and CD69 (middle blot) or CD49b and CXCR3 (right blot) in spleen (upper panel) and BM (lower panel) on day 37 p.I. The percentage of each subset is indicated in the respective gate. **G:** Bar graph displays percentages of CD49b$^+$CD69$^+$ cells in OVA-TCR$^+$CD4$^+$CD44^{hi}B220$^-$NK1.1$^-$PI$^-$ T cells in spleen and BM on day 37 p.I. N= 4. Data are presented as mean ± SEM. Statistical significance between groups was determined by Mann-Whitney U test as *$p < 0.05$. **H:** Bar graph displays percentages of CD49b$^+$CXCR3$^+$ cells in OVA-TCR$^+$CD4$^+$CD44^{hi}B220$^-$NK1.1$^-$PI$^-$ T cells in spleen and BM on day 37 p.I. N = 4. Data are presented as mean ± SEM. Statistical significance between groups was determined by Mann-Whitney U test as *$p < 0.05$.

3.2 CD49b$^+$CXCR3$^+$ precursors of BM memory CD4 T cells are generated via enhanced proliferation

The first part of this thesis suggests that splenic antigen-specific CD49b$^+$T-bet$^+$/CXCR3$^+$ CD4 T cells generated during a primary immune response include a population of cells that relocate to and remain in the BM throughout the memory phase and thus can be referred to as the precursors of BM memory CD4 T cells. In order to address the question how CD49b$^+$T-bet$^+$/CXCR3$^+$ precursors of BM memory CD4 T cells are generated in the spleen during a primary immune response, a comparative transcriptome analysis of sorted splenic antigen-specific CD49b$^+$ (single positive), CD49b$^+$T-bet$^+$ cells and DN (CD49b$^-$T-bet$^-$) cells harvested on day 6 after immunization was carried out. Interestingly, 57 and 27 genes involved in cell cycle activity and migration/homing, respectively, were differentially expressed in CD49b$^+$T-bet$^+$ antigen-specific CD4 T cells compared to CD49b$^+$-single positive cells or DN cells (fold change ≥2 or ≤0.5). Thus, differentially expressed candidates were validated on the protein level by flow cytometry and their role for the formation of precursors of BM memory CD4 T cells analyzed in the course of the second part of this thesis.

3.2.1 MP and antigen-specific CD49b$^+$CXCR3$^+$ CD4 T cells differentially express IL-2Rβ

IL-2 is known to be the major cytokine driving Th1 cell proliferation. After initial stimulation, naïve CD4 T cells secrete IL-2 which induces cell differentiation and increases the capacity of responding cells for memory survival and function (23, 127-130). To examine the role of IL-2 mediated signaling for the generation of CD4b$^+$CXCR3$^+$ memory precursors, at first, MP CD4 T cells of spleen and BM were analyzed for the expression of IL-2Rβ. As predicted from the transcriptome analysis, the expression of IL-2Rβ was significantly increased in CD49b$^+$CXCR3$^+$ MP CD4 T cells of the spleen (MFI 666.6 ± 43.12 SEM) compared to CD49b$^+$ (single positive) cells (MFI 282.6 ± 15.56 SEM), CXCR3$^+$ (single positive) cells (MFI 424.6 ± 21.14 SEM) or DN (double negative) cells (MFI 203.9 ± 9.1 SEM) (Figure 3.2.1 A and B). In the BM, the increased expression of IL-2Rβ in CD49b$^+$CXCR3$^+$ MP CD4 T cells was found to be even more prominent (CD49b$^+$: MFI 553.7 ± 19.21 SEM, CD49b$^+$CXCR3$^+$: MFI 1242 ± 29.63 SEM, CXCR3$^+$: MFI 726.9 ± 6.94 SEM, DN: MFI 485.1 ± 51.30 SEM) suggesting a decisive role for IL-2 signaling with regards to BM memory formation (Figure 3.2.1 C and D).

To further elucidate a potential role of increased IL-2Rβ expression for memory generation, purified Thy1.1$^+$LCMV-specific CD4 T cells were transferred into WT C57BL/6 mice followed by immunization with LCMV peptide $GP_{61–80}$ plus LPS. On day 6 after immunization, splenocytes were analyzed by flow cytometry. Thy1.1$^+$LCMV-TCR-specific CD49b$^+$CXCR3$^+$ cells contained slightly more IL-2$^+$ cells (13.48 % ± 1.45 SEM) than CD49b$^+$ (7.48 % ± 1.12 SEM) or CXCR3$^+$ (9.83 % ± 1.75 SEM), but included significantly more IL-2- producers than DN cells (4.76 % ± 0.54 SEM) (Figure 3.2.1. E and F).

The expression of IL-2Rβ by day 6 post immunization followed the same pattern as in MP CD4 T cells of the spleen. The major population including IL-2Rβ$^+$ cells in Thy1.1$^+$ LCMV-TCR-specific cells were CD49b$^+$CXCR3$^+$ (80.78 % ± 3.15 SEM) cells, followed by CXCR3$^+$ cells (67.78 % ± 4.38 SEM) and CD49b$^+$ cells (50.35 % ± 7.12 SEM). DN cells only included 43.7 % (± 5.87 SEM) of IL-2Rβ$^+$ cells (Figure 3.2.1. E and G).

Thus, this data indicated that IL-2 mediated signalling and the proliferative capacity of cells plays a role for BM memory CD4 T cell generation.

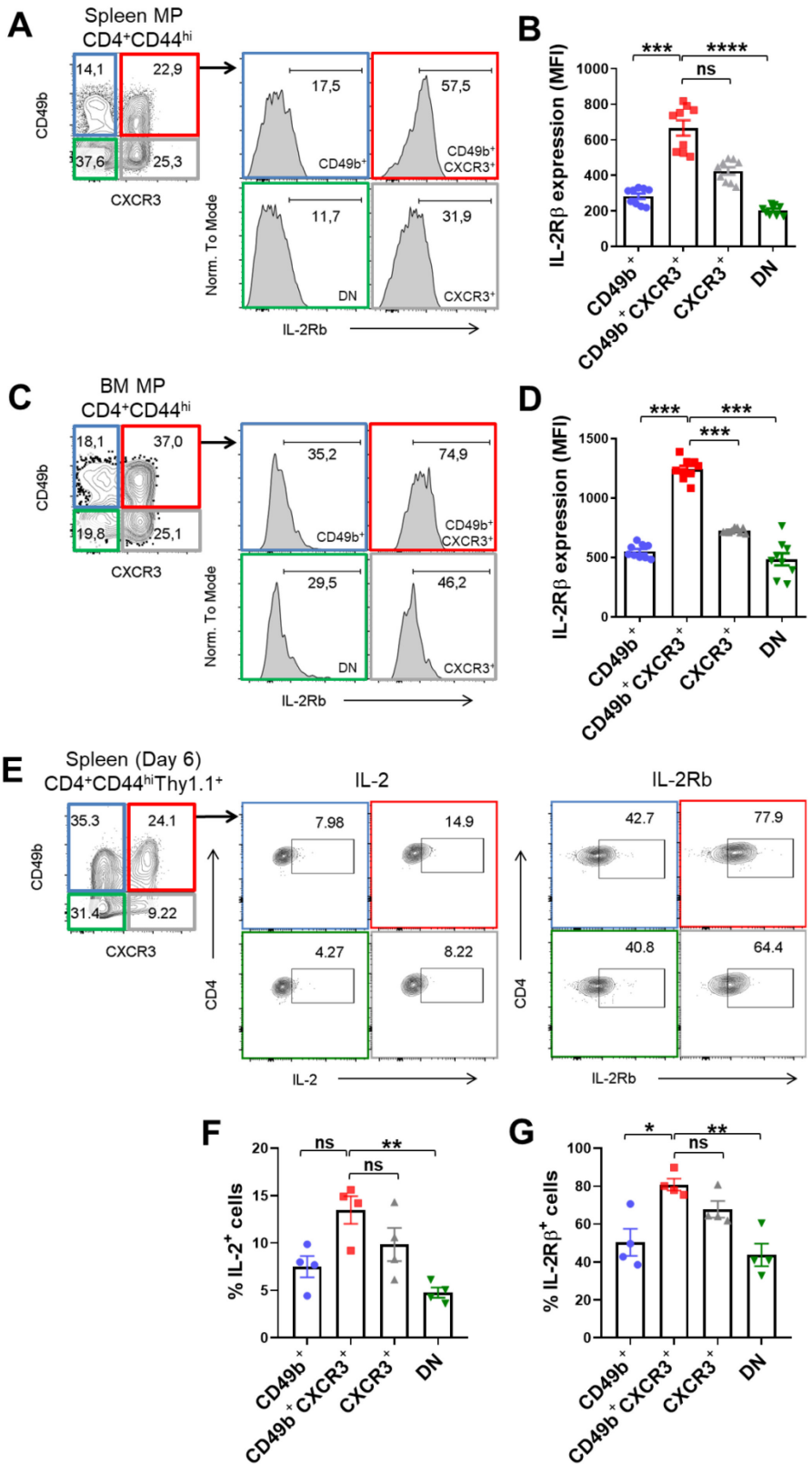

Figure 3.2.1: Memory phenotype and antigen-specific CD49b+CXCR3+ CD4 T cells differentially express IL-2Rb in spleen and BM. **A, B:** Gating blot displays CD49b and CXCR3 expressing cells in previously gated memory phenotype $CD4^+CD44^{hi}B220^-NK1.1^-PI^-$ cells in spleen (A) and BM (B). Further gating these populations (blue: $CD49b^+$, red: $CD49b^+CXCR3^+$, grey: $CXCR3^+$, green: double negative (DN)) displays their expression of IL-2Rb (histograms). The percentage of $IL\text{-}2Rb^+$ cells in the respective subsets is indicated in the histogram. **B, D:** Bar graph displays percentages of $IL\text{-}2Rb^+$ cells in spleen (B) and BM (D) subsets of CD49b and CXCR3 expressing cells in memory phenotype CD4 T cells. Data represent pooled results from two experiments with 4-5 mice per experiment (total n=9). Data are presented as mean ± SEM. Statistical significance between subsets was determined by Kruskal-Wallis test with Dunn's multiple comparison test as $^{***}p < 0.001$, $^{****}p < 0.0001$ and ns= not significant. **E:** Purified LCMV-TCR^+

(SMARTA, Thy1.1$^+$) CD4 T cells were transferred into WT C57BL/6 mice followed by immunization with 100 µg LCMV-peptide gp61-80 and 10 µg LPS. On day 6 p.I Thy1.1$^+$ CD4 T cells of the spleen were analyzed by flow cytometry for the expression of CD49b, CXCR3, IL-2Rb and intracellularly stained for IL-2. Gating blot displays CD49b and CXCR3 expressing cells in Thy1.1$^+$CD4$^+$CD44^{hi}B220$^-$NK1.1$^-$PI$^-$ T cells of the spleen on day 6 p.I. Further gating these populations (blue: CD49b$^+$, red: CD49b$^+$CXCR3$^+$, grey: CXCR3$^+$, green: double negative (DN)) displays their expression of IL-2 and IL-2Rb (contour blots).The percentage of IL-2$^+$ cells and IL-2Rb$^+$ cells in the respective subsets are indicated in above the gates. **F-G:** Bar graph displays percentages of IL-2$^+$ cells (**F**) or IL-2Rb+ cells (**G**) in splenic subsets of CD49b and CXCR3 expressing cells in Thy1.1$^+$CD4$^+$CD44^{hi}B220$^-$NK1.1$^-$PI$^-$ T cells on day 6 p.I. Data represent results from one experiment with n= 4. Data are presented as mean ± SEM. Statistical significance between subsets was determined by Kruskal-Wallis test with Dunn's multiple comparison as $^{**}p < 0.001$ or ns= not significant.

3.2.2 CD49b$^+$CXCR3$^+$ antigen-specific CD4 T cells differentially express Ki-67 on day 6 after immunization

Ki-67 is a marker strictly associated with cell proliferation and present during all active phases of the cell cycle (G_1, S, G_2, and mitosis), but is absent in resting (quiescent) cells (G_0) (189). To elaborate on the hypothesis that splenic CD49b$^+$CXCR3$^+$ precursors of BM memory CD4 T cells possess an increased proliferative capacity, purified Thy1.1$^+$LCMV-specific CD4 T cells were transferred into WT C57BL/6 mice followed by immunization with LCMV peptide $GP_{61–80}$ plus LPS. On day 4, 6 and 21 after immunization, splenic subsets of CD49b- and/or CXCR3- expressing cells in Thy1.1$^+$LCMV-TCR-specific CD4 T cells were analyzed for the percentage of Ki-67$^+$ cells (Figure 3.2.2). On day 4 after immunization, all subsets in Thy1.1$^+$CD44^{hi} LCMV-TCR-specific CD4 T cells positively stained for Ki-67 (Figure 3.2.2 A and D) (CD49b$^+$: 95.2 % ± 0.93 SEM, CD49b$^+$CXCR3$^+$: 95.8% ± 0.71 SEM, CXCR3$^+$: 95.8 % ± 0.77 SEM, DN: 95.7 % ± 0.83 SEM). Interestingly, with progression towards the beginning of the contraction phase by day 6, CD49b$^+$CXCR3$^+$ cells still contained 61.8 % (± 2.77 SEM) of Ki-67$^+$ cells, while percentages of Ki-67$^+$ cells decreased in other populations (CD49b$^+$: 28.4 % ± 3.5 SEM, CXCR3$^+$: 46.1 % ± 4.2 SEM, DN: 26.9 % ± 4.1 SEM) (Figure 3.2.2, B and D). However, during the early memory phase by day 21 after immunization, Thy1.1$^+$LCMV-TCR-specific CD4 T cells only included minor frequencies of Ki-67$^+$ cells regardless of CD49b and CXCR3 expression (CD49b$^+$: 3.4 % ± 2.2 SEM, CD49b$^+$CXCR3$^+$: 2.44 % ± 0.7 SEM, CXCR3$^+$: 2.7 % ± 1.66 SEM, DN: 2.6 % ± 0.88 SEM) demonstrating that by day 21 after immunization the cells are not proliferating anymore (Figure 3.2.2, C and D).

The BM harbored comparable percentages of Ki-67$^+$ cells within polyfunctional endogenous MP CD4$^+$CD44^{hi} T cells (27.9 % ± 1.48 SEM) on day 6 and day 21 (26.47 % ± 1.31 SEM) after immunization (Figure 3.2.2. E and F). Correspondingly, also endogenous naïve CD44^{lo} CD4 T cells included comparable percentages of Ki-67$^+$ cells on day 6 (7.4 % ± 0.52 SEM) and day 21 (8.8 % ± 0.57 SEM) after immunization, indicating that the immunization with LPS itself did not affect the endogenous CD4 T cell compartment in the BM (Figure 3.2.2. E and F). Interestingly, Thy1.1$^+$ LCMV-specific CD4 T

cells included 15.56 % (± 0.6 SEM) Ki-67$^+$ cells on day 6 after immunization, whereas this percentage decreased to 6.82 % (± 0.95 SEM) of Ki-67$^+$ cells on day 21 after immunization and thus reflected the percentage of Ki-67$^+$ cells in the endogenous naïve CD4 T cell compartment (Figure 3.2.2 E and F).

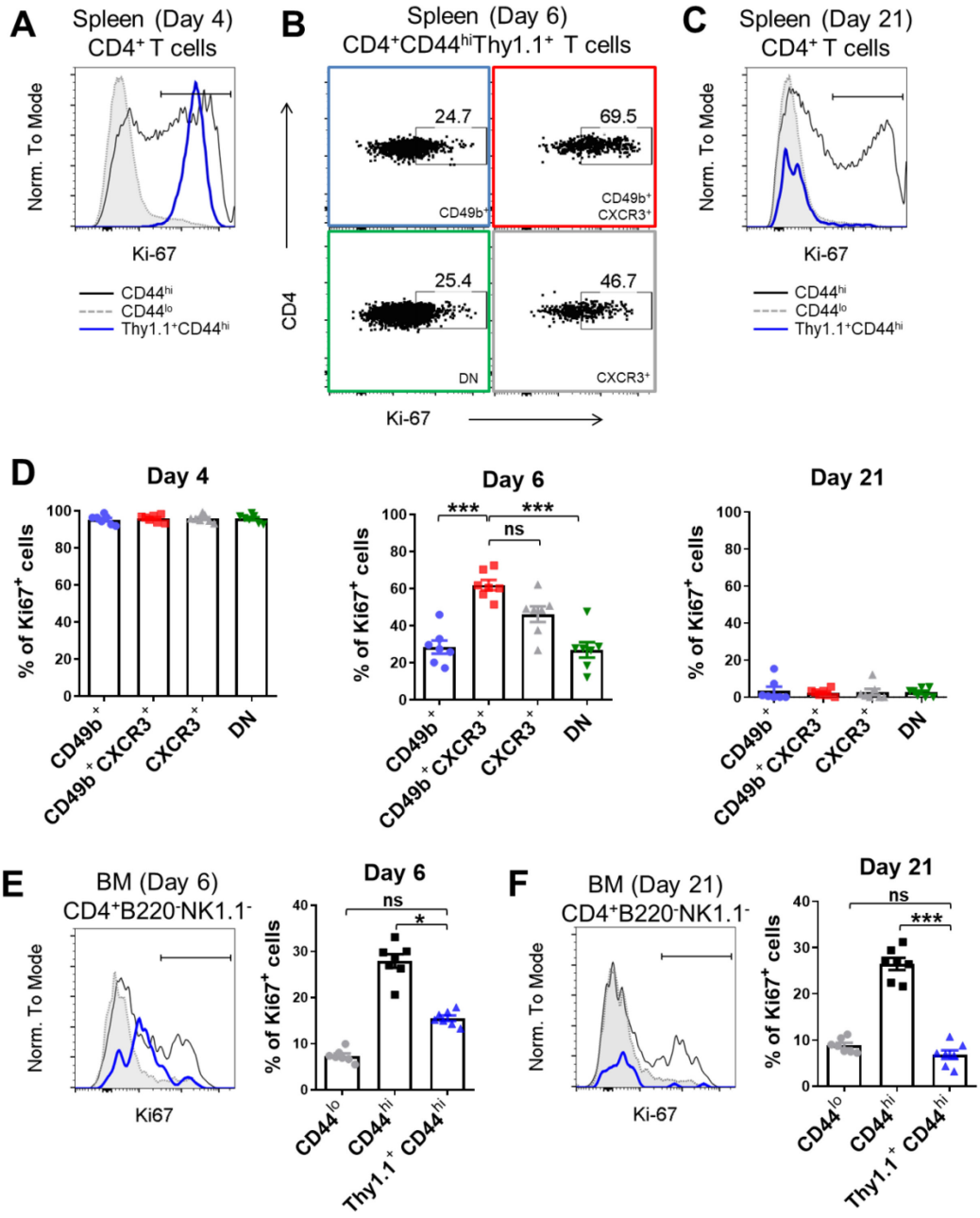

Figure 3.2.2: Antigen-specific CD49b$^+$CXCR3$^+$ CD4 T cells differentially express the proliferation marker Ki-67 on day 6 p.I. Purified Thy1.1$^+$ LCMV–TCR CD4 T cells were transferred into WT C57BL/6 mice followed by immunization with 100 µg LCMV-gp-61 and 10 µg LPS. On days 4, 6 and 21 p.I., Thy1.1$^+$ cell population within CD4$^+$CD44^{hi}B220$^-$NK1.1$^-$PI$^-$ cells in spleen and BM (day 6 and 21) was analyzed. **A:** Histogram displays Ki-67 expression levels in splenic CD4$^+$CD44^{lo} (dashed grey), CD4$^+$CD44^{hi} (black) and Thy1.1$^+$CD4$^+$CD44^{hi} cells on day 4 p.I. **B:** Dot blots display Ki-67 expression in splenic subsets of CD49b and CXCR3 expressing cells in Thy1.1$^+$CD4$^+$CD44^{hi} cells on day 6 p.I. (CD49b$^+$ cells: blue frame, CD49b$^+$CXCR3$^+$ cells: red frame, CXCR3$^+$ cells: grey frame, DN (double negative) cells: green frame) **C:** Histogram displays Ki-67 expression levels in splenic CD4$^+$CD44^{lo} (dashed grey), CD4$^+$CD44^{hi} (black) and Thy1.1$^+$CD4$^+$CD44^{hi} (blue) cells on day 21 p.I. **D:** Bar graph displays percentages of Ki-67$^+$ cells within splenic Thy1.1$^+$CD4$^+$CD44^{hi} cell subsets of CD49b and CXCR3 expressing cells on day 4 (left bar graph), day 6 (middle bar graph) and day 21 (right bar graph) p.I. **E:** Histogram displays Ki-67 expression levels in BM CD4$^+$CD44^{lo} (dashed grey), CD4$^+$CD44^{hi} (black) and Thy1.1$^+$CD4$^+$CD44^{hi} cells on day 6 p.I. Bar graph displays percentages of Ki-67$^+$ cells within CD4$^+$CD44^{lo} cells, CD4$^+$CD44^{hi} cells and Thy1.1$^+$CD4$^+$CD44^{hi} cells in the BM on day 6

p.l. **F:** Histogram displays Ki-67 expression levels in BM $CD4^+CD44^{lo}$ (dashed grey), $CD4^+CD44^{hi}$ (black) and $Thy1.1^+CD4^+CD44^{hi}$ cells on day 21 p.l. Bar graph displays percentages of $Ki\text{-}67^+$ cells within $CD4^+CD44^{lo}$ cells, $CD4^+CD44^{hi}$ cells and $Thy1.1^+CD4^+CD44^{hi}$ cells in the BM on day 21 p.l. **A-F:** Data represent pooled results from two independent experiments with 3-4 mice per experiment (total n=7). Data are presented as mean ± SEM. Statistical significance between subsets was determined by Kruskal-Wallis test with Dunn's multiple comparison test as $^{***}p < 0.001$, $^{*}p < 0.05$ and ns= not significant

3.2.3 $CD49b^+CXCR3^+$ antigen-specific CD4 T cells are highly proliferative and develop after 7 rounds of cell division

To examine how many rounds of cell division are required for the generation of $CD49b^+CXCR3^+$ precursors of BM memory CD4 T cells, purified carboxyfluorescein diacetate succinimidyl ester (CFSE)-labeled $Thy1.1^+$LCMV-TCR specific CD4 T cells were transferred into WT C57BL/6 mice followed by immunization with LCMV peptide $GP_{61–80}$ plus LPS. CFSE is commonly applied to monitor lymphocyte proliferation, owing to the progressive halving of CFSE fluorescence within daughter cells following each cell division (190).

On day 5 after immunization, splenic subsets of CD49b- and/or CXCR3-expressing $Thy1.1^+$LCMV-TCR specific CD4 T cells were analyzed for experienced rounds of cell division in terms of CFSE dilution. Day 5 was chosen, as by day 6 after immunization some cells have already undergone more than 8 rounds of cell division and CFSE fluorescence was too low to be distinguished above the auto fluorescence background. On day 5 after immunization, 80.36 % (± 3.98 SEM) of $CD49b^+CXCR3^+$ cells had experienced more or equal to 7 cell divisions, representing the most proliferated population. While 63.8 % (± 5.28 SEM) of $CXCR3^+$- single positive cells also experienced more than 7 cell divisions, only 47.03 % (± 6.73 SEM) of $CD49b^+$- single positive and 41.7 % (± 6.7 SEM) of double-negative cells (DN) included $CFSE^+$ cells that had divided ≥ 7 times (Figure 3.2.3 B). Interestingly, in the BM, 84.9 % (± 5.17 SEM) of $Thy1.1^+$LCMV-TCR specific CD4 T cells that could be detected on day 5 after immunization had experienced more than 7 cell divisions (Figure 3.2.3 E). Furthermore, $CD49b^+CXCR3^+$ cells are only generated after 7 rounds of cell division as determined by the inverse analysis of $Thy1.1^+$LCMV-TCR specific CD4 T cells (Figure 3.2.3 D).

This result consolidates the finding that, antigen-specific $CD49b^+CXCR3^+$ precursors of BM memory CD4 T cells include more proliferating ($Ki\text{-}67^+$) cells (Figure 3.2.2) and furthermore indicates that $CD49b^+CXCR3^+$ cells are generated via accelerated cell proliferation and have experienced more cell divisions within the first days after activation compared to other sub-populations.

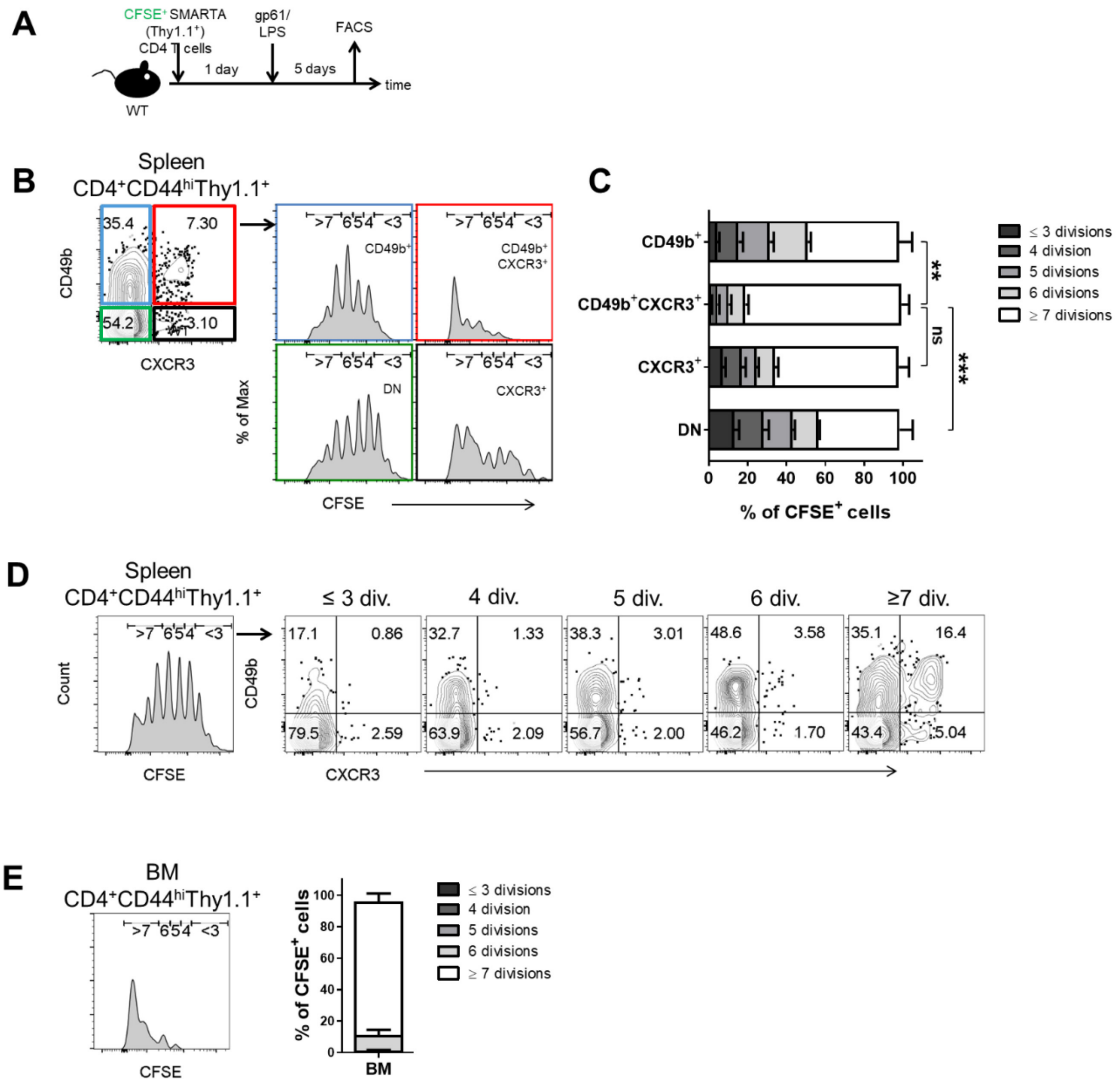

Figure 3.2.3: CD49b$^+$CXCR3$^+$ activated CD4 T cells are highly proliferative. **A:** Experimental outline. Purified CFSE-labeled Thy1.1$^+$ LCMV-TCR-specific CD4 T cells were transferred into WT C57BL/6 mice followed by immunization with 100 µg LCMV-gp-61 and 10 µg LPS. On day 5 p.I. Thy1.1$^+$ cells in spleen and BM were analyzed by flow cytometry. **B:** Gating plot (left) shows subsets of CD49b- and CXCR3- expressing cells within CD4$^+$CD44^{hi}Thy1.1$^+$B220$^-$NK1.1$^-$PI$^-$. The subsets are indicated by different colours (CD49b$^+$ -blue, CD49b$^+$CXCR3$^+$ -red, CXCR3$^+$ -black, DN -green). Further gating of those subsets allows for display of rounds of cell division that CFSE-labeled Thy1.1$^+$ cells have undergone by by day 5 p.I. (gates in histograms). **C:** Bar chart represents the percentages of CFSE$^+$ cells in each subset of CD49b- or CXCR3-expressing cells with regards to the number of rounds of cell division the subset has undergone by day 5 p.I. **D:** Gating plots display the subsets of CD49b and CXCR3 expressers in different divided generations of CFSE$^+$Thy1.1$^+$ cells (histogram) from **(B)**. **E:** Gatin plot displays populations of CFSE$^+$Thy1.1$^+$ cells in the BM. Bar graph displays quantification of experienced round of cell division in CFSE$^+$Thy1.1$^+$ cells by day 5 p.I. **B-E:** Data represent pooled results from three independent experiments with 3-4 mice per experiment (total n=10). Data are presented as mean ± SEM. Statistical significance between CD49b$^+$ and/or CXCR3$^+$ subsets that have undergone more than 7 rounds of cell division was determined by Kruskal-Wallis test with Dunn's multiple comparison test as $^{**}p < 0.01$, $^{***}p < 0.001$ or ns= not significant.

3.2.4 CD49b$^+$CXCR3$^+$ antigen-specific CD4 T cells are cycling even at late stages of the primary immune response

To examine if CD49b$^+$CXCR3$^+$ precursors of memory CD4 T cells continuously proliferate beyond the peak of the primary immune response (that is, day 4 after immunization), purified Thy1.1$^+$LCMV-specific CD4 T cells were transferred into WT C57BL/6 mice followed by immunization with LCMV peptide $GP_{61–80}$ plus LPS. Subsequently, mice were divided into 3 groups either receiving 6 x 1 mg BrdU (6x BrdU) i.p. on days 0 to 5, 1 x 1 mg BrdU (1x BrdU) on day 5 p.I. or no treatment (no BrdU) (Figure 3.2.4 A). At sufficient concentrations, BrdU incorporates as a thymidine substitute into newly synthesized DNA of replicating cells and can be detected by BrdU-specific antibodies upon DNA denaturation. On day 6 after immunization, splenic Thy1.1$^+$LCMV-TCR-specific CD4 T cells were analyzed for expression of CD49b and CXCR3 in relation to incorporation of BrdU.

Even though the effect of BrdU itself on the proliferation of activated dividing T cells has been a matter of contrary debate in the field (73, 191), no significant difference in the percentage of Thy1.1$^+$LCMV-specific CD4 T cells was detected regardless of BrdU treatment (No BrdU: 3.78 % ± 0.32 SEM, 6x BrdU: 3.44 % ± 0.42 SEM, 1x BrdU: 4.56 % ± 0.47 SEM) (Figure 3.2.4 B).

The analysis of CD49b- and CXCR3-expressing subpopulations within Thy1.1$^+$LCMV-TCR-specific CD4 T cells regarding incorporation of BrdU revealed that all subsets included comparable percentages of BrdU$^+$ cells after 6 BrdU injections (CD49b$^+$: 44.56 % ± 4.48 SEM, CD49b$^+$CXCR3$^+$: 47.18 % ± 3.9 SEM, CXCR3$^+$: 42.34 % ± 3.62 SEM, DN: 37.1 % ± 3.84 SEM). In turn, mice that received only one injection of BrdU on day 5 after immunization, included significantly more BrdU$^+$ cells within the CD49b$^+$CXCR3$^+$ population at 11.03 % (±1.82 SEM) compared to CD49b$^+$ (2.67 % ± 0.75 SEM), CXCR3$^+$ (5.18 % ± 0.71 SEM) or DN cells (2.08 % ± 0.34 SEM) (Figure 3.2.4 E and F).

Comparable results have been obtained in a third independent experiment (Supplementary Figure 2). Data could not be pooled here, since an amended flow cytometric staining panel was used in the supplemetary experiment.

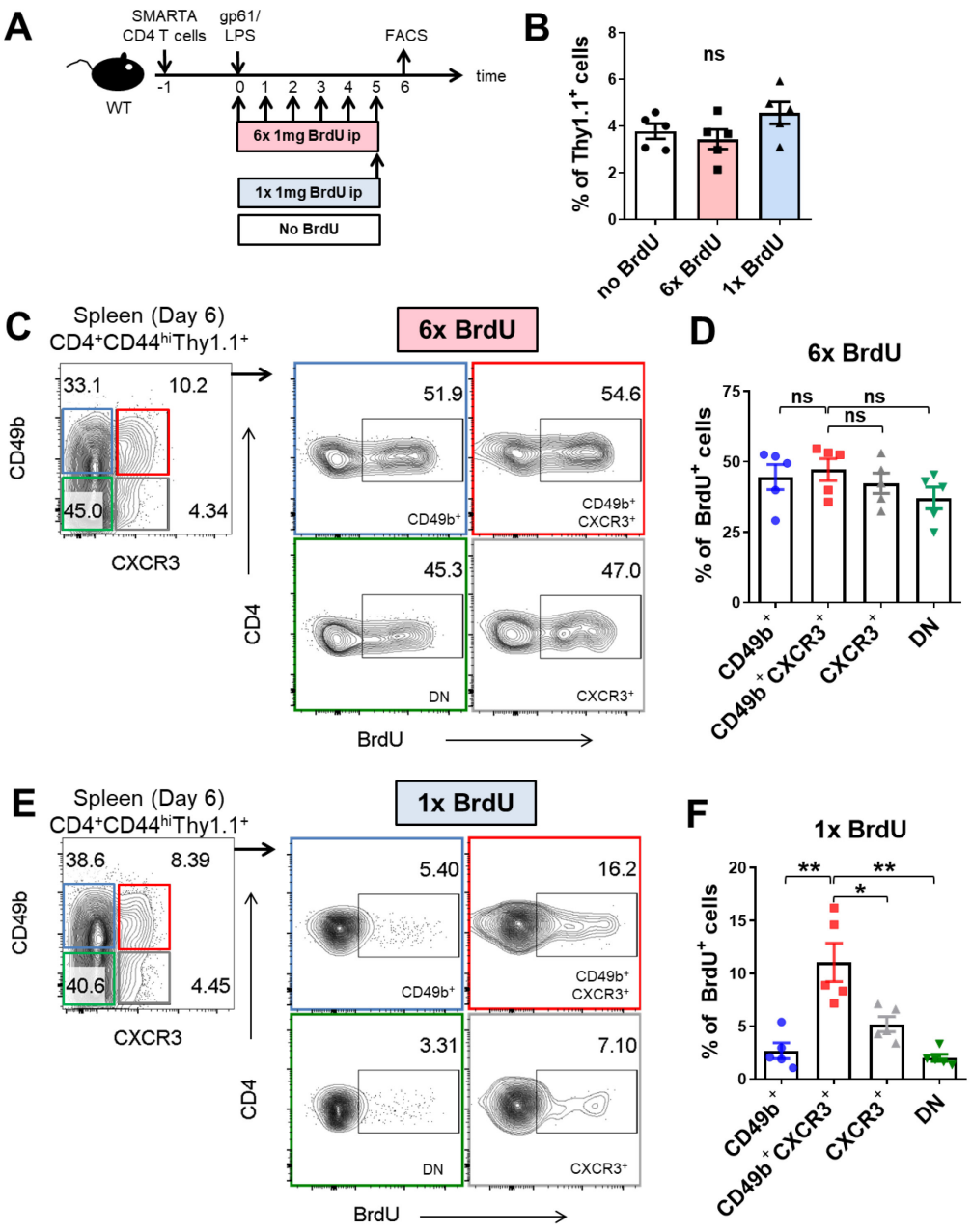

Figure 3.2.4: Antigen-specific CD49b$^+$CXCR3$^+$ CD4 T cells incorporate more BrdU than other subsets at the beginning of the contraction phase of a primary immune response. **A:** Experimental outline. Purified Thy1.1$^+$ LCMV-TCR CD4 T cells were transferred into WT C57BL/6 mice followed by immunization with 100 µg LCMV-gp-61 and 10 µg LPS. Mice were injected intraperitoneally with 1 mg BrdU on days 0-5 (6x BrdU) or day 5 (1x BrdU) after immunization. On day 6 p.I. splenocytes were analyzed by flow cytometry for incorporation of BrdU in subsets of CD49b and CXCR3 expressing Thy1.1$^+$LCMV-TCR CD4 T cells. **B:** Intraperitoneal treatment with BrdU does not alter frequencies in splenic Thy1.1$^+$CD44^{hi} CD4 T cells. Bar graph displays percentages of Thy1.1$^+$CD44^{hi} CD4 T cells on day 6 p.I. in the spleen of untreated (no BrdU - white bar), 6x BrdU treated (pink bar) or 1x BrdU treated (blue bar) mice. **C:** Contour plots display BrdU$^+$ cells in previously gated splenic subsets of CD49b and CXCR3 expressing CD4$^+$CD44^{hi}Thy1.1$^+$ cells in mice that were treated 6x with 1 mg BrdU. **D:** Bar graph displays percentages of BrdU$^+$ cells in subsets of CD49b and CXCR3 expressing cells after 6x BrdU treatment. **E:** Contour plots display BrdU$^+$ cells in previously gated splenic subsets of CD49b and CXCR3 expressing CD4$^+$CD44^{hi}Thy1.1$^+$ cells in mice that were treated 1x with 1 mg BrdU on day 5 p.I. and analyzed on day 6 p.I. **F:** Bar graph displays percentages of BrdU$^+$ cells in subsets of CD49b and CXCR3 expressing cells after 1x BrdU treatment. **B-F:** Data represent pooled results from two independent experiments with 1-4 mice per experiment (total n=5). Data are presented as mean ± SEM. Statistical significance between subsets was determined by Kruskal-Wallis test with Dunn's multiple comparison test as *$p < 0.05$, **$p < 0.01$ or ns= not significant.

3.2.5 Increased proliferation of splenic CD49b$^+$CXCR3$^+$ antigen-specific CD4 T cells can be blocked by cyclophosphamide

To determine if the generation of highly proliferative CD49b$^+$CXCR3$^+$ precursors of BM memory CD4 T cells can be blocked at a late stage of the primary immune response, purified Thy1.1$^+$LCMV-specific CD4 T cells were transferred into WT C57BL/6 mice followed by immunization with LCMV peptide $GP_{61–80}$ plus LPS.

On day 5 after immunization, mice were treated with 50 mg/kg body weight of the cytostatic drug cyclophosphamide (CyP). CyP is nitrogen mustard that adds alkyl groups to DNA leading to cross-linking of DNA which in turn impairs replication and thus directs cells attempting to divide into apoptosis (192). On day 6 after immunization, splenic Thy1.1$^+$LCMV-specific CD4 T cells were enumerated and analyzed for expression of CD49b and CXCR3 by flow cytometry (Figure 3.2.5 A). CyP treatment significantly reduced the frequency of CD49b$^+$CXCR3$^+$ cells in Thy1.1$^+$LCMV-TCR-specific CD4 T cells compared to a PBS control group (PBS: 10.3 % ± 0.88 SEM; CyP: 6.63 % ± 0.38 SEM) (Figure 3.2.5 B) demonstrating that the enhanced proliferative capacity of CD49b$^+$CXCR3$^+$ memory precursors can be abolished by treatment with CyP.

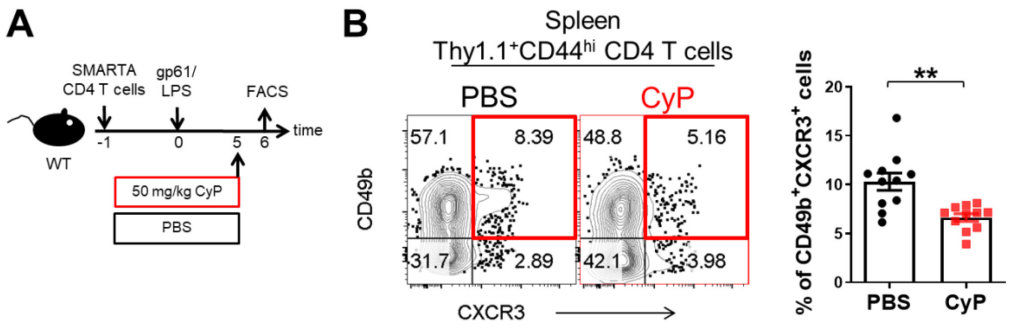

Figure 3.2.5: Cyclophosphamide treatment on day 5 p.i. reduces frequencies of CD49b$^+$CXCR3$^+$ memory Th cell precursors. **A:** Experimental outline. Purified Thy1.1$^+$ LCMV-TCR CD4 T cells were transferred into C57BL/6 mice followed by immunization with 100 µg LCMV-gp-61 and 10 µg LPS. On day 5 p.i. mice were treated intravenously with 50 mg/kg CyP or PBS. Mice were analyzed by flow cytometry on day 6 p.i. **B:** Gating plots display the expression of CD49b and CXCR3 within splenic Thy1.1$^+$ CD44^{hi} CD4$^+$ B220$^-$ NK1.1$^-$ PI$^-$ cells of CyP- or PBS-treated mice. Bar chart displays the percentage of CD49b$^+$CXCR3$^+$ cell population comparing CyP- and PBS-treated mice (framed in red in gating plot). Data represent pooled results from four independent experiments with 3-4 mice per experiment (total n=11 per group). Data are presented as mean ± SEM. Statistical significance between groups was determined by unpaired Student's t test as $^{**}p < 0.001$.

3.2.6 Late costimulatory blocking by CTLA-4 Ig impairs the expansion of CD49b$^+$CXCR3$^+$ antigen-specific CD4 T cells

Effector to memory T cell transition has been suggested to require late cognate interactions (127). In order to elucidate, whether the observed enhanced proliferation of CD49b$^+$CXCR3$^+$ precursors of BM memory CD4 T cells depends on late cognate APC:T cell interactions, an immunohistological approach was conducted. To that end, purified Thy1.1$^+$T-bet-(ZsGreen) reporter LCMV-TCR-specific CD4 T cells were transferred into WT C57BL/6 mice followed by immunization with LCMV peptide $GP_{61–80}$ plus LPS. On day 6 after immunization, spleen sections were cut and interactions of Thy1.1$^+$T-bet (ZsGreen$^+$) cells in contact with CD11c$^+$ DCs in the PALS quantified. Intriguingly, about 60 % of Thy1.1$^+$T-bet$^+$ were in contact with CD11c$^+$ cells whereas merely 26 % of Thy1.1$^+$T-bet$^-$ and 22 % of Thy1.1$^-$T-bet$^-$ endogenous CD4 T cells were found to be in contact with CD11c$^+$ DCs (Figure 3.2.6 A and B).

Costimulatory signals are crucial for T cell activation and differentiation and the CD28/B7 costimulatory pathway is required for activation of naïve CD4 T cells (193). To examine to which extent CD49b$^+$CXCR3$^+$ memory precursor formation depends on late costimulatory signals, blockage of the CD28-CD80/CD86 pathway with CTLA-4 Ig fusion protein was performed. The CTLA-4 Ig fusion protein binds with high avidity CD80/CD86 ligands and thus potently blocks naïve CD4 T cell activation and proliferation (194, 195, 196). To that end, purified Thy1.1$^+$LCMV-TCR specific CD4 T cells were transferred into WT C57BL/6 mice followed by immunization with LCMV peptide $GP_{61–80}$ plus LPS. On day 4 and 5 after immunization mice received either 200 µg CTLA-4 Ig or an isotype matched human IgG control (hu-IgG). On day 6 after immunization, splenic Thy1.1$^+$LCMV-TCR-specific CD4 T cells were analyzed by flow cytometry (Figure 3.2.6 C and D).

As anticipated, CTLA-4 Ig treatment reduced the frequency of CD49b$^+$CXCR3$^+$ cells significantly compared to hu-IgG control group (hu-IgG: 7.85 % ± 0.37 SEM; CTLA4-Ig: 5.17 % ± 0.42 SEM) (Figure 3.2.6 D). This result indicates that co-stimulatory signals via the CD28-CD80/CD86 pathway are crucial for the generation of CD49b$^+$CXCR3$^+$ memory precursor cells which continue being generated beyond the peak of the primary immune response by day 4 after immunization.

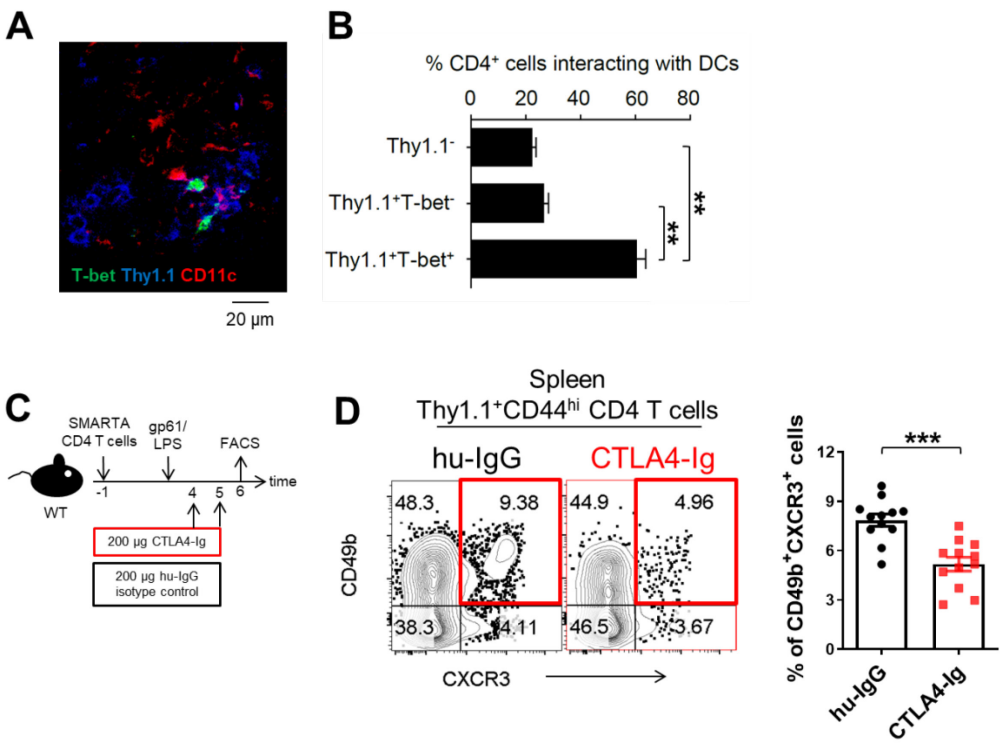

Figure 3.2.6: Formation of CD49b$^+$CXCR3$^+$ LCMV-TCR specific memory precursor CD4 T cells requires late cognate interactions and co-stimulatory signaling. **A:** Localization of T-bet$^+$ (ZsGreen$^+$) Thy1.1$^+$ CD4 T cells in a spleen section. Purified Thy1.1$^+$T-bet-ZsGreen reporter LCMV–TCR specific CD4 T cells were transferred into WT C57BL/6 mice followed by immunization with 100 µg LCMV-gp-61 and 10 µg LPS. On day 6 p.I. a frozen spleen sections were prepared and stained with anti-Thy1.1 (blue), anti-CD11c (red) and anti-CD4. **B:** Thy1.1$^-$ (endogenous CD4$^+$), T-bet$^-$Thy1.1$^+$ and T-bet$^+$Thy1.1$^+$ cells in contact with CD11c$^+$ cells in the PALS. Scale bar 20 µm. n=100-200 (from 3 mice). Data are shown as mean ± SD. Statistical significance between groups was determined by unpaired Student's t test as $^{**}p < 0.01$. **C:** Experimental outline. Purified Thy1.1$^+$LCMV-TCR CD4 T cells were transferred into WT C57BL/6 mice followed by immunization with 100 µg LCMV-gp-61 and 10 µg LPS. On day 4 and 5 p.I. mice were injected intraperitoneally with 200 µg CTLA-4 Ig or 200 µg human IgG. Mice were analyzed by flow cytometry on day 6 p.I. **D:** Gating plot displays subsets of CD49b and CXCR3 expressing cells in Thy1.1$^+$CD4$^+$CD44^{hi}B220$^-$NK1.1$^-$PI$^-$ cells of hu-IgG or CTLA4-Ig treated animals. Numbers indicate percentages. Bar chart displays the percentage of subsets of CD49b$^+$CXCR3$^+$ cells comparing hu-IgG and CTLA-4 Ig treated mice. Data represent pooled results from three independent experiments with 3-5 mice per experiment (total n=12). Data are presented as mean ± SEM. Statistical significance between groups was determined by unpaired Student's t test as $^{***}p < 0.001$.

3.2.7 Highly proliferated CD49b$^+$CXCR3$^+$ antigen-specific CD4 T cells quickly downregulate CCR7 expression and upregulate IL-2Rβ expression

It was previously described that BM resting memory CD4 T cells do not express CCR7 and are enriched for IL-2Rβ expression (96). CCR7 is a chemokine receptor that regulates T cell trafficking and compartmentalization within SLO. Although CCR7$^{-/-}$ T cells migrate to the spleen, they however fail to move into the PALS and remain in the red pulp. In turn, in order to leave the PALS, activated T cells must downregulate CCR7 (85, 197). Consequently, as shown above (Figure 3.1.9), CD49b$^+$T-bet$^+$ precursors of memory CD4 T cells start to re-locate from PALS to red pulp by day 6 after immunization.

To assess the expression of CCR7 in conjunction with IL-2Rβ, purified Thy1.1$^+$LCMV-specific CD4 T cells were transferred into WT C57BL/6 mice followed by immunization with LCMV peptide $GP_{61–80}$ plus LPS. On day 6 after immunization, CD49b$^+$CXCR3$^+$ LCMV-TCR-specific CD4 T cells included a major population of 23.3 % (± 2.78 SEM) IL-2Rβ$^+$CCR7^{lo} cells. While CXCR3$^+$- single positive cells also included a notable population of 12.36 % (± 1.53 SEM) IL-2Rβ$^+$CCR7^{lo} cells, CD49b$^+$- single positive cells (1.28 % ± 0.51 SEM) and DN cells (0.86 % ± 0.21 SEM) completely lacked this population (Figure 3.2.7 A-C). Notably, 63.5 % (± 3.7 SEM) of antigen-specific Thy1.1$^+$ CD4 T cells in the BM are IL-2Rb$^+$CCR7^{lo} cells (Figure 3.2.7 B-C).

To assess the kinetics of CCR7 downregulation in highly proliferating CD49b$^+$CXCR3$^+$ precursors of BM memory CD4 T cells, purified CFSE-labeled Thy1.1$^+$LCMV-specific CD4 T cells were transferred into WT C57BL/6 mice followed by immunization with LCMV peptide $GP_{61–80}$ plus LPS. On day 5 after immunization, CD49b$^+$CXCR3$^+$ splenic precursors of BM memory CD4 T cells were analyzed by flow cytometry for experienced cell divisions by means of CFSE with regard to the expression of CCR7 and IL-2Rβ (Figure 3.2.7 D-F). Expression of CCR7 was lowest in CD49b$^+$CXCR3$^+$ cells that have experienced ≥ 7 cell divisions (GMFI ≥7 div: 4593 ± 191 SEM) gradually decreasing with every round of cell division (GMFI div 5: 6601 ± 228 SEM; GMFI div 6: 6074 ± 280.9 SEM) and highest in less proliferated cells (GMFI 4 div: 7948 ± 357 SEM). On the contrary, IL-2Rβ expression increased gradually with growing numbers of cell divisions that CD49b$^+$CXCR3$^+$ cells have experienced (GMFI 4 div: 6215 ± 169 SEM; GMFI 5 div: 6836 ± 122.6 SEM; GMFI 6 div: 7553 ± 161.4 SEM; GMFI ≥7 div: 8262 ± 295 SEM). These results underline that CD49b$^+$CXCR3$^+$ precursors of BM memory CD4 T cells significantly upregulate IL-2Rβ and downregulate CCR7, thus displaying

an effector memory phenotype. The rapid downregulation of CCR7 potentially enables the cells to egress from the spleen and potentially migrate towards the BM.

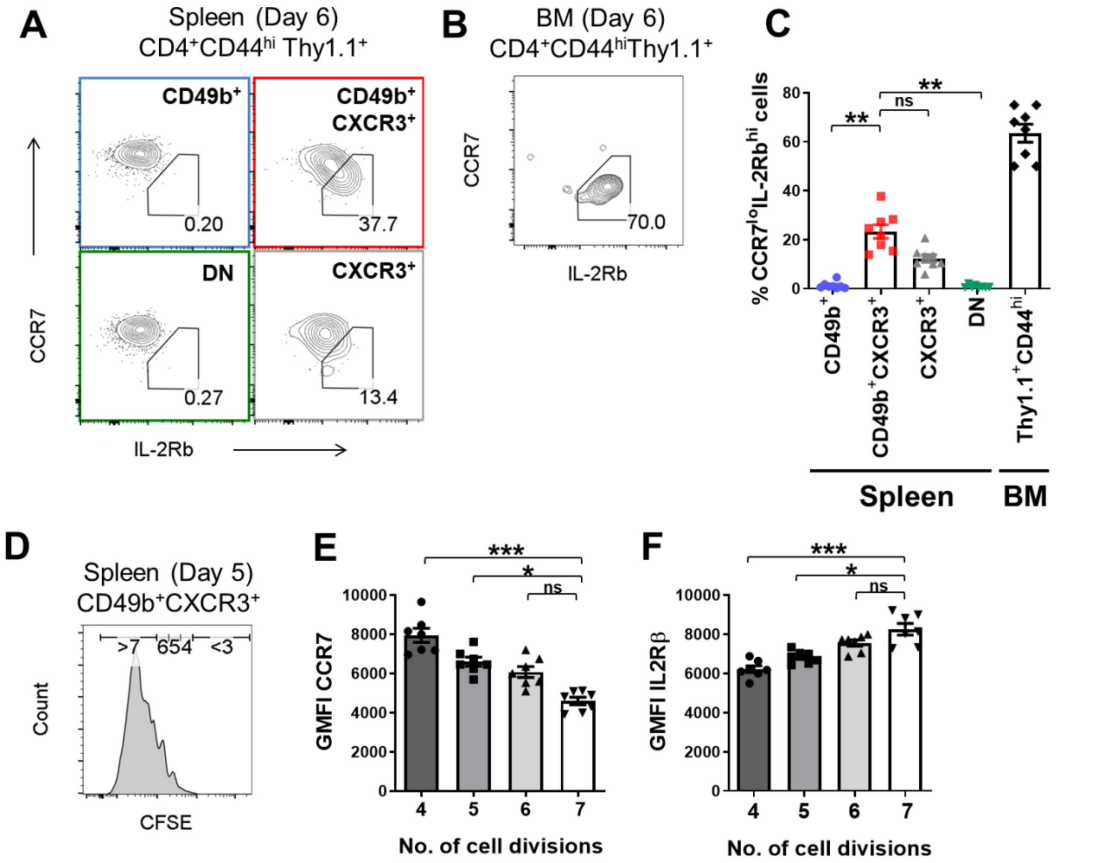

Figure 3.2.7: CD49b$^+$CXCR3$^+$ memory precursor CD4 T cells express low levels of CCR7 and high levels of IL-2Rβ. **A:** Purified Thy1.1$^+$ LCMV-TCR CD4 T cells were transferred into WT C57BL/6 mice followed by immunization with 100 µg LCMV-gp-61 and 10 µg LPS. Spleen and BM were analyzed by flow cytometry on day 6 p.I. for expression of CD49b, CXCR3, IL-2Rb and CCR7 in Thy1.1$^+$CD44^{hi} CD4 T cells. **A:** Gating plots display the expression of CCR7 and IL-2Rb in subsets of CD49b and CXCR3 expressing cells in Thy1.1$^+$CD44^{hi}CD4$^+$B220$^-$NK1.1$^-$PI$^-$ cells on day 6 p.I. **B:** Gating plot displays the expression of CCR7 and IL-2Rb in total Thy1.1$^+$CD44^{hi}CD4$^+$B220$^-$NK1.1$^-$PI$^-$ cells of the BM on day 6 p.I. **C:** Bar chart displays the percentage of CCR7^{lo}IL-2Rb^{hi}cells in subsets of CD49b and CXCR3 expressing cells of the spleen on day 6 p.I. (from **A**) and of total Thy1.1$^+$CD44^{hi}CD4$^+$ T cells in the BM on day 6 p.I. (from **B**). Data represent pooled results from two independent experiments with 3-5 mice per experiment (total n=8). Data are presented as mean ± SEM. Statistical significance between groups was determined by Kruskal-Wallis test with Dunn's multiple comparison test as $^{**}p < 0.01$ and ns= not significant. **D-F:** CD49b$^+$CXCR3$^+$ memory precursor CD4 T cells downregulate CCR7 and upregulate IL-2Rb expression with progressing number of experienced cell divisions. Purified CFSE-labeled Thy1.1$^+$LCMV-TCR CD4 T cells were transferred into WT C57BL/6 mice followed by immunization with 100 µg LCMV-gp-61 and 10 µg LPS. On day 5 p.I., Thy1.1$^+$LCMV-TCR CD4 T cells of the spleen were analyzed by flow cytometry. Histogram (D) displays generations of CFSE-diluted cells previously gated on CD49b$^+$CXCR3$^+$ cells. Gates in histogram indicate the rounds of cell division that CFSE-labelled cells have undergone by day 5 p.I. **E, F:** The GMFI of CCR7 (**E**) and IL-2Rβ (**F**) within the CD49b$^+$CXCR3$^+$ subpopulation is shown for each round of cell division. Data represent pooled results from two independent experiments with 3-4 mice per experiment (total n=7). Data are presented as mean ± SEM. Statistical significance between groups was determined by Kruskal-Wallis test with Dunn's multiple comparison test as $^{*}p < 0.05$, $^{***}p < 0.001$ and ns= not significant.

3.3 B cells negatively regulate the establishment of CD49b$^+$T-bet$^+$ CD4 T cells in the BM

3.3.1 B cell depletion/ deficiency increases accumulation of BM antigen-specific CD4 T cells

B cell depletion has been reported to inhibit the generation of splenic memory CD4 T cells, whereas the expansion of CD4 T cells is not affected under B cell deprived conditions (135-139).

In order to study the effect of B cells on the generation of memory CD4 T cells, WT C57BL/6 mice were treated with anti-IgD or isotype control antibody followed by injection of anti-rat IgG antibody that induces cross-linking and subsequently apoptosis of IgD$^+$ B cells (177). Two days after induction of B cell depletion, purified Thy1.1$^+$LCMV-specific CD4 T cells were transferred i.v. and mice immunized with LCMV peptide $GP_{61–80}$ plus LPS. On day 6 after immunization, a reduction of more than 80% of CD19$^+$ B cells in the spleen and mLNs and around 10% of CD19$^+$ B cells in the BM was observed (177, 225). Previous puplications have shown that BM B cell precursors, in particular pro-B cells, contact IL-7-expressing stromal niches, suggesting a spatial competition with memory CD4 T cells (183, 198). However, BM B cell precursors were not affected by anti-IgD treatment.

Even though Thy1.1$^+$LCMV-TCR-specific CD4 T cells in the spleen of B cell-depleted and control mice expanded equally by day 6 (Control: $1.84x10^5$ ± $2.05x10^4$ SEM; dB: $1.55x10^5$ ± $1.97x10^4$ SEM) more Thy1.1$^+$LCMV-specific CD4 T cells in the BM of B cell-depleted mice compared to control mice were detected (Control: $1.35x10^3$ ± 520 SEM; dB: $6.85x10^3$ ± 973 SEM) (Figure 3.3.1 A).

Additionally, the accumulation of antigen-specific CD4 T cells in the BM is also promoted in *Rag1*$^{-/-}$ host mice. Purified Thy1.1$^+$ LCMV-TCR-specific CD4 T cells were transferred into C57BL/6 (B6) or *Rag1*$^{-/-}$ mice followed by immunization with LCMV peptide $GP_{61–80}$ plus LPS. On day 4 after immunization, the Thy1.1$^+$ CD4 T cells in the spleen and BM were analyzed by flow cytometry and enumerated. While splenic numbers of Thy1.1$^+$LCMV-TCR-specific CD4 T cells did not differ significantly between WT C57BL/6 or *Rag1*$^{-/-}$ mice (B6: $1.72x10^6$ ± $5.71x10^5$ SEM; Rag1$^{-/-}$: $1.19x10^6$ ± $7.72x10^4$ SEM), considerably more Thy1.1$^+$LCMV-TCR-specific CD4 T cells were detected in the BM of Rag1$^{-/-}$ mice (Rag1$^{-/-}$: $2.15x10^4$ ± 784 SEM) already by day 4 after transfer when compared to B cell-sufficient WT C57BL/6 mice (B6: $2.43x10^3$ ± 700 SEM) (Figure 3.3.1 B).

When wild-type splenic polyclonal B cells were co-transferred together with Thy1.1^{+}LCMV-TCR-specific CD4 T cells into Rag1$^{-/-}$ mice, the accumulation of LCMV-TCR-specific CD4 T cells in the BM was significantly reduced (+B cells: 3.0x10^{4} ± 2.8x10^{3} SEM) by day 6 after immunization compared to animals that did not receive wild-type splenic polyclonal B cells (-B cells: 8.82x10^{4} ± 6.9x10^{3} SEM), despite normal expansion of Thy1.1^{+}LCMV-TCR-specific CD4 T cells in the spleen (-B cells: 1.0x10^{6} ± 1.06x10^{5} SEM; +B cells: 1.5x10^{6} ± 2.4x10^{5}) (Figure 3.3.1 C).

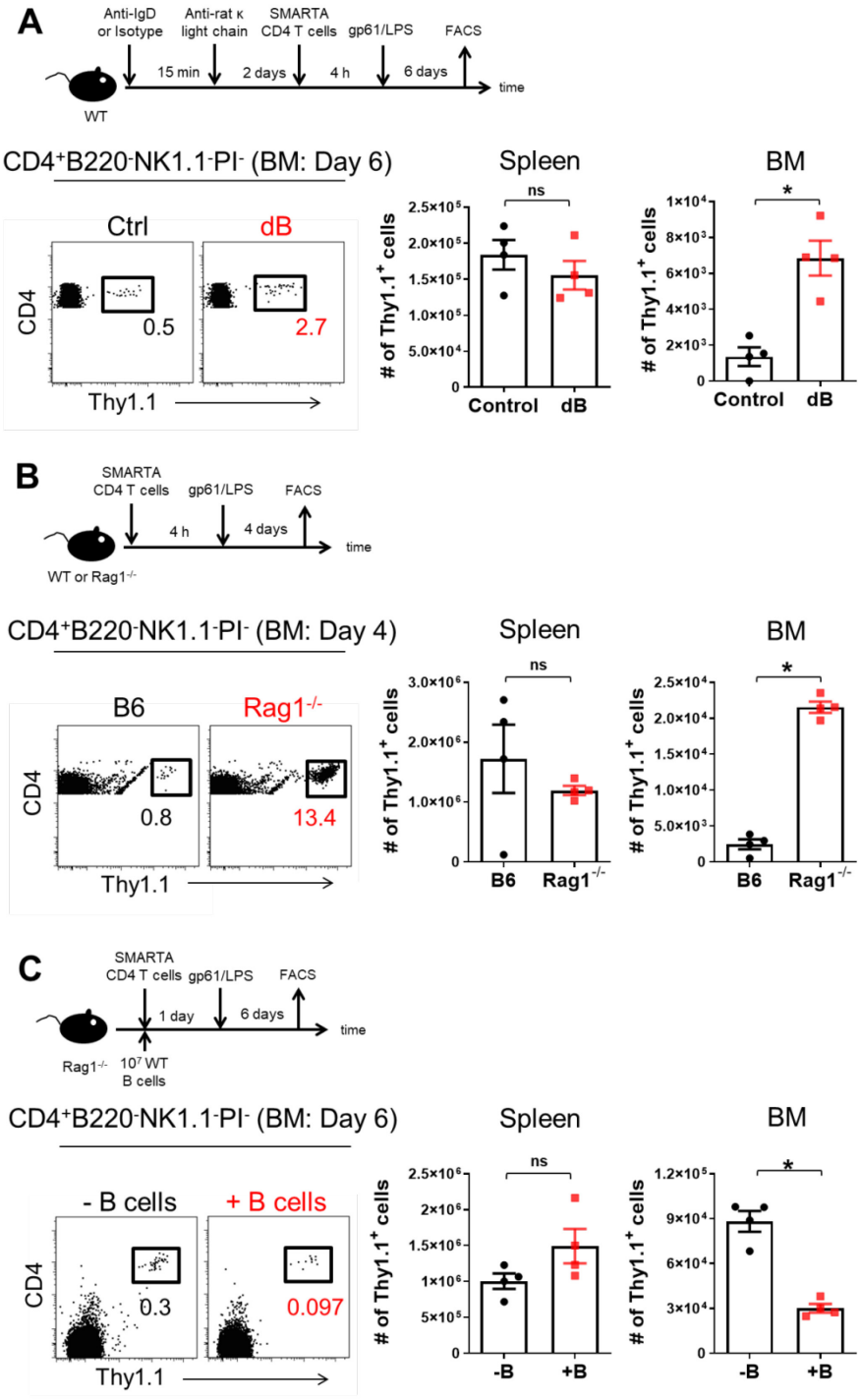

Figure 3.3.1: B cells negatively regulate the accumulation of activated antigen-specific CD4 T cells in the BM on day 6 p.I. All data presented in this figure is published in (225). **A:** B cell depletion promotes the accumulation of antigen-specific CD4 T cells in the BM. C57BL/6 mice were treated with isotype-matched control antibody or anti-IgD antibody followed by injection of anti-rat IgG antibody. Two days later, purified Thy1.1$^+$ LCMV-TCR CD4 T cells were transferred into the antibody-treated mice and mice immunized with 100 µg LCMV-gp-61 and 10 µg LPS. On day 6 p.I., the Thy1.1$^+$ CD4 T cells in the spleen and BM were analyzed by flow cytometry and enumerated. Gating plots show the Thy1.1$^+$ cell population in CD4$^+$B220$^-$NK1.1$^-$PI$^-$ cells of the BM. Bar charts represent the cell numbers of Thy1.1$^+$ cells in spleen and BM. N=4 per group. Data are presented as mean ± SEM. Statistical significance between subsets was determined by Mann-Whitney U test as $*p < 0.05$ or ns = not significant. **B:** Accumulation of antigen-specific CD4 T cells in the BM is also promoted in *Rag1*$^{-/-}$ host mice. Purified Thy1.1$^+$ LCMV-TCR-specific CD4 T cells were transferred into C57BL/6 or Rag1$^{-/-}$ mice followed by immunization with 100 µg LCMV-gp-61 and 10 µg LPS. On day 4, the Thy1.1$^+$ CD4 T cells in the spleen and BM were analyzed by flow cytometry and enumerated. Bar charts represent the cell numbers of Thy1.1$^+$ cells in spleen and BM. N=4 per group. Data are presented as mean ± SEM. Statistical significance between subsets was determined by Mann-Whitney U test as $*p < 0.05$ or ns = not significant. **C:** B cell co-transfer suppresses the accumulation of antigen-specific CD4 T cells in the BM. Purified Thy1.1$^+$ LCMV-TCR-specific CD4 T cells were transferred into Rag1$^{-/-}$ mice with or without B cells followed by immunization with 100 µg LCMV-gp-61 and 10 µg LPS. On day 6 p.I., the Thy1.1$^+$ CD4 T cells in the spleen and BM were analyzed by flow cytometry and enumerated. Bar charts represent the cell numbers of Thy1.1$^+$ cells in spleen and BM. N=4 per group. Data are presented as mean ± SEM. Statistical significance between subsets was determined by Mann-Whitney U test as $*p < 0.05$ or ns = not significant.

3.3.2 B cell depletion enhances the induction of CD49b$^+$T-bet$^+$ antigen-specific CD4 T cells

Splenic CD49b$^+$ antigen-specific activated CD4 T cells have previously been described to preferentially migrate into the BM (98). In order to understand how B cell depletion affects antigen-specific CD4 T cells in the spleen, the expression of CD49b in Thy1.1$^+$LCMV-TCR-specific CD4 T cells was analyzed under B cell depleted conditions on day 6 after mmunization. Interestingly, splenic Thy1.1$^+$LCMV-TCR-specific CD4 T cells in B cell-depleted mice expressed significantly more CD49b (MFI 1.41 ± 0.1 SEM, normalized to Control (=1)) compared to control mice (MFI 1.0 ± 0.05 SEM) (Figure 3.3.2 A). This result was also reflected in the number of CD49b$^+$ cells in Thy1.1$^+$LCMV-TCR-specific CD4 T cells (Control: 40.3 % ± 1.8 SEM; dB: 49.8 % ± 2.2 SEM) (Figure 3.3.2 A).

Conversely, Thy1.1$^+$LCMV-TCR-specific CD4 T cells in B cell-replenished Rag1$^{-/-}$ mice displayed a decreased expression of CD49b (MFI 0.75 ± 0.03 SEM, normalized to Control (=1)) compared to Rag1$^{-/-}$ mice that did not receive B cells (MFI 1.0 ± 0.02 SEM), which was also reflected in the frequency of CD49b$^+$ cells in Thy1.1$^+$LCMV-TCR-specific CD4 T cells (-B: 63.37 % ± 0.44 SEM; +B: 54.03 % ± 1.5 SEM) (Figure 3.3.2 B). This data indicates that B cells negatively regulate the expression of CD49b and consequently reduce the accumulation of antigen-specific CD4 T cells in the BM.

Misumi and Whitmire have previously suggested that B cell depletion affects the expression T-bet in splenic antigen-specific CD4 T cells (136-139). Since T-bet marks precursors of BM memory CD4 T cells, the effect of B cell depletion on the expression of T-bet was determined. To that end, purified T-bet ZsGreen (ZsGreen$^+$) Thy1.1$^+$LCMV-TCR-specific CD4 T cells were transferred into B cell depleted mice and the expression of T-bet analyzed by flow cytometry. The frequency of T-

bet$^+$Thy1.1$^+$LCMV-TCR-specific CD4 T cells were significantly increased in the spleen (Control: 14.57 % ± 1.1 SEM; dB: 26.25 % ± 2.7 SEM) and blood (Control: 20.15 % ± 1.93 SEM; dB: 34.32 % ± 3.85 SEM) after B cell depletion, whereas the BM population was likely saturated (Control: 46.95 % ± 12.62 SEM; dB: 60.57 ± 4.9 SEM) (Figure 3.3.3 C).

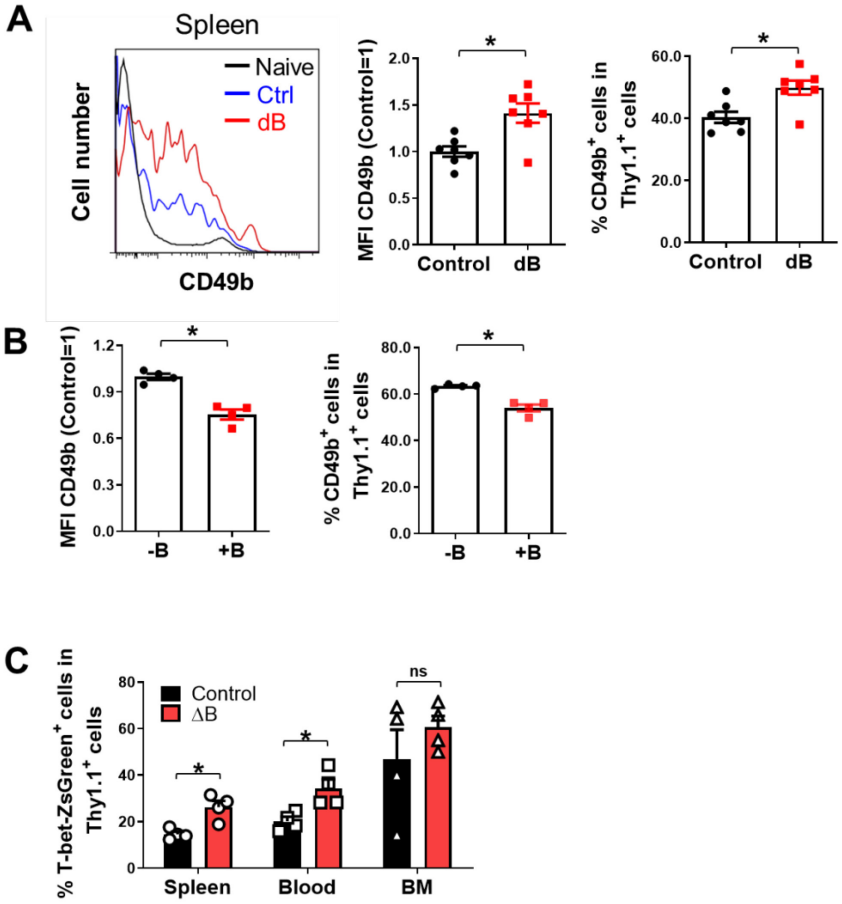

Figure 3.3.2: CD49b$^+$ and T-bet$^+$ antigen-specific CD4 T cells are increased by B cell-depletion. All data presented in this figure is published in (225). **A:** CD49b$^+$ antigen-specific CD4 T cells are increased in the spleen of B cell-depleted mice. WT C57BL/6 mice were treated with isotype-matched control antibody or anti-IgD antibody followed by injection of anti-rat IgG antibody. Two days later, purified Thy1.1$^+$LCMV-TCR-specific CD4 T cells were transferred into the antibody-treated mice and mice immunized with 100 µg LCMV-gp-61 and 10 µg LPS. On day 6 p.i., the CD49b$^+$ population in the spleen was analyzed by flow cytometry. Histograms show CD49b expression in CD4$^+$Thy1.1$^+$B220$^-$NK1.1$^-$PI$^-$ cells and CD4$^+$Thy1.1$^-$B220$^-$NK1.1$^-$PI$^-$ (naive) cells in the spleen. Bar charts represent the relative ratio of mean fluorescent intensity (MFI) of CD49b (left bar chart) expression and CD49b$^+$ cell population (right bar chart) in CD4$^+$Thy1.1$^+$B220$^-$NK1.1$^-$PI$^-$ cells in the spleen of Control or B cell depleted (dB) mice. N=7 per group. Data are presented as mean ± SEM. Statistical significance between groups was determined by Mann-Whitney U test as $*p < 0.05$. **B:** CD49b$^+$ antigen-specific CD4 T cells are decreased in the spleen by B cell co-transfer. The CD49b$^+$ cell population in the spleen of mice described in *Figure 3.3.1 C* was analyzed by flow cytometry. Bar charts represent the relative ratio of MFI of CD49b (left bar chart) and CD49b$^+$ cell population (right bar chart) in CD4$^+$Thy1.1$^+$B220$^-$NK1.1$^-$PI$^-$ cells in the spleen. N=4 per group. Data are presented as mean ± SEM. Statistical significance between groups was determined by Mann-Whitney U test as $*p < 0.05$. **C:** T-bet-ZsGreen$^+$ antigen-specific CD4 T cells are increased in the spleen of B cell-depleted mice. WT C57BL/6 mice were treated with isotype-matched control antibody or anti-IgD antibody followed by injection of anti-rat IgG antibody. Two days later, purified Thy1.1$^+$ T-bet-ZsGreen reporter LCMV-TCR-specific CD4 T cells were transferred into B cell-depleted or control C57BL/6 mice followed by immunization with 100 µg LCMV-gp-61 and 10 µg LPS. On day 6 p.i., the T-bet-ZsGreen$^+$ population in spleen, blood and BM was analyzed by flow cytometry. Bar chart represents the Thy1.1$^+$T-bet-ZsGreen$^+$ cell population in CD4$^+$B220$^-$NK1.1$^-$PI$^-$ cells in spleen, blood or BM. N=4 per group. Data are presented as mean ± SEM. Statistical significance between control or B cell depleted mice was determined by Mann-Whitney U test as $*p < 0.05$ or ns = not significant.

3.3.3 B cell depletion does not affect the proliferative capacity of CD49b$^+$CXCR3$^+$ precursors of BM memory CD4 T cells

The previous results indicated that CD49b$^+$T-bet/CXCR3$^+$ antigen-specific CD4 T cells are the precursors of BM memory CD4 T cells and that these precursors are generated via enhanced proliferation during the primary immune response. Furthermore, B cells were shown to negatively regulate the establishment of LCMV-TCR-specific CD4 T cells in the BM. To test to which extent B cell depletion affects the proliferative capacity of CD49b$^+$CXCR3$^+$ precursors of BM memory CD4 T cells during the primary immune response, purified CFSE-labeled Thy1.1$^+$LCMV-TCR-specific CD4 T cells were transferred into WT C57BL/6 mice that were pre-treated with anti-IgD or isotype control antibody followed by treatment of anti-rat IgG. After transfer of CFSE$^+$Thy1.1$^+$LCMV-TCR-specific CD4 T cells, mice were immunized with LCMV peptide $GP_{61–80}$ plus LPS. On day 4 and 6 after immunization, splenic Thy1.1$^+$LCMV-TCR-specific CD4 T cell were enumerated and the proliferative capacity of CD49b$^+$CXCR3$^+$ cells analyzed with regards to experienced rounds of cell division (Figure 3.3.3 A).

On day 4 after immunization, no differences in the percentage of CD49b$^+$CXCR3$^+$ cells could be observed comparing control (11.14 % ± 0.48 SEM) and B cell depleted mice (11.68 % ± 0.43 SEM) (Figure 3.3.3 B).

However, on day 6 after immunization, the percentage of CD49b$^+$CXCR3$^+$ cells increased significantly from 8,7 % (± 1.59 SEM) in control mice to 16.15 % (± 2.1 SEM) in B cell depleted mice (Figure 3.3.3 D) confirming the result from Figure 3.3.2 that demonstrated that CD49b and T-bet expression are increased upon B cell depletion, respectively.

The analysis of generations of divided cells in CD49b$^+$CXCR3$^+$ cells under control or B cell depleted conditions revealed that B cell depletion does not affect the proliferative capacity of CD49b$^+$CXCR3$^+$ precursors of BM memory CD4 T cells. No differences between normal and B cell depleted conditions with regards to the generations of divided cells according to CFSE dilution could be detected on days 4 and 6 after immunization (Figure 3.3.4 C and E).

Comparable results for day 4 have been obtained in a second independent experiment (Supplementary Figure 3). Data could not be pooled here, since an amended flow cytometric staining panel was used in the supplementary experiment.

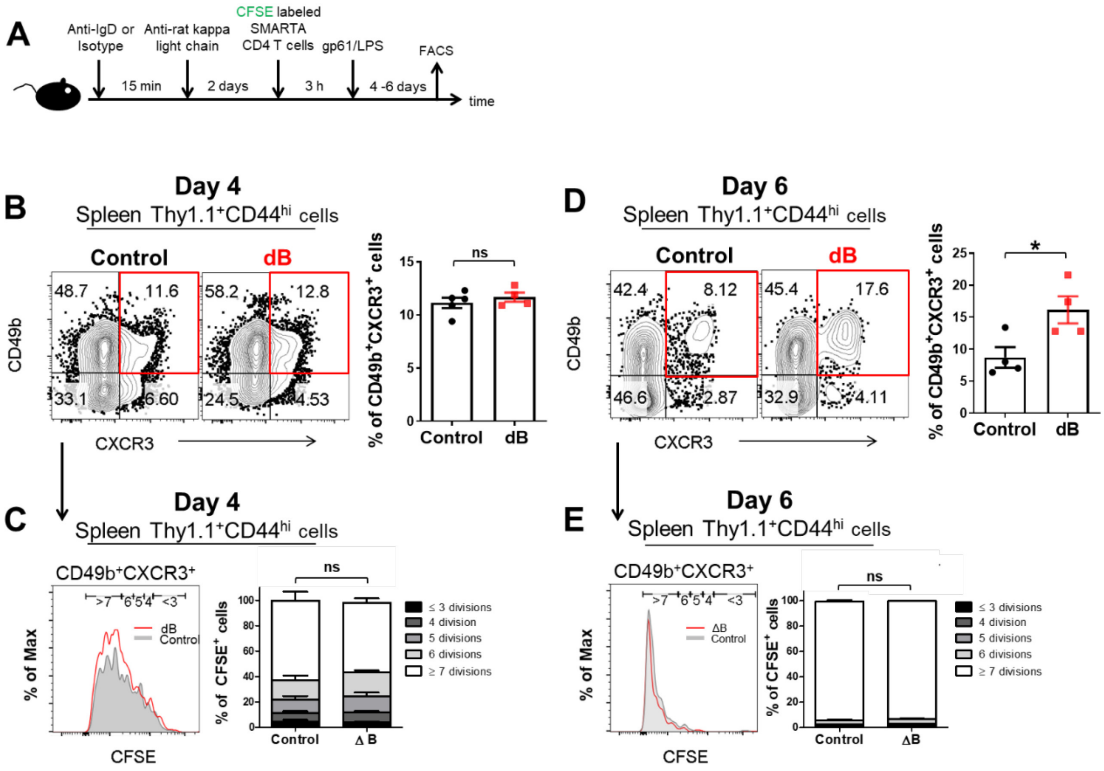

Figure 3.3.3: B cell depletion does not affect the proliferation of antigen-specific CXCR3$^+$CD49b$^+$ memory precursor CD4 T cells in the spleen. **A:** Experimental outline. C57BL/6 mice were treated with isotype-matched control antibody or anti-IgD antibody followed by injection of anti-rat IgG antibody. Two days later, purified CFSE-labeled Thy1.1$^+$ LCMV-TCR CD4 T cells were transferred into the antibody-treated mice and mice immunized with 100 µg LCMV-gp-61 and 10 µg LPS. On days 4-6 p.I., the CFSE$^+$ Thy1.1$^+$ CD4 T cells in the spleen were analyzed by flow cytometry. **B & D:** Gating plots show the expression of CD49b and CXCR3 in Thy1.1$^+$CD4$^+$B220$^-$NK1.1$^-$PI$^-$ cells of the spleen in control and B cell depleted (dB) mice on day 4 (B) and day 6 (D) p.I. Numbers indicate percentages. Bar charts display the percentage of CD49b$^+$CXCR3$^+$ cells in control and B cell depleted (dB) mice on day 4 (B) and day 6 (D) p.I. N=4 per group. Data are presented as mean ± SEM. Statistical significance between groups was determined by Mann-Whitney U test as ns = not significant (day 4) or *$p < 0.05$ (day 6) for % of CD49b$^+$CXCR3$^+$ cells in control and dB mice. **C & E:** Histograms show CD49b$^+$CXCR3$^+$ CFSE-labelled cells of the spleen on day 4 (C) and day 6 (E) p.I. In Thy1.1$^+$CD4$^+$B220$^-$NK1.1$^-$PI$^-$ cells (from B and D). Gates in histograms indicate the divisions that CFSE-labeled cells have undergone in CD49b and/or CXCR3 expressing subsets by day 4 (C) and day 6 (E) p.I. Bar charts represent the quantification of percentages of CFSE$^+$ cells in different divided generations (≤ 3 to ≥ 7 divisions) that subsets of CD49b and CXCR3 expressing cells have undergone by day 4 and 6 p.I. n = 4 per group. Data are presented as mean ± SEM. Statistical significance between groups was determined by Wilcoxon test as ns = not significant.

4 Discussion

Memory CD4 T cells contribut5e to long-term protection against repetitive exposure to pathogens by providing critical signals to cognate B cells and CD8 T cells and persist in the body in the absence of antigen. During an immune reaction, some antigen-experienced CD4 T cells relocate from SLOs to the BM and reside and rest there as professional memory CD4 T cells marked by high expression of Ly-6C and a resting phenotype in terms of transcriptional activity and proliferation (96). Moreover, it has been previously reported that CD49b and CD69 molecules are required for the migration and retention of activated CD4 T cells in the BM (97-99). However, how the precursors of BM memory CD4 T cells are generated in SLOs during the activation phase and which are the cellular and molecular cues leading to their formation and survival remains elusive. In sum, this doctoral thesis identifies the phenotype of the precursors of BM memory CD4 T cells in the spleen, describes the CD4 T cell-intrinsic requirements and the role of B cells for the generation and early accumulation of the precursors of memory CD4 T cells in the BM.

4.1 Splenic CD49b$^+$T-bet$^+$/CXCR3$^+$ CD4 T cells are the precursors of BM memory CD4 T cells

Since the expression of CD49b, CD69 and Ly-6C has been previously described to mark or modulate the generation of BM memory CD4 T cells, the expression of these molecules set the ground for the initial identification of splenic precursors of BM memory CD4 T cells. At first, the analysis of splenic memory phenotype (MP) CD44^{hi}CD62L^{lo} CD4 T cells demonstrates that a substantial population of cells co-expresses CD49b and CD69 and that this population is enriched in the BM. The fact that splenic CD49b$^+$CD69$^+$ MP CD4 T cells contain the majority of Ly-6C$^+$ cells (about 10%) compared to other populations, and BM MP CD49b$^+$CD69$^+$ CD4 T cells comprise of 33 % Ly-6C$^+$ cells, raised the question if splenic CD49b$^+$CD69$^+$Ly-6C$^+$ cells display the precursors of CD49b$^+$CD69$^+$Ly-6C$^+$ MP CD4 T cells found in the BM. Unfortunately, not much is known about the functional role of Ly-6C for CD4 and CD8 memory formation. Ly-6C is also a marker of memory CD8 T cells and has previously been described to support homing of CD8 T_{CM} cells into lymph nodes (150, 151). Furthermore, Ly-6C has been shown to act as a costimulatory molecule for T cells (149), but a definite functional characterization of this molecule remains to be determined. During the

development of Vα14i NKT cells, the transcription factor T-bet drives the expression of Ly-6C and in the absence of T-bet, Ly-6C expression is impaired (180). Moreover, in NK and Vα14i NKT cells, T-bet regulates the terminal maturation and homeostasis of these cells and a deficiency in T-bet expression leads to a significant downregulation of CD49b expression, but an increase in the expression of CD69 (199). Interestingly, the transcriptomic comparison of sorted splenic and BM MP $CD44^{hi}CD62L^{lo}$ CD4 T cells previously conducted to this study identified T-bet as a differentially upregulated molecule in the BM (96). The present study further demonstrates that T-bet expression is significantly increased in $CD49b^{+}CD69^{+}$ MP CD4 T cells of spleen and BM and that T-bet deficiency drastically impairs the appearance of $CD49b^{+}CD69^{+}$ MP CD4 T cells in both organs. This data initially suggested that T-bet may play a regulatory role for the generation of BM $CD49b^{+}CD69^{+}$Ly-$6C^{+}$ MP CD4 T cells. In line with previous reports on NK and Vα14i NKT cells, the analysis of splenic and BM MP CD4 T cells demonstrates that T-bet deficiency particularly reduces expression of Ly-6C in $CD49b^{+}$ cells, including $CD49b^{+}CD69^{+}$ cells, but not $CD49b^{-}CD69^{+}$ cells. In an antigen-specific immune response against OVA, some splenic antigen-specific activated CD4 T cells co-express CD49b and CD69, but primarily $CD49b^{+}$ CD4 T cells (including $CD49b^{+}CD69^{+}$ cells) highly co-express T-bet and Ly-6C. Unexpectedly, conditional loss of T-bet in antigen-specific CD4 T cells does not impair the appearance of $CD49b^{+}CD69^{+}$ cells by day 6 *in vivo* or after 48 hours of *in vitro* anti-CD3 stimulation of sorted naïve CD4 T cells from WT or T-bet deficient mice. However, Ly-6C expression in antigen-specific CD4 T cells is, just as in MP CD4 T cells, particularly reduced in $CD49b^{+}$ cells. This suggests a similar regulatory role of T-bet for the concomitant expression of Ly-6C and CD49b as in Vα14iNKT cells (180, 199). On the contrary, the enumeration of total CD4 T cells and MP $CD44^{hi}CD62L^{lo}$ CD4 T cells displayed no difference between WT and T-$bet^{-/-}$ mice. One explanation may be that T-$bet^{-/-}$ mice suffer from splenomegaly and thus generally harbor a vastly increased number of lymphocytes, including subsets of CD4 T cells that potentially also populate other tissues in the body (179). Another possibility may be that CD4 T cells deficient in T-bet expression instead upregulate GATA-3 and thus convert towards a Th2 lineage phenotype. However, this remains a formal possibility as experimental evidence is lacking.

In order to ultimately determine the role of T-bet for the accumulation of activated CD4 T cells in the BM, OVA-specific CD4 T cells sufficient or deficient in T-bet were transferred into WT mice and the accumulation of antigen-specific CD4 T cells tracked in spleen and BM on day 6 after immunization. Moreover, splenic activated antigen-specific T-$bet^{+/+}$ or T-$bet^{-/-}$ CD4 T cells were sorted on day 6 after immunization and re-transferred into lymphopenic SCID mice and their accumulation in the BM assessed

two hours after transfer. In both experiments, no difference in frequency or cell number of antigen-specific CD4 T cells was detected regardless of T-bet expression, suggesting that T-bet is dispensable for the accumulation of antigen-specific CD4 T cells in the BM. This result is also in line with the observations made for MP CD4 T cells. Rather, the upstream signaling pathway (T-bet inducing signal) may be critical in this process in parallel with the control of CD49b expression. T-bet and CD49b are not expressed by naïve T cells. While T-bet is induced via IFN-γR and IL-2R signaling pathways (30, 31), CD49b (and the VLA-2 heterodimer of CD49b and CD29) is induced *in vitro* independently of IFN-γ and IL-12 signals (200). Thus, contrarily to the upregulation of T-bet and CD49b upon T cell- DC engagement, B cell mediated signals may commonly downregulate the expression of these molecules.

Despite the redundancy of T-bet expression for the accumulation of activated CD4 T cells in the BM, CD49b$^+$T-bet$^+$ antigen-specific CD4 T cells are detected at the highest percentage in the BM on day 6 after immunization, indicating that CD49b$^+$T-bet$^+$ antigen-specific CD4 T cells display the precursors of BM memory CD4 T cells. Moreover, Marshall et *al.* suggested that a differential expression of Ly-6C distinguishes splenic effector Th1 and memory cells. P-selectin glycoprotein ligand 1 (PSGL1)^{hi} Ly-6C^{hi} cells are marked by increased expression of T-bet, CXCR3 and IFN-γ, whereas PSGL1^{hi}Ly-6C^{lo} cells displayed less differentiated cells and highly expressed CD62L and CCR7, thus identifying them as T_{CM} cells (152). The study provided evidence that similarly to antigen-specific CD8 T cells, elevated T-bet expression is required for maximal clonal expansion and the formation of PSGL1^{hi}Ly-6C^{hi}CD4$^+$ T cells (152). Notably, the study by Marshall et al. used a viral infection model as compared to the results presented here (peptide immunization) and they did not focus on the establishment of BM memory CD4 T cells. However, some analogies to the results presented her can be found: BM memory CD4 T cells highly express T-bet and Ly-6C, but do not express CD62L or CCR7 (96), thus displaying a classical effector memory phenotype (T_{EM}). Furthermore, preliminary results on splenic and BM CD49b$^+$Ly-6C$^+$ MP and OVA-specific CD4 T cells revealed that those cells are highly enriched in PSGL1$^+$ cells (data not shown).

The chemokine receptor CXCR3 is rapidly induced on naïve cells following activation, preferentially remains highly expressed on Th1 CD4 T cells and is important for the migration of antigen-specific CD4 T cells out of the PALS into the interfollicular regions (site of T cell and DC interactions) (38). Furthermore, CXCR3 has been shown to be critical for directing activated T cells to peripheral sites of inflammation (39).

CXCR3 ligands include CXCL9, CXCL10, and CXCL11 that can be induced by IFNγ. CXCL10 can also be upregulated by IFNα/β as well as NF-κB induction (38). Defects in migration of T-bet deficient CD4 T cells are primarily due to loss of CXCR3 expression, since T-bet directly transactivates CXCR3 (29, 185). In addition to a potential role during primary responses, CXCR3 expression by T cells in LNs has been described to be important for the induction of T cell memory. $CXCR3^+$ cells make up between 60–90% of memory CD8 T cells (186, 187) and 40% of memory CD4 T cells (188). CXCR3 expression has also been proposed as a reliable marker for memory T cell responses, as viral recall responses for both CD8 and CD4 T cells are largely restricted to $CXCR3^+$ cells (187, 188). The results presented here demonstrate that CXCR3 is indeed highly expressed on activated BM CD4 T cells (memory phenotype and antigen-specific), in particular on $CD49b^+T\text{-}bet^+$ CD4 T cells that also express Ly-6C and exhibit no expression of CD62L. This suggests that CXCR3 may be used as a marker to identify the splenic precursors of BM memory CD4 T cells during the course of an immune response. Loss of T-bet does not impair the accumulation of activated CD4 T cells in the BM and due to the activating role of T-bet for the induction of CXCR3 expression, CXCR3 may not be the guiding chemokine receptor for the homing of activated CD4 T cells to the BM. Other chemokine receptors, e.g. CXCR4, may play a more prominent role and $CD49b^+T\text{-}bet^+/CXCR3^+$ cells include a substantial portion of $CXCR4^+$ cells (personal communication with Dr. Shintaro Hojyo). Interestingly, on day 6 after immunization, splenic antigen-specific T-bet $(ZsGreen)^+$ CD4 T cells preferentially localize in the red pulp of the spleen, indicating that they are about to egress the spleen and migrate to other tissues, e.g. the BM. Similar aspects to plasma blast migration to the BM after secondary antigen-exposure may be interpreted from this: During an immune response, some antigen-specific activated B cells differentiate into memory B cells and short-lived plasma cells (201). Upon antigen re-challenge, memory B cells differentiate into plasma blasts that migrate from the spleen to the BM in a CXCR4-CXCL12 and S1P1-S1P dependent manner where they eventually become memory plasma cells and rest in defined CXCL12-secreting $VCAM\text{-}1^+$ stromal survival niches (182, 183, 202). It is thus tempting to speculate that precursors of BM memory CD4 T cells may use similar ways to migrate to the BM and may be focus of future investigations.

The role of CD69 for the formation of BM memory CD4 T cells remains controversial and enigmatic at the same time. CD69 protein expression can be detected as early as 2- 3 hours after stimulation, entitling CD69 as a perfect early activation marker and effector T cells may only transiently express CD69 (89, 203). Furthermore, CD69 has been attributed a fundamental role as retention molecule for T_{RM} cells in both CD8 and CD4 T cell memory and the establishment of BM memory CD4 T cells is defect in the

absence of CD69 (97). CD69 can physically interact with S1P1 after exposure to IFNα/β leading to S1P1 internalization and degradation and consequently block S1P-mediated lymphocyte egress from lymphoid structures (158-160). Accordingly, inhibition or deficiency in CD69 may be expected to increase lymphocyte egress from SLOs into the periphery, but increased cell numbers in peripheral blood were not observed in adoptively transferred antigen-specific $CD69^{-/-}$ CD4 T cells at various time points after immunization (97). Likewise, following virus infection, numbers of re-circulating $CD69^{-/-}$ CD8 T cells are comparable to $CD69^{+/+}$ cell numbers in the blood indicating that S1P1 mediated egress from SLOs may have little impact on the expansion of activated CD8 T cells and that additional mechanisms control T cell expansion and SLO egress (160, 204-206).

The results presented here indicate that CD69 certainly marks MP CD4 T cells of the BM, and a distinct population of $CD49b^{+}CD69^{+}$ MP and antigen-specific activated CD4 T cells can be detected in the spleen. However, only few cells simultaneously express CD49b, T-bet/CXCR3 and CD69 on day 6 after immunization in the spleen. Moreover, Tfh cells were found to highly express CD69 in parallel to Tfh lineage markers such as Bcl-6 or the concomitant expression of CXCR5 and PD-1. CD49b on the other hand was not expressed in Tfh cells, suggesting a bifurcation of $CD49b^{+}$ effector/memory precursor CD4 T cells and CD69 dependent retention of Tfh cells in the spleen Supplementary Figure 1). Taken together, this data indicates that CD69 is not a suitable marker to distinguish early splenic precursors of BM memory CD4 T cells from other effector CD4 T cells or Tfh cells.

In summary, the first part of the thesis identified activated $CD49b^{+}T\text{-}bet^{+}/CXCR3^{+}$ CD4 T cells as the splenic precursors of BM memory CD4 T cells and displayed that $CD49b^{+}CXCR3^{+}$ antigen-specific CD4 T cells remain in the BM even during the memory phase of an immune response. Importantly, during the memory phase, a great population within antigen-specific CD4 T cells also express CD69 in the BM. This leaves further room for investigation on a dual role for CD69 on antigen-specific CD4 T cells: as an early activation marker and a tissue retention marker during the memory phase.

4.2 CD49b$^+$CXCR3$^+$ precursors of BM memory CD4 T cells are generated following enhanced cell proliferation

Indispensable aspects of successful memory T cell generation are the affinity and duration of interaction between TCR and p:MHC molecules, adequate costimulatory signaling and the appropriate cytokine milieu and microenvironment. High-affinity T cells differentiate into a large numbers of memory cells due to their greater expansion (111, 207). On the contrary, in case of infection or lymphopenia, even very low-affinity antigens support memory development (118, 120), suggesting that TCR affinity alone is not predictive of memory formation. Indeed, other studies have found that the duration of the TCR-p:MHCII interaction can serve as a more reliable predictor of memory fate (208-210). In support of these findings, recent work by Kim et *al.* revealed that Th1 memory fate correlates with the duration of TCR-p:MHCII interaction and not with the affinity of the TCR-p:MHCII interaction or the ability to expand (123). On the molecular level, the duration of TCR signaling affects the number of cell division as well as chromatin remodeling and expression of key transcription factors and cytokine/chemokine receptors. Yet, *in vitro* differentiated effector cells were capable to differentiate into memory cells in MHCII-deficient host mice (82), raising questions of the importance of the duration of cognate CD4 T cell interaction with APCs. Moreover, it is tempting to ask how many rounds of cell divisions are required to generate precursors of BM memory CD4 T cells *in vivo*.

It has remained controversial whether memory CD4 T cells have differential requirements for cell division to obtain longevity. Chang et *al*. have previously suggested an asymmetric division model for effector and memory T cell differentiation (145). To become an effector cell, T cells need to contact APCs proximally and divide more. By contrast, T cells located distally to the APCs stop cell division earlier and are proposed to favor memory generation. However, we show here that BM memory precursors are in prolonged contact with DCs and divide more than other responding subpopulations.

In particular, the results presented here demonstrate that CD49b$^+$CXCR3$^+$ precursors of BM antigen-specific memory CD4 T cells are generated via enhanced proliferation and sustained late cognate CD4 T cell- DC interactions during the late activation phase. After the peak of the primary response, which occurs around day 4 after immunization, CD49b$^+$CXCR3$^+$ precursors of BM memory CD4 T cells have experienced considerably more rounds of cell divisions than other populations, or rather, a distinct population of CD49b$^+$CXCR3$^+$ cells can only be detected after antigen-specific CD4 T

cells have experienced at least 7 rounds of cell division. Furthermore, CD49b$^+$CXCR3$^+$ precursors of BM memory CD4 T cells incorporated significantly more BrdU when mice were injected after the peak of the primary immune response. Moreover, on day 6 after immunization CD49b$^+$CXCR3$^+$ precursors of BM memory CD4 T cells included significantly more Ki-67$^+$ cells, a marker strictly associated with cell proliferation and absent in resting (quiescent) cells (G_0) (189), when compared to other populations. Notably, even though the effect of BrdU itself on the proliferative capacity of activated dividing T cells has been a matter of contrary debate in the field (73, 191), no significant difference in the frequency of antigen-specific CD4 T cells or differing distributions of CD49b and/or CXCR3 expressing cells was detected after BrdU treatment compared to untreated mice. This result indicates that intraperitoneal BrdU application in a defined concentration of 1 mg does not induce default proliferation of susceptible cells, differently as proposed by Sercan et *al.* who applied BrdU plus sugar in the drinking water *ad libitum*, making it more difficult to control the exact amount of BrdU taken up (73).

In accordance with the observation of highly proliferative CD49b$^+$CXCR3$^+$ precursors of BM memory CD4 T cells, treatment with the cytostatic drug cyclophosphamide specifically reduced frequencies in CD49b$^+$CXCR3$^+$ precursors of BM memory CD4 T cells.

Costimulatory signals are crucial for T cell activation and differentiation. In particular the CD28/B7 costimulatory pathway has been assigned significant importance, as interaction of the CD28 costimulatory receptor with its ligands B7-1/B7-2 (CD80/CD86) on APCs is required for activation of naïve CD4 T cells (193). Blocking this pathway with CTLA-4 Ig fusion molecule that binds with high avidity CD80/86 ligands potently blocks naïve CD4 T cell activation and proliferation (194-196). Consistently, the treatment with CTLA-4 Ig on days 4 and 5 after immunization significantly impaired the generation of CD49b$^+$CXCR3$^+$ precursors of BM memory CD4 T cells. The results highlight the requirement of prolonged cell division in the late activation phase of a primary immune response and strengthen the importance of costimulatory signaling by DCs for effective memory formation. In sum, this data indicates that highly proliferative CD49b$^+$CXCR3$^+$ activated CD4 T cells are continuously generated even during late time points of the primary immune response and that this generation is dependent on co-stimulatory signaling via CD28.

The transition from effector to memory has been described to be dependent on IL-2, co-stimulation and antigen signals at a defined “memory checkpoint”, that occurs around the peak of effector cell numbers (127, 128, 211, 212). Additionally, IL-2 signaling during priming has been associated with enhanced long-term survival of CD4 T cells (130). The analysis of CD49b$^+$CXCR3$^+$ MP CD4 T cells underlines this notion, as

the cells highly express IL-2Rβ in both spleen and BM. The analysis of splenic antigen-specific CD4 T cells on day 6 after immunization illustrates that particularly CD49b$^+$CXCR3$^+$ cells are susceptible to increased IL-2 signaling, as they contain more IL-2$^+$- and IL-2Rβ$^+$ cells than other populations. Notably, IL-2 neutralization with antibodies efficiently suppresses the appearance of BM memory CD4 T cells and their splenic precursors (unpublished data from Dr. Shintaro Hojyo). It is thus tempting to assume that the enhanced proliferation of CD49b$^+$CXCR3$^+$ precursors of BM memory CD4 T cells that coincides with increased IL-2 signaling enables the cells to avoid default apoptosis during the contraction phase thereby fostering survival and transition to memory.

In the process of deciphering why precursor formation of BM memory CD4 T cells requires enhanced cell division, cellular mechanisms of egress from the PALS and ultimately SLOs as well as interaction of antigen-specific CD4 T cells with DCs in the PALS on day 6 were assessed. A major fraction of antigen-specific T-bet$^+$ cells that can still be detected in the PALS are in contact with DCs, whereas antigen-specific T-bet$^-$ cells are not. Moreover, the majority of splenic precursors of BM memory CD4 T cells can be detected in the red pulp by day 6 after immunization, suggesting that a rapid downregulation of CCR7 occurs previously to this re-location from the PALS. CCR7 is a chemokine receptor that regulates T cell trafficking and compartmentalization within SLOs. Although CCR7$^{-/-}$ T cells migrate to the spleen, they however fail to move into the PALS and remain in the red pulp. In turn, in order to leave the PALS, activated T cells must downregulate CCR7 (85, 197). Consequently, resting BM memory CD4 T cells do not express CCR7 (96). Indeed, the analysis of MP CD44^{hi}CD4 T cells in spleen and BM revealed that particularly CD49b$^+$CXCR3$^+$ cells significantly downregulate CCR7. Accordingly, splenic antigen-specific CD49b$^+$CXCR3$^+$ precursors of BM memory CD4 T cells include a major population of IL-2Rβ$^+$CCR7^{lo} cells on day 6 after immunization, whereas other populations are not or only negligibly enriched in IL-2Rβ$^+$CCR7^{lo} cells. Notably, about 70 % of antigen-specific CD49b$^+$CXCR3$^+$ CD4 T cells in the BM are IL-2Rβ$^+$CCR7^{lo} cells.

Similarly to expression levels of CCR7, BM memory CD4 T cells do also not express CD62L (96). The combination of these markers distinguishes T_{EM} and T_{CM} cells and thus associates BM memory CD4 T cells with a T_{EM} phenotype. Intracellular fluorescent-dye labeling experiments previously demonstrated that the more effector cells divide, the more likely they are to lose CD62L expression (213). In line with this observation, the results displayed here illustrate that the expression of CCR7 gradually decreased in CD49b$^+$CXCR3$^+$ cells with progressing rounds of experienced cell divisions. Simultaneously, IL-2Rβ expression increased progressively with each round of cell

division and thus enhanced the cellular survival capacity by enabling the cells to escape from a default contraction phase.

The transcription factor Foxo1 regulates the expression of crucial T cell migration molecules CD62L and CCR7 via its direct regulation of the transcription factor Klf2 (156, 214, 215). Transcriptomic analyses revealed that Foxo1 mRNA in CD49b^{+}T-bet^{+} sorted antigen-specific CD4 T cells on day 6 after immunization is 2- or 4.5-fold reduced compared to CD49b^{+}T-bet^{-} or CD49b^{-}T-bet^{-} antigen-specific CD4 T cells, respectively (data not shown). This suggests a regulatory role of Foxo1 during the transition from effector to memory, but further in-depths-analyses must be carried out to confirm this proposition. In sum, the data presented here suggest that the downregulation of CCR7 enables highly proliferated CD49b^{+}CXCR3^{+} precursors of BM memory CD4 T cells to rapidly egress from the spleen and potentially migrate towards the BM for further differentiation into resting memory cells.

4.3 B cells negatively regulate the formation of precursors of BM memory CD4 T cells

B cell depletion inhibits the generation of splenic CD4 T cell memory, whereas the expansion of CD4 T cells is not affected under B cell deprived conditions (135-139). On the contrary, the establishment of lung CD4 T_{RM} cells has been reported to be negatively regulated by B cells (211, 216). In line with this finding, the results obtained here demonstrate that the depletion or deficiency in B cells actually promotes the accumulation of antigen-specific activated CD4 T cells in the BM, and in contrast the co-transfer of B cells suppresses their accumulation, suggesting that B cells are a negative regulator for the generation of CD4 T cell memory in the BM. Moreover, B cells suppress the expression of T-bet and CD49b in splenic antigen-specific CD4 T cells suggesting a direct regulatory role of B cells on BM CD4 T cell generation.

Early differentiation steps of the Th1 lineage overlap with the early Tfh pathway (217). Interestingly, T-bet expression suppresses the induction of Tfh cell specific genes by inhibiting the expression of Bcl-6, the master transcription factor of Tfh cells. Surprisingly, even in terminal differentiated Th1 cells, the Bcl-6 locus is not fully repressed by T-bet, and a Bcl-6/T-bet complex facilitates the repression of alternative Th lineages (218, 219). IL-2 plays a predominant role in defining the T-bet/Bcl-6 ratio: A high concentration of IL-2 keeps the concentration of Bcl-6 at a low level (220). Additionally, a report on the opposing signals from Bcl-6 and IL-2R stated that Th1 effector memory and Tfh-like central memory cells are generated from early effector cell populations

after infection with *Listeria monocytogenes* with an additional dependency on ICOS ligand expressed on B cells (93). In line with this report, others have described that ICOS costimulation via B cells is crucial to maintain the Tfh phenotype through the downregulation of the transcription factor Klf2 and that the blockade of ICOS ligand on B cells increases T-bet transcripts in antigen-specific CD4 T cells (215, 221). Moreover, transcripts of CD49b have been found to be increased in a Klf2-transduced HUVEC cell line (222). These reports support the results displayed here, which indicate that B cell depletion facilitates the upregulation of CD49b and T-bet expression. However, up to this point it remains unclear whether B cells suppress T-bet and CD49b in activated CD4 T cells in a Klf2-dependent manner.

The here presented data confirms the general paradigm that DCs activate CD4 T cells and license some of them to differentiate into precursors of BM memory CD4 T cells in the course of a primary immune response, while some activated CD4 T cells contact bystander B cells as follow-up APCs through cognate interaction. These cells then further differentiate into Tfh cells (78, 93, 152, 223). Thus, additional activation by B cells following DCs may induce the differentiation of Tfh cells (52), in turn suppressing the differentiation program for precursors of BM memory CD4 T cells.

Resting memory CD4 T cells in the BM are more functional *in vitro* and *in vivo* compared to spleen-resident memory cells (96). Adoptively transferred memory CD4 T cells from the BM can efficiently help B cells to produce high-affinity antibodies, suggesting that BM memory CD4 T cells can differentiate into Tfh cells during recall responses. Persisting antigens emulsified in adjuvants of oil and aluminum hydroxide augment the expansion of antigen-specific CD4 T cells in SLOs, namely Tfh cells (224), whereas the number of antigen-specific CD4 T cells in the BM is not affected by antigen persistence (99). It is thus tempting to speculate that the ratio of splenic Tfh cells and BM resting memory CD4 T cells is distinctly affected by antigen persistence which may also suggest that the duration of antigen presence defines the quantitative balance of splenic effector and resting BM memory.

In addition to their inhibitory role for the accumulation of precursors of BM memory CD4 T cells, the results obtained here demonstrate that B cells do not affect the cell division or proliferative capacity of precursors of BM memory CD4 T cells as analyzed by intracellular CFSE labelling experiments. Remarkably though, on day 4 after immunization, the frequency in $CD49b^{+}CXCR3^{+}$ precursors of BM memory CD4 T cells in the spleen were not different between B cell depleted and normal mice (Supplementary figure 3). On day 6 after immunization however, B cell depleted mice harbored more $CD49b^{+}CXCR3^{+}$ precursors of BM memory CD4 T cells in the spleen, confirming the

notion that B cell depletion indirectly augments T-bet and CD49b expression due to lack of Tfh lineage commitment. In turn, the increased frequency in $CD49b^+CXCR3^+$ precursors of BM memory CD4 T cells may foster the accumulation of these cells in the BM. The fact that $CD49b^+CXCR3^+$ activated CD4 T cells do not differ in terms of cell division properties underlines the paradigm that DCs are the responsible APC for priming, activation and fostering cell proliferation during the initiation of a primary immune response in SLOs. However, it remains to be further investigated if the division of activated CD4 T cells may be affected in B cell depleted mice after activated CD4 T cells have experienced more than 7 rounds of cell division, as CFSE labeling is too diluted to be distinguished from non-CFSE labeled cells after 7 cell divisions. In sum, it requires further research on how, where and at what time during the activation phase B cells affect the generation of memory CD4 T cells in the BM.

4.4 Limitations of the study

Some limitations in the methodology may be considered for this study. Throughout the study, a TCR-transgenic CD4 T cell adoptive transfer model has been employed. $5x10^5$ to $1x10^6$ antigen-specific naïve CD4 T cells have been adoptively transferred into syngenic non-transgenic recipient mice, reflecting about 1.5- 3 % of all naïve CD4 T cells post transfer. While this method offers unique possibilities to track a detectable population of antigen-specific CD4 T *in vivo* during an immune response using monoclonal antibodies, the frequency of transferred naïve CD4 T cells does not reflect physiological conditions. In addition, it is important to note that random integration of the TCR transgene into germline DNA may have unwanted consequences.

Alternatively, MHC tetramer staining is frequently used in some studies (226). This staining method permits the detection of endogeneous CD4 T cells specific for a certain antigen upon immunization without usage of transgenic mice. Taken into consideration that naïve antigen-specific CD4 T cells are continuously released from the thymus, Moon et *al.* estimated that the physiological number of naïve antigen-specific CD4 T cells only ranges from 20 to 200 cells per intact mouse. These estimates correspond to a frequency of 0.7 – 7 antigen-specific CD4 T cells per million cells, considering a mouse possesses approximately $3x10^7$ naïve CD4 T cells (227-228). This fact makes it difficult to specifically track these cells *in vivo* at this low frequency at the early time points chosen within this study, even after clonal expansion of activated CD4 T cells upon immunization. In sum, both, TCR-transgenic transfer model and tetramer staining model offer advantages and disadvantages. However, within this study, the kinetics of

activated CD4 T cells were primarily analyzed within a week after immunization. For this purpose, a prominent population of adoptively transferred naïve TCR-transgenic CD4 T cells was best suitable to show a simultaneous activation of CD4 T cells albeit the above mentioned disadvantages of this model.

The second limitation of this study applies to the antigens such as ovalbumin protein and LCMV peptide that were utilized to mimic vaccination. In particular ovalbumin has not been subject to pathogen/host co-evolution, and thus may not be representative for relevant cellular responses to infection or immunization and hence immune memory formation (229). However, infection with a pathogen or injection with protein/peptide are assumed to induce very distinct immune reactions. While the immunogenicity of an antigen is instrumental in directing antigen-specific lymphocytes to a dedicated response pathway during immunization/vaccination, pathogenic infection also stimulates many other innate pathways beyond TLR signaling. Hence, to understand the mechanism of memory formation upon a pathogen-specific infection, an injection with protein/peptide may not be suitable, as it does not reflect physiological conditions. However, in order to track antigen-specific CD4 T cells during the course of an immune reaction and to specifically understand how naive cells differentiate into memory cells, this study applied the simplified activation mechanism. Following the understanding of the differentiation mechanism gained from this study, the kinetics of memory precursor CD4 T cell generation should be investigated in a pathogenic infection model in the future.

It lies in the nature of animal experiments that individual mice vary between one another, even if they possess the same genetic background, are housed under the same conditions and are treated equally. In addition, handling and preparation of sacrificed mice brings further variance into the data. For instance, specific cell numbers of e.g. BM cells (e.g. Figure 3.3.1) strongly depend on the handling of the bone and the way the BM is flushed out of the bone, adding variance from mouse to mouse. Even though this sample handling induced variance can be expected between mice and thus can be seen as a systematic non-group-specific error, an increase in the sample size number would be beneficial to compensate this additional variance.

Hence, a further major limitation of this study refers to the sample size. In some experiments, the sample size was limited due to the breeding difficulties of transgenic mice (in particular T-bet KO mice) and low yield of TCR transgenic CD4 T cells for adoptive cell transfer into WT host mice. In addition, for the experiments presented in Figure 3.2.4 and Figure 3.3.3 technical obstacles required unforeseen changes in the flow cytometric panel design for the third repetition (Supplementary Figure 2) or second

repetition (Supplementary Figure 3) of the experiment leading to data that could not be pooled to increase statistical power of the results. Thus, some results are presented with low sample size and hence with low statistical power. Those results have to be seen as preliminary indicative results rather than results of strong quantitative power.

P values have been used as measures of significance for decades; the lower the *P* value, the less likely it is that the results are owed to coincidence, considering that the null hypothesis is true (no relationship between the measured phenomena). However, it is a matter of controversial debate in the scientific community, if setting a threshold such as a *P* value is generally useful to differ a true from a false effect and thus it is important to see the data generated within this study in the light of statistical limitations (230, 231). Statisticians and researchers have suggested that a possible loophole of categorizing results as significant or not significant would be in reporting effect sizes and confidence intervals (230, 231). This would inform about the magnitude and relative importance of an effect rather than a threshold for significance such as the *P* value and should be considered for future studies.

4.5 Conclusion

In conclusion, the results presented in this doctoral thesis suggest that CD49b$^+$T-bet$^+$/CXCR3$^+$ activated CD4 T cells are the precursors of BM memory CD4 T cells in the spleen (Figure 4.1).

Following their phenotypical identification within the pool of splenic activated CD4 T cells, the results illustrate that precursors of BM memory CD4 T cells are generated via enhanced cell division and sustained cognate interaction with DCs. Moreover, the data indicate that CD49b$^+$CXCR3$^+$ activated CD4 T cells are primarily generated during late time points of the primary immune response. Treatment with a cytostatic drug or blockage of CD28/B7 costimulatory pathway in the late activation phase in turn abrogates the generation of precursors of BM memory CD4 T cells. Moreover, fluorescent-dye labeling experiments demonstrate that the more CD49b$^+$CXCR3$^+$ activated CD4 T cells divide, the more they are likely to lose the expression of CCR7, a chemokine receptor crucial for cell persistence in the PALS of SLOs, and to gain the expression of IL-2Rβ, a cytokine receptor crucial for long-term survival.

Since B cells have been previously described to modulate the formation of memory CD4 T cells in the spleen, the third part of this thesis uncovers the role of B cells as suppressors for the formation of CD4 T cell memory in the BM by using B cell-depleted or B cell-deficient mice. However, B cells do not affect the proliferative capacity of activated CD4 T cells in the spleen during the activation phase, raising further questions on the regulatory role of B cells for the generation of BM resident memory CD4 T cells.

In sum, the results obtained in this thesis provide new insight into the generation of BM memory CD4 T cells that may help for the therapeutic strengthening of memory in the context of vaccination or its abolishment within the scope of autoimmune diseases.

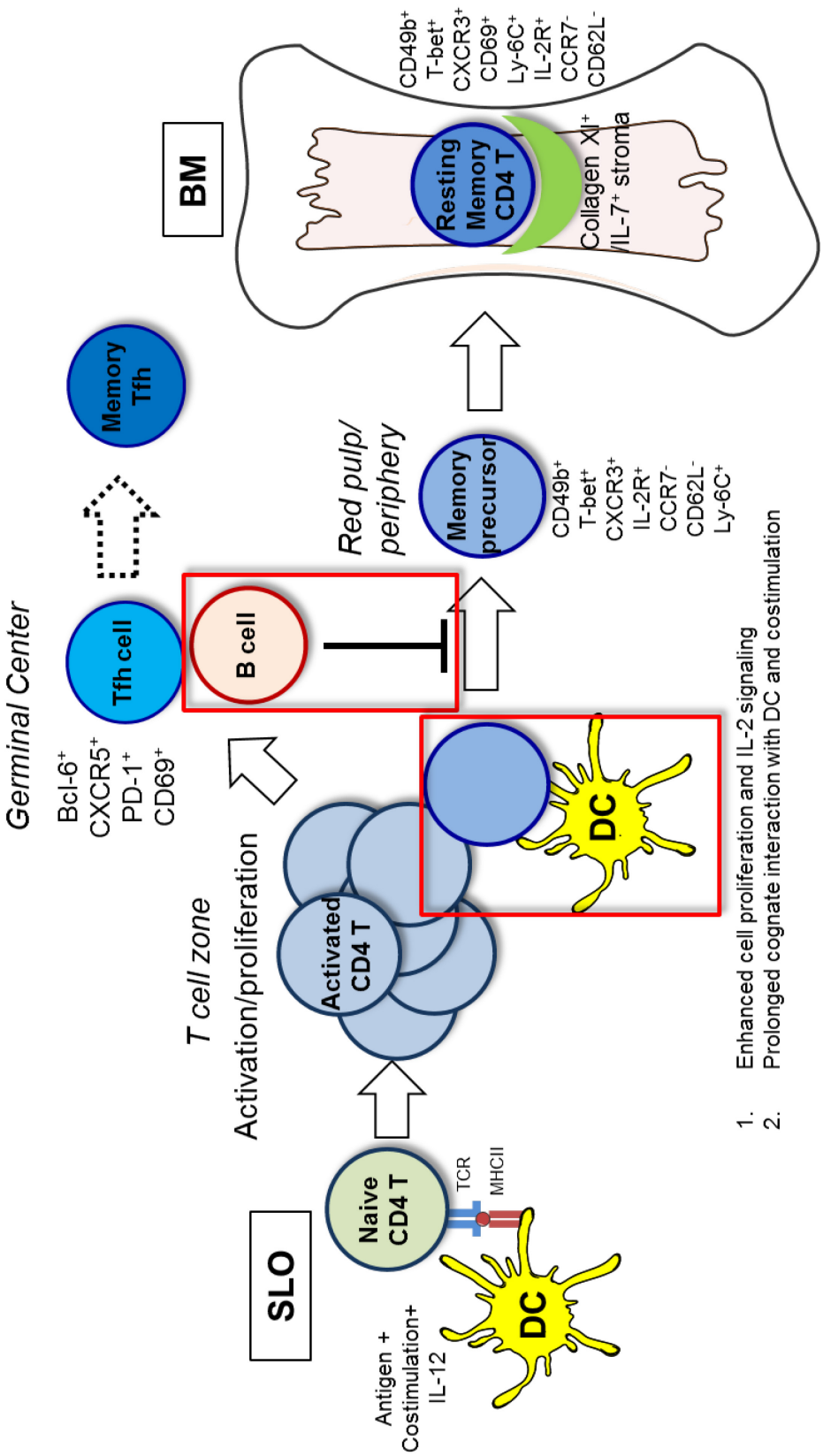

Figure 4.1: Schematic model for the generation of precursors of BM memory CD4 T cells on the basis of the results obtained within this doctoral thesis.

Appendix

1. T follicular helper cells express CD69, but not CD49b

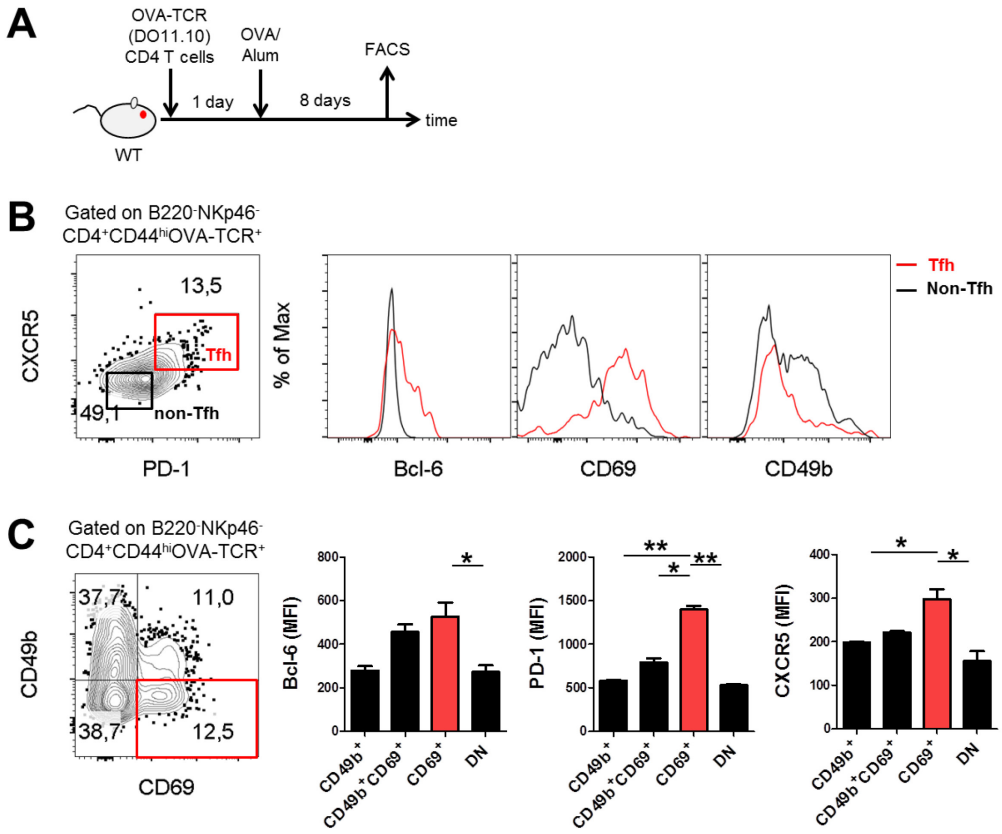

Supplementary Figure 1: Tfh cells express CD69 but not CD49b. **A:** Experimental outline. Purified OVA-TCR$^+$ (DO11.10) CD4 T cells were transferred into WT Balb/c mice followed by immunization with 100 µg OVA-peptide emulsified in 100 µl Alum. On day 8 after immunization, splenic OVA-TCR$^+$ CD4 T cells were analyzed by flow cytometry. **B:** Gating plots show a OVA-TCR$^+$ population in CD4$^+$CD44^{hi}B220$^-$PI$^-$ cells in the spleen. CXCR5$^-$PD-1$^-$ (non-Tfh, highlighted in black) and CXCR5$^+$PD-1$^+$ (Tfh, highlighted in red) cells were analyzed for their expression of Bcl-6, CD69 and CD49b. **C:** Gating plots show an OVA-TCR$^+$ population in CD4$^+$CD44^{hi}B220$^-$PI$^-$ cells in the spleen. The expression of the Tfh markers Bcl-6, CXCR5 and PD-1 was analyzed on the different subsets of CD69$^+$ and CD49b$^+$ expressing cells and the respective MFI compared between the subets. n=3; Mean ± SD; ns= not significant, **P*<0.05, ***P*<0.01, Student's t test.

2. CD49b⁺CXCR3⁺ antigen-specific CD4 T cells are highly proliferative and develop after 7 rounds of cell division

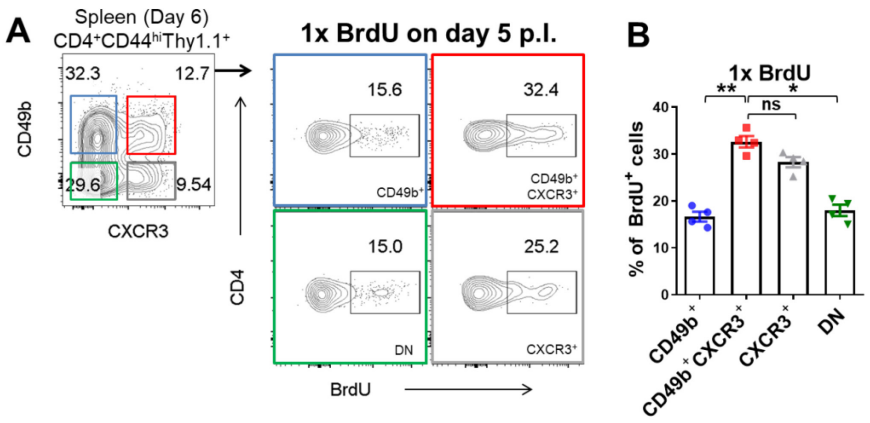

Supplementary Figure 2 (Appendix to Figure 3.2.4): Antigen-specific CD49b⁺CXCR3⁺ CD4 T cells incorporate more BrdU than other subsets at the beginning of the contraction phase of a primary immune response. **A:** Contour plots display BrdU⁺ cells in previously gated splenic subsets of CD49b and CXCR3 expressing CD4⁺CD44ʰⁱThy1.1⁺ cells in mice that were treated 1x with 1 mg BrdU on day 5 p.l. and analyzed on day 6 p.l. **B:** Bar graph displays percentages of BrdU⁺ cells in subsets of CD49b and CXCR3 expressing cells after 1x BrdU treatment (CD49b⁺: 16,63±1,043, CD49b⁺CXCR3⁺: 32,63±1,229, CXCR3⁺:28,25±1,090, DN (double negative): 17,98±1,209). Data represent results from a third experiments with n=4 per group. Data are presented as mean ± SEM. Statistical significance between subsets was determined by Kruskal-Wallis test with Dunn's multiple comparison test as $*p < 0.05$, $**p < 0.01$ or ns= not significant.

3. B cell depletion does not affect the proliferation of antigen-specific CXCR3⁺CD49b⁺ memory precursor CD4 T cells in the spleen

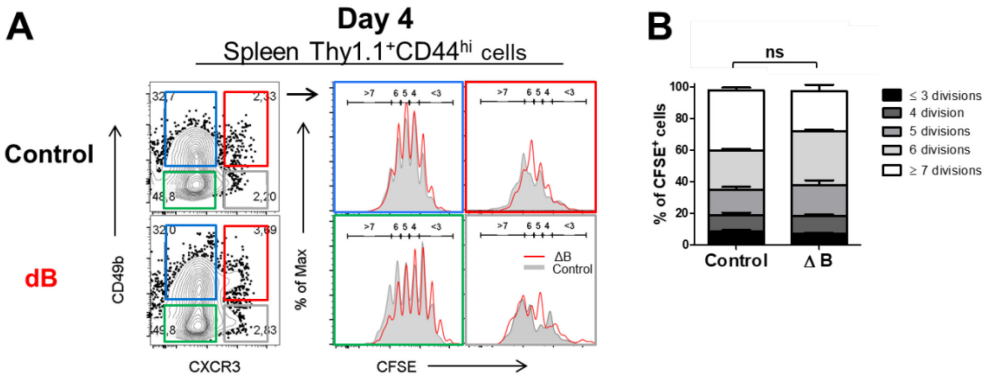

Supplementary Figure 3 (Appendix to Figure 3.3.3 B&C): B cell depletion does not affect the proliferation of ag-specific CXCR3⁺CD49b⁺ memory precursor CD4 T cells in the spleen. **A:** Gating plots show the expression of CD49b and CXCR3 in Thy1.1⁺CD4⁺ T cells of the spleen in control and B cell depleted (dB) mice on day 4 p.l. Histograms show splenic CD49b⁺CXCR3⁺ CFSE-labeled cells on day 4 p.l. In Thy1.1⁺CD4⁺cells. Filled grey histograms: control. Red line histograms: B cell depleted mice. Gates in histograms indicate rounds of cell division that CFSE-labeled cells have undergone in subsets of CD49b and/or CXCR3 expressing cells. **B:** Bar chart represents the precentages of CFSE⁺ cells in different divided generations (≤ 3 to ≥ 7 divisions) of CD49b⁺CXCR3⁺ cells. n=3 per group. Data are presented as mean ± SEM. Statistical significance between groups was determined by Wilcoxon test as ns = not significant.

Acknowledgements

It is a pleasure for me to thank all those who made this dissertation possible. First of all, I would like to thank my supervisor Dr. Koji Tokoyoda for giving me the opportunity to work in his lab and on the project and for his guidance and support during the last years.

I would like to thank the reviewers Prof. Radbruch, Prof. Thiel and Prof. Zychlinsky for reviewing this doctoral thesis. In particular Prof. Radbruch provided helpful comments and ideas for the project along the years in his function as Director of the DRFZ.

I am indebted to the DRFZ and all the co-workers for creating a great working atmosphere and providing help and support whenever needed, for fruitful discussions in clubs and seminars and for sharing great moments inside and outside the laboratory. I am particularly thankful for my lab mates Mathias Mursell, Shintaro Hojyo, Christian Männe, Asami Hanazawa, Tsung-Yen Wu and Yuzuru Yamasaki for the nice research atmosphere and precious help at any time.

I also would like to thank Dr. Katrin Moser, the Coordinator of the Leibniz Graduate School for Rheumatology (LGRh), for her support throughout the years and always an open office door for any problem or issue whatsoever.

I would like to thank my family for all their love and support: my parents and my siblings and not less importantly my “other” parents Angelika and Frieder. I would certainly not be the person I am today without all their constant help and unconditional love.

I need to thank Berni for always standing by my side, for encouraging me to do my best and for pushing me forward, and my sweet son Linus who is certainly the best biological experiment I’ll ever have done and who is able to easily break things down to what really matters in life. 11

Selbstständigkeitserklärung

Hiermit erkläre ich, die Dissertation selbstständig und nur unter Verwendung der angegebenen Hilfen und Hilfsmittel angefertigt zu haben. Ich habe mich anderwärts nicht um einen Doktorgrad beworben und besitze keinen entsprechenden Doktorgrad. Ich erkläre, dass ich die Dissertation oder Teile davon nicht bereits bei einer anderen wissenschaftlichen Einrichtung eingereicht habe und, dass sie dort weder angenommen noch abgelehnt wurde. Ich erkläre die Kenntnisnahme der dem Verfahren zugrunde liegenden Promotionsordnung der Mathematisch-Naturwissenschaftlichen Fakultät I (jetzt Lebenswissenschaftliche Fakultät) der Humboldt-Universität zu Berlin vom 27. Juni 2012. Weiterhin erkläre ich, dass keine Zusammenarbeit mit gewerblichen Promotionsberaterinnen/Promotionsberatern stattgefunden hat und dass die Grundsätze der Humboldt-Universität zu Berlin zur Sicherung guter wissenschaftlicher Praxis eingehalten wurden.

Berlin, Datum

Literature

1. Meylan E, Tschopp J, Karin M. Intracellular pattern recognition receptors in the host response. Nature. 2006;442(7098):39-44.
2. Medzhitov R. Toll-like receptors and innate immunity. Nat Rev Immunol. 2001;1(2):135-45.
3. Germain RN. MHC-dependent antigen processing and peptide presentation: providing ligands for T lymphocyte activation. Cell. 1994;76(2):287-99.
4. Inaba K, Turley S, Iyoda T, Yamaide F, Shimoyama S, Reis e Sousa C, et al. The formation of immunogenic major histocompatibility complex class II-peptide ligands in lysosomal compartments of dendritic cells is regulated by inflammatory stimuli. J Exp Med. 2000;191(6):927-36.
5. Steinman RM, Swanson J. The endocytic activity of dendritic cells. J Exp Med. 1995;182(2):283-8.
6. Stoltze L, Nussbaum AK, Sijts A, Emmerich NP, Kloetzel PM, Schild H. The function of the proteasome system in MHC class I antigen processing. Immunology today. 2000;21(7):317-9.
7. Jensen PE, Weber DA, Thayer WP, Chen X, Dao CT. HLA-DM and the MHC class II antigen presentation pathway. Immunologic research. 1999;20(3):195-205.
8. Gao GF, Jakobsen BK. Molecular interactions of coreceptor CD8 and MHC class I: the molecular basis for functional coordination with the T-cell receptor. Immunology today. 2000;21(12):630-6.
9. Al-Daccak R, Mooney N, Charron D. MHC class II signaling in antigen-presenting cells. Curr Opin Immunol. 2004;16(1):108-13.
10. Holling TM, Schooten E, van Den Elsen PJ. Function and regulation of MHC class II molecules in T-lymphocytes: of mice and men. Hum Immunol. 2004;65(4):282-90.
11. Banchereau J, Steinman RM. Dendritic cells and the control of immunity. Nature. 1998;392(6673):245-52.
12. Iwasaki A, Medzhitov R. Toll-like receptor control of the adaptive immune responses. Nat Immunol. 2004;5(10):987-95.
13. MacLeod MKL, Clambey ET, Kappler JW, Marrack P. CD4 memory T cells: What are they and what can they do? Seminars in Immunology. 2009;21(2):53-61.
14. Kapsenberg ML. Dendritic-cell control of pathogen-driven T-cell polarization. Nat Rev Immunol. 2003;3(12):984-93.
15. Grewal IS, Flavell RA. The role of CD40 ligand in costimulation and T-cell activation. Immunological reviews. 1996;153:85-106.
16. Greenwald RJ, Freeman GJ, Sharpe AH. The B7 family revisited. Annual review of immunology. 2005;23:515-48.
17. Parry RV, Chemnitz JM, Frauwirth KA, Lanfranco AR, Braunstein I, Kobayashi SV, et al. CTLA-4 and PD-1 receptors inhibit T-cell activation by distinct mechanisms. Mol Cell Biol. 2005;25(21):9543-53.
18. Said EA, Dupuy FP, Trautmann L, Zhang Y, Shi Y, El-Far M, et al. Programmed death-1-induced interleukin-10 production by monocytes impairs CD4+ T cell activation during HIV infection. Nature medicine. 2010;16(4):452-9.
19. Gershon RK, Paul WE. Effect of thymus-derived lymphocytes on amount and affinity of anti-hapten antibody. J Immunol. 1971;106(3):872-4.
20. Francus T, Francus Y, Siskind GW. Memory T cells enhance the expression of high-avidity naive B cells. Cellular immunology. 1991;134(2):520-7.

21. Crotty S, Kersh EN, Cannons J, Schwartzberg PL, Ahmed R. SAP is required for generating long-term humoral immunity. Nature. 2003;421(6920):282-7.
22. MacLennan IC, Gulbranson-Judge A, Toellner KM, Casamayor-Palleja M, Chan E, Sze DM, et al. The changing preference of T and B cells for partners as T-dependent antibody responses develop. Immunological reviews. 1997;156:53-66.
23. Williams MA, Tyznik AJ, Bevan MJ. Interleukin-2 signals during priming are required for secondary expansion of CD8+ memory T cells. Nature. 2006;441(7095):890-3.
24. Janssen EM, Droin NM, Lemmens EE, Pinkoski MJ, Bensinger SJ, Ehst BD, et al. CD4+ T-cell help controls CD8+ T-cell memory via TRAIL-mediated activation-induced cell death. Nature. 2005;434(7029):88-93.
25. Janssen EM, Lemmens EE, Wolfe T, Christen U, von Herrath MG, Schoenberger SP. CD4+ T cells are required for secondary expansion and memory in CD8+ T lymphocytes. Nature. 2003;421(6925):852-6.
26. Shedlock DJ, Shen H. Requirement for CD4 T cell help in generating functional CD8 T cell memory. Science. 2003;300(5617):337-9.
27. Sun JC, Bevan MJ. Defective CD8 T Cell Memory Following Acute Infection Without CD4 T Cell Help. Science (New York, NY). 2003;300(5617):339-42.
28. Sun JC, Williams MA, Bevan MJ. CD4+ T cells are required for the maintenance, not programming, of memory CD8+ T cells after acute infection. Nat Immunol. 2004;5(9):927-33.
29. Szabo SJ, Kim ST, Costa GL, Zhang X, Fathman CG, Glimcher LH. A novel transcription factor, T-bet, directs Th1 lineage commitment. Cell. 2000;100(6):655-69.
30. Afkarian M, Sedy JR, Yang J, Jacobson NG, Cereb N, Yang SY, et al. T-bet is a STAT1-induced regulator of IL-12R expression in naive CD4+ T cells. Nat Immunol. 2002;3(6):549-57.
31. Schulz EG, Mariani L, Radbruch A, Hofer T. Sequential polarization and imprinting of type 1 T helper lymphocytes by interferon-gamma and interleukin-12. Immunity. 2009;30(5):673-83.
32. Lugo-Villarino G, Maldonado-Lopez R, Possemato R, Penaranda C, Glimcher LH. T-bet is required for optimal production of IFN-gamma and antigen-specific T cell activation by dendritic cells. Proceedings of the National Academy of Sciences of the United States of America. 2003;100(13):7749-54.
33. Sullivan BM, Juedes A, Szabo SJ, von Herrath M, Glimcher LH. Antigen-driven effector CD8 T cell function regulated by T-bet. Proceedings of the National Academy of Sciences of the United States of America. 2003;100(26):15818-23.
34. Mosmann TR, Coffman RL. TH1 and TH2 cells: different patterns of lymphokine secretion lead to different functional properties. Annual review of immunology. 1989;7:145-73.
35. Glimcher LH, Murphy KM. Lineage commitment in the immune system: the T helper lymphocyte grows up. Genes Dev. 2000;14(14):1693-711.
36. Abbas AK, Murphy KM, Sher A. Functional diversity of helper T lymphocytes. Nature. 1996;383(6603):787-93.
37. Ahlers JD, Belyakov IM, Matsui S, Berzofsky JA. Signals delivered through TCR instruct IL-12 receptor (IL-12R) expression: IL-12 and tumor necrosis factor-alpha synergize for IL-12R expression at low antigen dose. Int Immunol. 2001;13(11):1433-42.
38. Groom JR, Richmond J, Murooka TT, Sorensen EW, Sung JH, Bankert K, et al. CXCR3 chemokine receptor-ligand interactions in the lymph node optimize CD4+ T helper 1 cell differentiation. Immunity. 2012;37(6):1091-103.
39. Xie JH, Nomura N, Lu M, Chen SL, Koch GE, Weng Y, et al. Antibody-mediated blockade of the CXCR3 chemokine receptor results in diminished recruitment of T helper 1 cells into sites of inflammation. J Leukoc Biol. 2003;73(6):771-80.

40. Paul WE, Seder RA. Lymphocyte responses and cytokines. Cell. 1994;76(2):241-51.
41. Couper KN, Blount DG, Riley EM. IL-10: the master regulator of immunity to infection. J Immunol. 2008;180(9):5771-7.
42. Harrington LE, Hatton RD, Mangan PR, Turner H, Murphy TL, Murphy KM, et al. Interleukin 17-producing CD4+ effector T cells develop via a lineage distinct from the T helper type 1 and 2 lineages. Nat Immunol. 2005;6(11):1123-32.
43. Afzali B, Lombardi G, Lechler RI, Lord GM. The role of T helper 17 (Th17) and regulatory T cells (Treg) in human organ transplantation and autoimmune disease. Clinical and experimental immunology. 2007;148(1):32-46.
44. Weaver CT, Harrington LE, Mangan PR, Gavrieli M, Murphy KM. Th17: an effector CD4 T cell lineage with regulatory T cell ties. Immunity. 2006;24(6):677-88.
45. Chen Z, Laurence A, O'Shea JJ. Signal transduction pathways and transcriptional regulation in the control of Th17 differentiation. Semin Immunol. 2007;19(6):400-8.
46. Ivanov, II, McKenzie BS, Zhou L, Tadokoro CE, Lepelley A, Lafaille JJ, et al. The orphan nuclear receptor RORgammat directs the differentiation program of proinflammatory IL-17+ T helper cells. Cell. 2006;126(6):1121-33.
47. Mangan PR, Harrington LE, O'Quinn DB, Helms WS, Bullard DC, Elson CO, et al. Transforming growth factor-beta induces development of the T(H)17 lineage. Nature. 2006;441(7090):231-4.
48. Veldhoen M, Hocking RJ, Atkins CJ, Locksley RM, Stockinger B. TGFbeta in the context of an inflammatory cytokine milieu supports de novo differentiation of IL-17-producing T cells. Immunity. 2006;24(2):179-89.
49. Sakaguchi S. Naturally arising CD4+ regulatory t cells for immunologic self-tolerance and negative control of immune responses. Annual review of immunology. 2004;22:531-62.
50. Sakaguchi S, Yamaguchi T, Nomura T, Ono M. Regulatory T cells and immune tolerance. Cell. 2008;133(5):775-87.
51. Bettelli E, Carrier Y, Gao W, Korn T, Strom TB, Oukka M, et al. Reciprocal developmental pathways for the generation of pathogenic effector TH17 and regulatory T cells. Nature. 2006;441(7090):235-8.
52. Crotty S. T follicular helper cell differentiation, function, and roles in disease. Immunity. 2014;41(4):529-42.
53. Chtanova T, Tangye SG, Newton R, Frank N, Hodge MR, Rolph MS, et al. T follicular helper cells express a distinctive transcriptional profile, reflecting their role as non-Th1/Th2 effector cells that provide help for B cells. J Immunol. 2004;173(1):68-78.
54. Nurieva RI, Chung Y, Hwang D, Yang XO, Kang HS, Ma L, et al. Generation of T follicular helper cells is mediated by interleukin-21 but independent of T helper 1, 2, or 17 cell lineages. Immunity. 2008;29(1):138-49.
55. Fazilleau N, Mark L, McHeyzer-Williams LJ, McHeyzer-Williams MG. Follicular helper T cells: lineage and location. Immunity. 2009;30(3):324-35.
56. Sivakumar PV, Foster DC, Clegg CH. Interleukin-21 is a T-helper cytokine that regulates humoral immunity and cell-mediated anti-tumour responses. Immunology. 2004;112(2):177-82.
57. Crotty S. Follicular helper CD4 T cells (TFH). Annual review of immunology. 2011;29:621-63.
58. Fenner F. A successful eradication campaign. Global eradication of smallpox. Rev Infect Dis. 1982;4(5):916-30.
59. Rappuoli R, Miller HI, Falkow S. Medicine. The intangible value of vaccination. Science. 2002;297(5583):937-9.
60. Sarkander J, Hojyo S, Tokoyoda K. Vaccination to gain humoral immune memory. Clin Transl Immunology. 2016;5(12):e120.

61. Chang HD, Radbruch A. Targeting pathogenic T helper cell memory. Ann Rheum Dis. 2011;70 Suppl 1:i85-7.
62. Manz RA, Thiel A, Radbruch A. Lifetime of plasma cells in the bone marrow. Nature. 1997;388(6638):133-4.
63. Slifka MK, Antia R, Whitmire JK, Ahmed R. Humoral immunity due to long-lived plasma cells. Immunity. 1998;8(3):363-72.
64. Fairfax KA, Kallies A, Nutt SL, Tarlinton DM. Plasma cell development: from B-cell subsets to long-term survival niches. Semin Immunol. 2008;20(1):49-58.
65. Cassese G, Arce S, Hauser AE, Lehnert K, Moewes B, Mostarac M, et al. Plasma cell survival is mediated by synergistic effects of cytokines and adhesion-dependent signals. J Immunol. 2003;171(4):1684-90.
66. Tellier J, Kallies A. Finding a home for plasma cells--a niche to survive. European journal of immunology. 2014;44(8):2243-6.
67. Chu VT, Beller A, Nguyen TT, Steinhauser G, Berek C. The long-term survival of plasma cells. Scandinavian journal of immunology. 2011;73(6):508-11.
68. Chu VT, Frohlich A, Steinhauser G, Scheel T, Roch T, Fillatreau S, et al. Eosinophils are required for the maintenance of plasma cells in the bone marrow. Nat Immunol. 2011;12(2):151-9.
69. O'Connor BP, Raman VS, Erickson LD, Cook WJ, Weaver LK, Ahonen C, et al. BCMA is essential for the survival of long-lived bone marrow plasma cells. J Exp Med. 2004;199(1):91-8.
70. Tan JT, Ernst B, Kieper WC, LeRoy E, Sprent J, Surh CD. Interleukin (IL)-15 and IL-7 jointly regulate homeostatic proliferation of memory phenotype CD8+ cells but are not required for memory phenotype CD4+ cells. J Exp Med. 2002;195(12):1523-32.
71. Becker TC, Coley SM, Wherry EJ, Ahmed R. Bone marrow is a preferred site for homeostatic proliferation of memory CD8 T cells. J Immunol. 2005;174(3):1269-73.
72. Mazo IB, Honczarenko M, Leung H, Cavanagh LL, Bonasio R, Weninger W, et al. Bone marrow is a major reservoir and site of recruitment for central memory CD8+ T cells. Immunity. 2005;22(2):259-70.
73. Sercan Alp O, Durlanik S, Schulz D, McGrath M, Grun JR, Bardua M, et al. Memory CD8(+) T cells colocalize with IL-7(+) stromal cells in bone marrow and rest in terms of proliferation and transcription. European journal of immunology. 2015;45(4):975-87.
74. Siracusa F, Alp OS, Maschmeyer P, McGrath M, Mashreghi MF, Hojyo S, et al. Maintenance of CD8(+) memory T lymphocytes in the spleen but not in the bone marrow is dependent on proliferation. European journal of immunology. 2017;47(11):1900-5.
75. Ahmed R, Gray D. Immunological memory and protective immunity: understanding their relation. Science. 1996;272(5258):54-60.
76. Gasper DJ, Tejera MM, Suresh M. CD4 T-cell memory generation and maintenance. Crit Rev Immunol. 2014;34(2):121-46.
77. Stockinger B, Kassiotis G, Bourgeois C. CD4 T-cell memory. Semin Immunol. 2004;16(5):295-303.
78. Hale JS, Youngblood B, Latner DR, Mohammed AU, Ye L, Akondy RS, et al. Distinct memory CD4+ T cells with commitment to T follicular helper- and T helper 1-cell lineages are generated after acute viral infection. Immunity. 2013;38(4):805-17.
79. Boyman O, Letourneau S, Krieg C, Sprent J. Homeostatic proliferation and survival of naive and memory T cells. European journal of immunology. 2009;39(8):2088-94.
80. Kassiotis G, Garcia S, Simpson E, Stockinger B. Impairment of immunological memory in the absence of MHC despite survival of memory T cells. Nat Immunol. 2002;3(3):244-50.

81. Seddon B, Tomlinson P, Zamoyska R. Interleukin 7 and T cell receptor signals regulate homeostasis of CD4 memory cells. Nat Immunol. 2003;4(7):680-6.
82. Swain SL, Hu H, Huston G. Class II-independent generation of CD4 memory T cells from effectors. Science. 1999;286(5443):1381-3.
83. Sallusto F, Lenig D, Forster R, Lipp M, Lanzavecchia A. Two subsets of memory T lymphocytes with distinct homing potentials and effector functions. Nature. 1999;401(6754):708-12.
84. Campbell JJ, Bowman EP, Murphy K, Youngman KR, Siani MA, Thompson DA, et al. 6-C-kine (SLC), a lymphocyte adhesion-triggering chemokine expressed by high endothelium, is an agonist for the MIP-3beta receptor CCR7. J Cell Biol. 1998;141(4):1053-9.
85. Forster R, Schubel A, Breitfeld D, Kremmer E, Renner-Muller I, Wolf E, et al. CCR7 coordinates the primary immune response by establishing functional microenvironments in secondary lymphoid organs. Cell. 1999;99(1):23-33.
86. Sallusto F, Geginat J, Lanzavecchia A. Central memory and effector memory T cell subsets: function, generation, and maintenance. Annual review of immunology. 2004;22:745-63.
87. Ahlers JD, Belyakov IM. Memories that last forever: strategies for optimizing vaccine T-cell memory. Blood. 2010;115(9):1678-89.
88. Park CO, Kupper TS. The emerging role of resident memory T cells in protective immunity and inflammatory disease. Nature medicine. 2015;21(7):688-97.
89. Beura LK, Masopust D. SnapShot: resident memory T cells. Cell. 2014;157(6):1488- e1.
90. Takada K, Wang X, Hart GT, Odumade OA, Weinreich MA, Hogquist KA, et al. Kruppel-like factor 2 is required for trafficking but not quiescence in postactivated T cells. J Immunol. 2011;186(2):775-83.
91. Weber JP, Fuhrmann F, Hutloff A. T-follicular helper cells survive as long-term memory cells. European journal of immunology. 2012;42(8):1981-8.
92. Ise W, Inoue T, McLachlan JB, Kometani K, Kubo M, Okada T, et al. Memory B cells contribute to rapid Bcl6 expression by memory follicular helper T cells. Proceedings of the National Academy of Sciences of the United States of America. 2014;111(32):11792-7.
93. Pepper M, Pagan AJ, Igyarto BZ, Taylor JJ, Jenkins MK. Opposing signals from the Bcl6 transcription factor and the interleukin-2 receptor generate T helper 1 central and effector memory cells. Immunity. 2011;35(4):583-95.
94. MacLeod MK, David A, McKee AS, Crawford F, Kappler JW, Marrack P. Memory CD4 T cells that express CXCR5 provide accelerated help to B cells. J Immunol. 2011;186(5):2889-96.
95. Choi YS, Yang JA, Yusuf I, Johnston RJ, Greenbaum J, Peters B, et al. Bcl6 expressing follicular helper CD4 T cells are fate committed early and have the capacity to form memory. J Immunol. 2013;190(8):4014-26.
96. Tokoyoda K, Zehentmeier S, Hegazy AN, Albrecht I, Grun JR, Lohning M, et al. Professional memory CD4+ T lymphocytes preferentially reside and rest in the bone marrow. Immunity. 2009;30(5):721-30.
97. Shinoda K, Tokoyoda K, Hanazawa A, Hayashizaki K, Zehentmeier S, Hosokawa H, et al. Type II membrane protein CD69 regulates the formation of resting T-helper memory. Proceedings of the National Academy of Sciences of the United States of America. 2012;109(19):7409-14.
98. Hanazawa A, Hayashizaki K, Shinoda K, Yagita H, Okumura K, Lohning M, et al. CD49b-dependent establishment of T helper cell memory. Immunol Cell Biol. 2013;91(8):524-31.
99. Hanazawa A, Lohning M, Radbruch A, Tokoyoda K. CD49b/CD69-Dependent Generation of Resting T Helper Cell Memory. Front Immunol. 2013;4(183).

100. Tokoyoda K, Hauser AE, Nakayama T, Radbruch A. Organization of immunological memory by bone marrow stroma. Nat Rev Immunol. 2010;10(3):193-200.
101. Tokoyoda K, Radbruch A. Signals controlling rest and reactivation of T helper memory lymphocytes in bone marrow. Cell Mol Life Sci. 2012;69(10):1609-13.
102. Herndler-Brandstetter D, Landgraf K, Jenewein B, Tzankov A, Brunauer R, Brunner S, et al. Human bone marrow hosts polyfunctional memory CD4+ and CD8+ T cells with close contact to IL-15-producing cells. J Immunol. 2011;186(12):6965-71.
103. Okhrimenko A, Grün JR, Westendorf K, Fang Z, Reinke S, von Roth P, et al. Human memory T cells from the bone marrow are resting and maintain long-lasting systemic memory. Proceedings of the National Academy of Sciences of the United States of America. 2014;111(25):9229-34.
104. Isogai S, Miyata S, Taha R, Yoshizawa Y, Martin JG, Hamid Q. CD4+ T cells migrate from airway to bone marrow after antigen inhalation in rats. J Allergy Clin Immunol. 2004;113(3):455-61.
105. Kaech SM, Wherry EJ, Ahmed R. Effector and memory T-cell differentiation: implications for vaccine development. Nat Rev Immunol. 2002;2(4):251-62.
106. Kwok WW, Tan V, Gillette L, Littell CT, Soltis MA, LaFond RB, et al. Frequency of epitope-specific naive CD4(+) T cells correlates with immunodominance in the human memory repertoire. J Immunol. 2012;188(6):2537-44.
107. Whitmire JK, Benning N, Whitton JL. Precursor frequency, nonlinear proliferation, and functional maturation of virus-specific CD4+ T cells. J Immunol. 2006;176(5):3028-36.
108. Geiger R, Duhen T, Lanzavecchia A, Sallusto F. Human naive and memory CD4+ T cell repertoires specific for naturally processed antigens analyzed using libraries of amplified T cells. J Exp Med. 2009;206(7):1525-34.
109. Moon JJ, Chu HH, Pepper M, McSorley SJ, Jameson SC, Kedl RM, et al. Naive CD4(+) T cell frequency varies for different epitopes and predicts repertoire diversity and response magnitude. Immunity. 2007;27(2):203-13.
110. Celli S, Lemaitre F, Bousso P. Real-time manipulation of T cell-dendritic cell interactions in vivo reveals the importance of prolonged contacts for CD4+ T cell activation. Immunity. 2007;27(4):625-34.
111. Corse E, Gottschalk RA, Allison JP. Strength of TCR-peptide/MHC interactions and in vivo T cell responses. J Immunol. 2011;186(9):5039-45.
112. Daniels MA, Teixeiro E. TCR Signaling in T Cell Memory. Front Immunol. 2015;6:617.
113. Masopust D, Kaech SM, Wherry EJ, Ahmed R. The role of programming in memory T-cell development. Curr Opin Immunol. 2004;16(2):217-25.
114. Malherbe L, Hausl C, Teyton L, McHeyzer-Williams MG. Clonal selection of helper T cells is determined by an affinity threshold with no further skewing of TCR binding properties. Immunity. 2004;21(5):669-79.
115. Williams MA, Ravkov EV, Bevan MJ. Rapid culling of the CD4+ T cell repertoire in the transition from effector to memory. Immunity. 2008;28(4):533-45.
116. Lanzavecchia A, Sallusto F. Progressive differentiation and selection of the fittest in the immune response. Nat Rev Immunol. 2002;2(12):982-7.
117. Kieper WC, Jameson SC. Homeostatic expansion and phenotypic conversion of naive T cells in response to self peptide/MHC ligands. Proceedings of the National Academy of Sciences of the United States of America. 1999;96(23):13306-11.
118. Zehn D, Lee SY, Bevan MJ. Complete but curtailed T-cell response to very low-affinity antigen. Nature. 2009;458(7235):211-4.
119. Corse E, Gottschalk RA, Krogsgaard M, Allison JP. Attenuated T cell responses to a high-potency ligand in vivo. PLoS Biol. 2010;8(9).

120. Sabatino JJ, Jr., Huang J, Zhu C, Evavold BD. High prevalence of low affinity peptide-MHC II tetramer-negative effectors during polyclonal CD4+ T cell responses. J Exp Med. 2011;208(1):81-90.
121. Sprent J, Surh CD. Normal T cell homeostasis: the conversion of naive cells into memory-phenotype cells. Nat Immunol. 2011;12(6):478-84.
122. Obst R, van Santen HM, Mathis D, Benoist C. Antigen persistence is required throughout the expansion phase of a CD4(+) T cell response. J Exp Med. 2005;201(10):1555-65.
123. Kim C, Wilson T, Fischer KF, Williams MA. Sustained interactions between T cell receptors and antigens promote the differentiation of CD4(+) memory T cells. Immunity. 2013;39(3):508-20.
124. Koguchi Y, Buenafe AC, Thauland TJ, Gardell JL, Bivins-Smith ER, Jacoby DB, et al. Preformed CD40L is stored in Th1, Th2, Th17, and T follicular helper cells as well as CD4+ 8- thymocytes and invariant NKT cells but not in Treg cells. PLoS One. 2012;7(2):e31296.
125. Pagan AJ, Pepper M, Chu HH, Green JM, Jenkins MK. CD28 promotes CD4+ T cell clonal expansion during infection independently of its YMNM and PYAP motifs. J Immunol. 2012;189(6):2909-17.
126. Boise LH, Minn AJ, Noel PJ, June CH, Accavitti MA, Lindsten T, et al. CD28 costimulation can promote T cell survival by enhancing the expression of Bcl-XL. Immunity. 1995;3(1):87-98.
127. McKinstry KK, Strutt TM, Bautista B, Zhang W, Kuang Y, Cooper AM, et al. Effector CD4 T-cell transition to memory requires late cognate interactions that induce autocrine IL-2. Nat Commun. 2014;5:5377.
128. Bautista BL, Devarajan P, McKinstry KK, Strutt TM, Vong AM, Jones MC, et al. Short-Lived Antigen Recognition but Not Viral Infection at a Defined Checkpoint Programs Effector CD4 T Cells To Become Protective Memory. J Immunol. 2016;197(10):3936-49.
129. Feau S, Arens R, Togher S, Schoenberger SP. Autocrine IL-2 is required for secondary population expansion of CD8(+) memory T cells. Nat Immunol. 2011;12(9):908-13.
130. Dooms H, Wolslegel K, Lin P, Abbas AK. Interleukin-2 enhances CD4+ T cell memory by promoting the generation of IL-7R alpha-expressing cells. J Exp Med. 2007;204(3):547-57.
131. Zhang J, Bardos T, Shao Q, Tschopp J, Mikecz K, Glant TT, et al. IL-4 potentiates activated T cell apoptosis via an IL-2-dependent mechanism. J Immunol. 2003;170(7):3495-503.
132. Harrington LE, Janowski KM, Oliver JR, Zajac AJ, Weaver CT. Memory CD4 T cells emerge from effector T-cell progenitors. Nature. 2008;452(7185):356-60.
133. Zhang X, Giangreco L, Broome HE, Dargan CM, Swain SL. Control of CD4 effector fate: transforming growth factor beta 1 and interleukin 2 synergize to prevent apoptosis and promote effector expansion. J Exp Med. 1995;182(3):699-709.
134. Yuseff MI, Pierobon P, Reversat A, Lennon-Dumenil AM. How B cells capture, process and present antigens: a crucial role for cell polarity. Nat Rev Immunol. 2013;13(7):475-86.
135. Linton PJ, Harbertson J, Bradley LM. A critical role for B cells in the development of memory CD4 cells. J Immunol. 2000;165(10):5558-65.
136. Misumi I, Whitmire JK. B cell depletion curtails CD4+ T cell memory and reduces protection against disseminating virus infection. J Immunol. 2014;192(4):1597-608.
137. Mollo SB, Zajac AJ, Harrington LE. Temporal requirements for B cells in the establishment of CD4 T cell memory. J Immunol. 2013;191(12):6052-9.
138. van Essen D, Dullforce P, Gray D. Role of B cells in maintaining helper T-cell memory. Philosophical transactions of the Royal Society of London Series B, Biological sciences. 2000;355(1395):351-5.

139. Whitmire JK, Asano MS, Kaech SM, Sarkar S, Hannum LG, Shlomchik MJ, et al. Requirement of B cells for generating CD4+ T cell memory. J Immunol. 2009;182(4):1868-76.
140. Gray D, Matzinger P. T cell memory is short-lived in the absence of antigen. J Exp Med. 1991;174(5):969-74.
141. Burton GF, Kosco MH, Szakal AK, Tew JG. Iccosomes and the secondary antibody response. Immunology. 1991;73(3):271-6.
142. Lohning M, Hegazy AN, Pinschewer DD, Busse D, Lang KS, Hofer T, et al. Long-lived virus-reactive memory T cells generated from purified cytokine-secreting T helper type 1 and type 2 effectors. J Exp Med. 2008;205(1):53-61.
143. Pepper M, Jenkins MK. Origins of CD4(+) effector and central memory T cells. Nat Immunol. 2011;12(6):467-71.
144. Moulton VR, Bushar ND, Leeser DB, Patke DS, Farber DL. Divergent generation of heterogeneous memory CD4 T cells. J Immunol. 2006;177(2):869-76.
145. Chang JT. Polarity and lymphocyte fate determination. Curr Opin Cell Biol. 2012;24(4):526-33.
146. Oliaro J, Van Ham V, Sacirbegovic F, Pasam A, Bomzon Z, Pham K, et al. Asymmetric cell division of T cells upon antigen presentation uses multiple conserved mechanisms. J Immunol. 2010;185(1):367-75.
147. King CG, Koehli S, Hausmann B, Schmaler M, Zehn D, Palmer E. T cell affinity regulates asymmetric division, effector cell differentiation, and tissue pathology. Immunity. 2012;37(4):709-20.
148. Choi YS, Kageyama R, Eto D, Escobar TC, Johnston RJ, Monticelli L, et al. ICOS receptor instructs T follicular helper cell versus effector cell differentiation via induction of the transcriptional repressor Bcl6. Immunity. 2011;34(6):932-46.
149. Bamezai A. Mouse Ly-6 proteins and their extended family: markers of cell differentiation and regulators of cell signaling. Arch Immunol Ther Exp (Warsz). 2004;52(4):255-66.
150. Walunas TL, Bruce DS, Dustin L, Loh DY, Bluestone JA. Ly-6C is a marker of memory CD8+ T cells. J Immunol. 1995;155(4):1873-83.
151. Hanninen A, Maksimow M, Alam C, Morgan DJ, Jalkanen S. Ly6C supports preferential homing of central memory CD8+ T cells into lymph nodes. European journal of immunology. 2011;41(3):634-44.
152. Marshall HD, Chandele A, Jung YW, Meng H, Poholek AC, Parish IA, et al. Differential expression of Ly6C and T-bet distinguish effector and memory Th1 CD4(+) cell properties during viral infection. Immunity. 2011;35(4):633-46.
153. Yamashita I, Nagata T, Tada T, Nakayama T. CD69 cell surface expression identifies developing thymocytes which audition for T cell antigen receptor-mediated positive selection. Int Immunol. 1993;5(9):1139-50.
154. Ziegler SF, Ramsdell F, Alderson MR. The activation antigen CD69. Stem Cells. 1994;12(5):456-65.
155. Spiegel S, Milstien S. The outs and the ins of sphingosine-1-phosphate in immunity. Nat Rev Immunol. 2011;11(6):403-15.
156. Carlson CM, Endrizzi BT, Wu J, Ding X, Weinreich MA, Walsh ER, et al. Kruppel-like factor 2 regulates thymocyte and T-cell migration. Nature. 2006;442(7100):299-302.
157. Skon CN, Lee JY, Anderson KG, Masopust D, Hogquist KA, Jameson SC. Transcriptional downregulation of S1pr1 is required for the establishment of resident memory CD8+ T cells. Nat Immunol. 2013;14(12):1285-93.
158. Shiow LR, Rosen DB, Brdickova N, Xu Y, An J, Lanier LL, et al. CD69 acts downstream of interferon-alpha/beta to inhibit S1P1 and lymphocyte egress from lymphoid organs. Nature. 2006;440(7083):540-4.
159. Bankovich AJ, Shiow LR, Cyster JG. CD69 suppresses sphingosine 1-phosophate receptor-1 (S1P1) function through interaction with membrane helix 4. J Biol Chem. 2010;285(29):22328-37.

160. Mackay LK, Rahimpour A, Ma JZ, Collins N, Stock AT, Hafon ML, et al. The developmental pathway for CD103(+)CD8+ tissue-resident memory T cells of skin. Nat Immunol. 2013;14(12):1294-301.
161. Richter M, Ray SJ, Chapman TJ, Austin SJ, Rebhahn J, Mosmann TR, et al. Collagen distribution and expression of collagen-binding alpha1beta1 (VLA-1) and alpha2beta1 (VLA-2) integrins on CD4 and CD8 T cells during influenza infection. J Immunol. 2007;178(7):4506-16.
162. Kassiotis G, Gray D, Kiafard Z, Zwirner J, Stockinger B. Functional specialization of memory Th cells revealed by expression of integrin CD49b. J Immunol. 2006;177(2):968-75.
163. Hynes RO. Integrins: versatility, modulation, and signaling in cell adhesion. Cell. 1992;69(1):11-25.
164. Kern A, Eble J, Golbik R, Kuhn K. Interaction of type IV collagen with the isolated integrins alpha 1 beta 1 and alpha 2 beta 1. European journal of biochemistry. 1993;215(1):151-9.
165. Tuckwell D, Calderwood DA, Green LJ, Humphries MJ. Integrin alpha 2 I-domain is a binding site for collagens. Journal of cell science. 1995;108 (Pt 4):1629-37.
166. DeNucci CC, Shimizu Y. beta1 integrin is critical for the maintenance of antigen-specific CD4 T cells in the bone marrow but not long-term immunological memory. J Immunol. 2011;186(7):4019-26.
167. Homann D, Teyton L, Oldstone MB. Differential regulation of antiviral T-cell immunity results in stable CD8+ but declining CD4+ T-cell memory. Nature medicine. 2001;7(8):913-9.
168. MacLeod M, Kwakkenbos MJ, Crawford A, Brown S, Stockinger B, Schepers K, et al. CD4 memory T cells survive and proliferate but fail to differentiate in the absence of CD40. J Exp Med. 2006;203(4):897-906.
169. Mata-Haro V, Cekic C, Martin M, Chilton PM, Casella CR, Mitchell TC. The vaccine adjuvant monophosphoryl lipid A as a TRIF-biased agonist of TLR4. Science. 2007;316(5831):1628-32.
170. Murphy KM, Heimberger AB, Loh DY. Induction by antigen of intrathymic apoptosis of CD4+CD8+TCRlo thymocytes in vivo. Science. 1990;250(4988):1720-3.
171. Oxenius A, Zinkernagel RM, Hengartner H. Comparison of activation versus induction of unresponsiveness of virus-specific CD4+ and CD8+ T cells upon acute versus persistent viral infection. Immunity. 1998;9(4):449-57.
172. Zhu J, Jankovic D, Oler AJ, Wei G, Sharma S, Hu G, et al. The transcription factor T-bet is induced by multiple pathways and prevents an endogenous Th2 cell program during Th1 cell responses. Immunity. 2012;37(4):660-73.
173. Mombaerts P, Iacomini J, Johnson RS, Herrup K, Tonegawa S, Papaioannou VE. RAG-1-deficient mice have no mature B and T lymphocytes. Cell. 1992;68(5):869-77.
174. Parish CR, Glidden MH, Quah BJ, Warren HS. Use of the intracellular fluorescent dye CFSE to monitor lymphocyte migration and proliferation. Current protocols in immunology. 2009;Chapter 4:Unit4 9.
175. Cossarizza A, Chang HD, Radbruch A, Akdis M, Andra I, Annunziato F, et al. Guidelines for the use of flow cytometry and cell sorting in immunological studies. European journal of immunology. 2017;47(10):1584-797.
176. Benner R, Hijmans W, Haaijman JJ. The bone marrow: the major source of serum immunoglobulins, but still a neglected site of antibody formation. Clinical and experimental immunology. 1981;46(1):1-8.
177. Tsubata T, Murakami M, Honjo T. Antigen-receptor cross-linking induces peritoneal B-cell apoptosis in normal but not autoimmunity-prone mice. Curr Biol. 1994;4(1):8-17.

178. Kawamoto T. Use of a new adhesive film for the preparation of multi-purpose fresh-frozen sections from hard tissues, whole-animals, insects and plants. Archives of histology and cytology. 2003;66(2):123-43.
179. Koch MA, Tucker-Heard G, Perdue NR, Killebrew JR, Urdahl KB, Campbell DJ. The transcription factor T-bet controls regulatory T cell homeostasis and function during type 1 inflammation. Nat Immunol. 2009;10(6):595-602.
180. Matsuda JL, Zhang Q, Ndonye R, Richardson SK, Howell AR, Gapin L. T-bet concomitantly controls migration, survival, and effector functions during the development of Valpha14i NKT cells. Blood. 2006;107(7):2797-805.
181. Manz RA, Arce S, Cassese G, Hauser AE, Hiepe F, Radbruch A. Humoral immunity and long-lived plasma cells. Curr Opin Immunol. 2002;14(4):517-21.
182. Hauser AE, Debes GF, Arce S, Cassese G, Hamann A, Radbruch A, et al. Chemotactic responsiveness toward ligands for CXCR3 and CXCR4 is regulated on plasma blasts during the time course of a memory immune response. J Immunol. 2002;169(3):1277-82.
183. Tokoyoda K, Egawa T, Sugiyama T, Choi B-I, Nagasawa T. Cellular Niches Controlling B Lymphocyte Behavior within Bone Marrow during Development. Immunity.20(6):707-18.
184. Hargreaves DC, Hyman PL, Lu TT, Ngo VN, Bidgol A, Suzuki G, et al. A coordinated change in chemokine responsiveness guides plasma cell movements. J Exp Med. 2001;194(1):45-56.
185. Lord GM, Rao RM, Choe H, Sullivan BM, Lichtman AH, Luscinskas FW, et al. T-bet is required for optimal proinflammatory CD4+ T-cell trafficking. Blood. 2005;106(10):3432-9.
186. Guarda G, Hons M, Soriano SF, Huang AY, Polley R, Martin-Fontecha A, et al. L-selectin-negative CCR7- effector and memory CD8+ T cells enter reactive lymph nodes and kill dendritic cells. Nat Immunol. 2007;8(7):743-52.
187. Hikono H, Kohlmeier JE, Takamura S, Wittmer ST, Roberts AD, Woodland DL. Activation phenotype, rather than central- or effector-memory phenotype, predicts the recall efficacy of memory CD8+ T cells. J Exp Med. 2007;204(7):1625-36.
188. Rivino L, Messi M, Jarrossay D, Lanzavecchia A, Sallusto F, Geginat J. Chemokine receptor expression identifies Pre-T helper (Th)1, Pre-Th2, and nonpolarized cells among human CD4+ central memory T cells. J Exp Med. 2004;200(6):725-35.
189. Scholzen T, Gerdes J. The Ki-67 protein: from the known and the unknown. Journal of cellular physiology. 2000;182(3):311-22.
190. Lyons AB, Parish CR. Determination of lymphocyte division by flow cytometry. Journal of immunological methods. 1994;171(1):131-7.
191. Parretta E, Cassese G, Santoni A, Guardiola J, Vecchio A, Di Rosa F. Kinetics of in vivo proliferation and death of memory and naive CD8 T cells: parameter estimation based on 5-bromo-2'-deoxyuridine incorporation in spleen, lymph nodes, and bone marrow. J Immunol. 2008;180(11):7230-9.
192. Hall AG, Tilby MJ. Mechanisms of action of, and modes of resistance to, alkylating agents used in the treatment of haematological malignancies. Blood reviews. 1992;6(3):163-73.
193. Linsley PS, Brady W, Grosmaire L, Aruffo A, Damle NK, Ledbetter JA. Binding of the B cell activation antigen B7 to CD28 costimulates T cell proliferation and interleukin 2 mRNA accumulation. J Exp Med. 1991;173(3):721-30.
194. Linsley PS, Brady W, Urnes M, Grosmaire LS, Damle NK, Ledbetter JA. CTLA-4 is a second receptor for the B cell activation antigen B7. J Exp Med. 1991;174(3):561-9.
195. Linsley PS, Wallace PM, Johnson J, Gibson MG, Greene JL, Ledbetter JA, et al. Immunosuppression in vivo by a soluble form of the CTLA-4 T cell activation molecule. Science. 1992;257(5071):792-5.

196. Wells AD, Gudmundsdottir H, Turka LA. Following the fate of individual T cells throughout activation and clonal expansion. Signals from T cell receptor and CD28 differentially regulate the induction and duration of a proliferative response. The Journal of clinical investigation. 1997;100(12):3173-83.
197. Junt T, Scandella E, Forster R, Krebs P, Krautwald S, Lipp M, et al. Impact of CCR7 on priming and distribution of antiviral effector and memory CTL. J Immunol. 2004;173(11):6684-93.
198. Hardy RR, Kincade PW, Dorshkind K. The protean nature of cells in the B lymphocyte lineage. Immunity. 2007;26(6):703-14.
199. Townsend MJ, Weinmann AS, Matsuda JL, Salomon R, Farnham PJ, Biron CA, et al. T-bet regulates the terminal maturation and homeostasis of NK and Valpha14i NKT cells. Immunity. 2004;20(4):477-94.
200. Sasaki K, Tsuji T, Jinushi T, Matsuzaki J, Sato T, Chamoto K, et al. Differential regulation of VLA-2 expression on Th1 and Th2 cells: a novel marker for the classification of Th subsets. Int Immunol. 2003;15(6):701-10.
201. Radbruch A, Muehlinghaus G, Luger EO, Inamine A, Smith KG, Dorner T, et al. Competence and competition: the challenge of becoming a long-lived plasma cell. Nat Rev Immunol. 2006;6(10):741-50.
202. Kabashima K, Haynes NM, Xu Y, Nutt SL, Allende ML, Proia RL, et al. Plasma cell S1P1 expression determines secondary lymphoid organ retention versus bone marrow tropism. J Exp Med. 2006;203(12):2683-90.
203. Cibrian D, Sanchez-Madrid F. CD69: from activation marker to metabolic gatekeeper. European journal of immunology. 2017;47(6):946-53.
204. Alari-Pahissa E, Notario L, Lorente E, Vega-Ramos J, Justel A, Lopez D, et al. CD69 does not affect the extent of T cell priming. PLoS One. 2012;7(10):e48593.
205. Lee YT, Suarez-Ramirez JE, Wu T, Redman JM, Bouchard K, Hadley GA, et al. Environmental and antigen receptor-derived signals support sustained surveillance of the lungs by pathogen-specific cytotoxic T lymphocytes. J Virol. 2011;85(9):4085-94.
206. Mackay LK, Braun A, Macleod BL, Collins N, Tebartz C, Bedoui S, et al. Cutting edge: CD69 interference with sphingosine-1-phosphate receptor function regulates peripheral T cell retention. J Immunol. 2015;194(5):2059-63.
207. Kuhns MS, Davis MM. TCR Signaling Emerges from the Sum of Many Parts. Front Immunol. 2012;3:159.
208. Govern CC, Paczosa MK, Chakraborty AK, Huseby ES. Fast on-rates allow short dwell time ligands to activate T cells. Proceedings of the National Academy of Sciences of the United States of America. 2010;107(19):8724-9.
209. Govern CC, Chakraborty AK. For T cell receptors, some breakups might not last forever. Immunity. 2010;32(2):141-2.
210. Tubo NJ, Pagan AJ, Taylor JJ, Nelson RW, Linehan JL, Ertelt JM, et al. Single naive CD4+ T cells from a diverse repertoire produce different effector cell types during infection. Cell. 2013;153(4):785-96.
211. Hondowicz BD, Kim KS, Ruterbusch MJ, Keitany GJ, Pepper M. IL-2 is required for the generation of viral-specific CD4(+) Th1 tissue-resident memory cells and B cells are essential for maintenance in the lung. European journal of immunology. 2018;48(1):80-6.
212. Devarajan P, Bautista B, Vong AM, McKinstry KK, Strutt TM, Swain SL. New Insights into the Generation of CD4 Memory May Shape Future Vaccine Strategies for Influenza. Front Immunol. 2016;7:136.
213. Caserta S, Kleczkowska J, Mondino A, Zamoyska R. Reduced functional avidity promotes central and effector memory CD4 T cell responses to tumor-associated antigens. J Immunol. 2010;185(11):6545-54.
214. Kerdiles YM, Beisner DR, Tinoco R, Dejean AS, Castrillon DH, DePinho RA, et al. Foxo1 links homing and survival of naive T cells by regulating L-selectin, CCR7 and interleukin 7 receptor. Nat Immunol. 2009;10(2):176-84.

215. Weber JP, Fuhrmann F, Feist RK, Lahmann A, Al Baz MS, Gentz LJ, et al. ICOS maintains the T follicular helper cell phenotype by down-regulating Kruppel-like factor 2. J Exp Med. 2015;212(2):217-33.
216. Hondowicz BD, An D, Schenkel JM, Kim KS, Steach HR, Krishnamurty AT, et al. Interleukin-2-Dependent Allergen-Specific Tissue-Resident Memory Cells Drive Asthma. Immunity. 2016;44(1):155-66.
217. Lazarevic V, Glimcher LH, Lord GM. T-bet: a bridge between innate and adaptive immunity. Nat Rev Immunol. 2013;13(11):777-89.
218. Nakayamada S, Kanno Y, Takahashi H, Jankovic D, Lu KT, Johnson TA, et al. Early Th1 cell differentiation is marked by a Tfh cell-like transition. Immunity. 2011;35(6):919-31.
219. Oestreich KJ, Huang AC, Weinmann AS. The lineage-defining factors T-bet and Bcl-6 collaborate to regulate Th1 gene expression patterns. J Exp Med. 2011;208(5):1001-13.
220. Oestreich KJ, Mohn SE, Weinmann AS. Molecular mechanisms that control the expression and activity of Bcl-6 in TH1 cells to regulate flexibility with a TFH-like gene profile. Nat Immunol. 2012;13(4):405-11.
221. Lee JY, Skon CN, Lee YJ, Oh S, Taylor JJ, Malhotra D, et al. The transcription factor KLF2 restrains CD4(+) T follicular helper cell differentiation. Immunity. 2015;42(2):252-64.
222. Parmar KM, Larman HB, Dai G, Zhang Y, Wang ET, Moorthy SN, et al. Integration of flow-dependent endothelial phenotypes by Kruppel-like factor 2. The Journal of clinical investigation. 2006;116(1):49-58.
223. Crotty S, Johnston RJ, Schoenberger SP. Effectors and memories: Bcl-6 and Blimp-1 in T and B lymphocyte differentiation. Nat Immunol. 2010;11(2):114-20.
224. Baumjohann D, Preite S, Reboldi A, Ronchi F, Ansel KM, Lanzavecchia A, et al. Persistent antigen and germinal center B cells sustain T follicular helper cell responses and phenotype. Immunity. 2013;38(3):596-605.
225. Hojyo S, Sarkander J, Männe C, Mursell M, Hanazawa A, Zimmel D, et al. B Cells Negatively Regulate the Establishment of CD49b^{+}T-bet^{+} Resting Memory T Helper Cells in the Bone Marrow. Front Immunol. 2016; 7:26.
226. Vollers SS, Stern LJ. Class II major histocompatibility complex tetramer staining: progress, problems, and prospects. Immunology. 2008 Mar;123(3):305-13.
227. Moon JJ, Chu HH, Pepper M, McSorley SJ, Jameson SC et al. Naive CD4(+) T cell frequency varies for different epitopes and predicts repertoire diversity and response magnitude. Immunity. 2007; 27:203–213.
228. Jenkins MK, Chu HH, McLachlan JB, Moon JJ. On the composition of the preimmune repertoire of T cells specific for Peptide-major histocompatibility complex ligands. Annu. Rev. Immunol. 2010; 28:275–294.
229. Zinkernagel RM, Hengartner H. Regulation of the immune response by antigen. Science. 2000; 293:251–253.
230. Nuzzo R. Scientific method: Statistical errors. P values, the 'gold standard' of statistical validity, are not as reliable as many scientists assume. Nature. 2014; 506:150–152.
231. Amrhein V, Greenland S, McShane B et al. Scientists rise up against statistical significance. Nature. 2019; 567:305–307.